The two-plasmon decay instability in a turbulent background



Rusko Todorov Ruskov
University College
University of Oxford

A thesis submitted for the degree of
Doctor of Philosophy

Trinity 2026

Abstract

Laser-plasma instabilities have impeded laser inertial confinement fusion since its inception. The direct-drive approach requires understanding the non-linearly saturated, strongly turbulent state of the two-plasmon decay (TPD) instability. Since wave propagation is significantly modified in a turbulent medium, so will be any process involving a resonant wave-wave interaction such as TPD. Therefore studying the turbulent steady-state demands a model of the influence of the turbulence upon its own forcing.

This thesis examines this phenomenon by applying the direct-interaction approximation (DIA) statistical closure to the Zakharov system extended to include the TPD non-linearity. The formalism naturally admits an externally imposed laser electric field with an arbitrary power spectrum, enabling the study of how broad laser bandwidth affects both the instability's linear and non-linear stages.

The turbulence provides an additional decorrelation mechanism that limits the effective interaction time of the triad of modes involved in the TPD resonance. The turbulent damping responsible for this is evaluated using the renormalised equations of the DIA. Scalings of the fluctuation level and of the power injected by TPD (equivalent to the laser power absorbed by the plasma) are derived in terms of the laser parameters. They align with numerical work reporting a constant hot-electron fraction and constant laser anomalous absorption. When the interaction time is dominated not by turbulent decorrelation, but by the laser coherence time, the injected power and the fluctuation level exhibit increased sensitivity to the laser parameters.

The influence of the laser frequency spectrum on the growth rate of the TPD instability is evaluated in the absence of the turbulent background. The range of excited modes is shown to be substantially broadened, and peak growth rates are calculated for different spectral shapes, including a discrete one.

Acknowledgements

Personal

I will be forever in debt to my supervisor Prof. Peter Norreys, who took me on as a student in 2019, and opened the world of inertial confinement fusion to me. Few people are as devoted and committed to the growth of their students as Peter is. I am beyond grateful for the intellectual freedom he gave me to follow my curiosity.

I would like to thank Bob Bingham who was instrumental in introducing me to the problems I ended up working on. While broadband parametric instabilities were the initial focus, Langmuir collapse was already discussed in our very first meeting in October of 2022! I am grateful for excellent conversations with Luis Silva, who also served as my Transfer of Status examiner, as well as with Jason Myatt and Russ Follett, who patiently answered numerous questions about TPD.

Thanks to all members of the Norreys group, past and present, especially to Ramy Aboushelbaya, for his weekly feedback and for keeping me from drifting into the abyss, and to the other two-thirds of the Norreys group laser fusion programme – Heath Martin and Jordan Lee – for countless fascinating (and speculative) discussions about fusion, and for making every conference trip an absolute joy.

My venture into physics would never have happened without the remarkable teachers I had during my school days in Bulgaria: Mariana Anastasova and Teodosii Teodosiev. Nothing has kindled the spirit of free learning in me more than the kind of environment they fostered. My dear friends from that time are too numerous to list, but I am especially indebted to Kamen Velev, who first brought me to Teo's lectures.

My years at Univ blessed me with the friendship of Radostin Chonev, Mikael Yeghiazaryan, Kaloyan Aleksiev, Maria Popova, and the other members of The White House: Darren Chan, Ethan Carragher, and Leonard Turica.

Finally, and most importantly, none of this would have mattered without my parents Tanya and Todor, my brother Alexander, my friend Borislav, and my wife Martina.

Funding

I would like to thank Mr. Bjorn Saven and the British taxpayer for funding, and the Oxford Department of Physics for awarding me, the Joint *Saven European Scholarship* and *Doctoral Training Partnership – Engineering and Physical Sciences Research Council Scholarship*. This work would not have been carried out without their contributions. Additional support provided by the John Adams Institute for Accelerator Science is also gratefully acknowledged.

Communications

The work presented in this thesis has resulted in the following communications to the scientific community:

Publications

- Ruskov, R. T., Bingham, R., Silva, L. O., Harper, M., Aboushelbaya, R., Myatt, J. F. & Norreys, P. A. 2024 Statistical theory of the broadband two-plasmon decay instability. *Journal of Plasma Physics* **90** (6), 905900621.

Conference presentations

- "The effects of laser bandwidth on the non-linearly saturated state of the two-plasmon decay instability," *Laboratory for Laser Energetics, Rochester NY, USA, November 24, 2025.* Seminar.
- "The effects of laser bandwidth on the non-linearly saturated state of the two-plasmon decay instability," 67^{th} *Annual Meeting of the APS Division of Plasma Physics, Long Beach CA, USA, November 20, 2025.* Talk.
- "The effect of broad laser bandwidth on the two-plasmon decay instability and its connection to turbulence," 2^{nd} *IFE-Star Conference, Breckenridge CO, USA, April 7-11, 2025.* Poster.
- "Statistical theory of the broadband two-plasmon decay instability," 52^{nd} *Anomalous Absorption Conferenece, Big Sky MT, USA, June 9-14, 2024.* Talk.
- "Statistical theory of the broadband two-plasmon decay instability," *UK Inertial Fusion Energy Consortium Annual Meeting, Imperial College, London, UK, March 26, 2024.* Poster.
- "Statistical theory of the broadband two-plasmon decay instability," *Oxford Centre for High Energy Density Science* 10^{th} *Annual Meeting, Oxford, UK, March 18, 2024.* Talk.
- "Theory of the broadband two-plasmon decay instability," 65^{th} *Annual Meeting of the APS Division of Plasma Physics, Denver CO, USA, October 31, 2023.* Talk.

Other work carried out during the course of doctoral studies has led to the following collaborative contributions:

Co-author publications

- Timmis, R., Fitzpatrick, C., Kennedy, J., Huddleston, H., Denis, E., James, A., Baird, C., Symes, D., McGonegle, D., Atonga, E., Martin, H., Rebenstock, J., Neely, J., Lee, J., Bourgeois, N., Finlay, O., *Ruskov, R.T.*, Astbury, S., Hawkes, S., Zhang, Z., Zepf, M., Krushelnick, K., Gumbrell, E., Pattathil, R., Yeung, M., Dromey, B., and Norreys, P. 2026 Efficiency-optimized relativistic plasma harmonics for extreme fields. *Nature*.

- Martin, H., Paddock, R.W., von der Leyen, M.W., Eliseev, V., *Ruskov, R.T.*, Timmis, R., Lee, J.J., James, A., and Norreys, P.A. 2024 Electrothermal Filamentation of Fusion Plasmas. *Physical Review E* **110**, 035205.

- Atonga, E., Martineau, K., Aboushelbaya, R., Barrau, A., von der Leyen, M.W., Howard, S., James, A., Lee, J.J., Lin, C., Martin, H., Ouatu, I., Paddock, R., *Ruskov, R.T.*, Timmis, R., and Norreys, P.A. 2024 Gravitational waves from high-power twisted light. *Phyiscal Review D* **110**, 044023.

Contents

List of Figures **viii**

1 Introduction **1**
1.1 Laser-plasma instabilities in inertial confinement fusion 1
1.2 Turbulence and saturation 4
1.3 Outline of the thesis 6

2 Background **7**
2.1 The two-plasmon decay 7
2.2 Plasma turbulence in the direct-interaction approximation 10
2.2.1 Wave propagation in a turbulent medium 10
2.2.2 Derivation of the DIA 15
2.2.3 Single-field DIA 19
2.2.4 Markovianisation 20
2.2.5 Energy conservation, realizability, and the random-coupling model 23
2.3 Langmuir collapse 24
2.4 Summary 26

3 Power injection by the two-plasmon decay into the turbulent steady state **28**
3.1 Introduction 28
3.2 The Zakharov system forced by the two-plasmon decay 30
3.2.1 Relevant temporal and spatial scales 30
3.2.2 Derivation 31
3.2.3 Time-enveloping, normalisation, and Fourier decomposition 35
3.3 Application of the DIA to the ZakTPD system 39
3.3.1 Statistical homogeneity and symmetries 39
3.3.2 Governing equations 43
3.3.3 Spectral balance and total power injected by TPD 47
3.4 Estimate of the non-linear growth rate and the injected power under a Markovian approximation 49
3.5 Scalings of the injected power with laser intensity and bandwidth 53
3.6 Summary 58

4 Linear regime of the two-plasmon decay driven by broad bandwidth laser fields 60
4.1 Introduction 60
4.2 Dependence of the growth rate on the laser spectrum 62
4.2.1 Dispersion relation 62
4.2.2 Single temporally incoherent beam 63
4.2.3 Relation of the DIA to other statistical approximations 67
4.3 Parametric instabilities driven by a discrete N-line spectrum 67
4.4 Summary 69

5 Concluding remarks and future work 71
5.1 Summary of the results 71
5.2 Open questions and future research 72

Appendices

A Relationship between real space and Fourier space response functions 75

B Equations for the ZakTPD system in the direct-interaction approximation 77
B.1 Coupling coefficients in the ZakTPD system 77
B.2 From the general DIA equations to the statistically homogeneous ones . . 78
B.3 The ZakTPD-DIA equations 80
B.3.1 Langmuir response and covariance 80
B.3.2 Ion response and covariance 81

Bibliography 83

List of Figures

1.1 (a) An illustration of a spherical ICF fuel pellet, directly driven by multiple laser beams. (b) A zoom-in of the coronal plasma region surrounding the target, showing the laser beams propagating up to the critical density surface n_c, together with the two-plasmon decay instability near the quarter-critical ($n_c/4$) surface responsible for generating energetic (hot) electrons. 2

2.1 Plot of the TPD growth rate $\gamma_{0\mathbf{k}}$ overlaid with the wave-vector diagram showing the laser wave vector $\mathbf{k}_0$ in white, together with the two Langmuir wave vectors in red (left panel). The red dashed hyperbolas satisfy $k_\perp^2 = k_\parallel \left(k_\parallel - k_0\right)$, and are the locations along which the growth rate is maximised. The normalisation is $\gamma_0 = k_0 v_{\mathrm{os}}/4$. 9

2.2 Perturbations of the turbulent medium. For a steady-state to exist, the response R must be a decaying function of time. 13

2.3 An illustration of the role of the two non-linear terms contributing to the spectral balance in (2.89) representing the forward decays *from* $\mathbf{k}$, and the mergers *into* $\mathbf{k}$. The solid lines are used to denote the covariances entering each term, and the dashed lines represent the responses which enter by way of the interaction time. 23

2.4 An illustration of a collapsing wave packet (a caviton) showing the four characteristic stages in the cycle. 25

3.1 Illustration of the wave-vector and field species coupling constraints leading to the diagonalisation of the DIA. 43

3.2 An illustration of a typical Langmuir frequency spectrum observed in simulations of the SLT state showing a free mode near $\delta\omega_{\mathbf{k}}$ as well as a *caviton continuum* of bound states having $\omega < \omega_{\mathrm{pe}}$ (which because of enveloping corresponds to $\omega < 0$). 46

3.3 An illustration of the scaling laws for the power injected by the two-plasmon decay into the saturated state as a function of laser bandwidth. 58

4.1 Plot of the growth rate of the TPD instability for different laser bandwidths. The laser has an intensity of $I_L = 10^{15}\,\mathrm{W/cm^2}$, a wavelength $\lambda_L = 351\,\mathrm{nm}$, and a Lorentzian power spectrum; the plasma conditions are $n_{0e}/n_c = 0.235$ and $T_e = 2\,\mathrm{keV}$ in (a), and $T_e = 5\,\mathrm{keV}$ in (b). The left panels show the monochromatic growth rates from the direct numerical solution of (4.6) for a single mode spectrum, and are normalised to γ_0. The middle and right panels show the analytic broadband growth rate $\gamma_{\mathbf{k}}$ (4.11) normalised to $\gamma_{\max} = 2\gamma_0^2/\Delta\omega$. $k_\perp$ and $k_\parallel$ refer to wave numbers perpendicular or parallel to the direction of propagation of the laser. 64

4.2 Plot of the growth rate $\gamma_{\mathbf{k}}$ obtained by the numerical evaluation of (4.6) along the lower branch of the TPD hyperbolas $k_\perp^2 = k_\parallel(k_\parallel - k_0)$. The inset shows the middle panel of figure 4.1 (a) along with the aforementioned hyperbola by the red dashed line. The laser and plasma parameters are identical to those in figure 4.1. The growth rate is normalised to the monochromatic one γ_0, and the horizontal axis is $k = \sqrt{k_\perp^2 + k_\parallel^2}$, evaluated along the hyperbola. The circles show the estimated peak growth rate from (4.18). 66

4.3 a) A power spectrum consisting of $N = 7$ discrete spectral lines spread over bandwidth $\Delta\omega$. b) The square of the correlation function $|g(\tau)|^2$ as a function of the time delay τ for a set of N discrete spectral lines spread over a bandwidth $\Delta\omega$. 68

Base metals can be transmuted into gold by stars,
and by intelligent beings who understand the processes that power stars,
but by nothing else in the universe.

— David Deutsch, *The Beginning of Infinity*

1 Introduction

Contents

1.1 Laser-plasma instabilities in inertial confinement fusion 1
1.2 Turbulence and saturation 4
1.3 Outline of the thesis 6

Fuelled by the promise of virtually limitless, clean energy, humankind has been on a quest to achieve controlled thermonuclear fusion for over 70 years. In laser-driven inertial confinement fusion (ICF)[1], powerful lasers spherically compress a millimetre-sized fuel pellet, concentrating roughly five hundred times more power on its surface than supported by the entirety of the United States' electrical grid. The pellet implodes with a velocity of 0.1 % of the speed of light, and at peak compression is 10 times hotter, and 10 times denser than the centre of the Sun. Pressures exceed 300 billion atmospheres. On December 5, 2022, the lasers at the National Ignition Facility fired 2.05 MJ of energy towards such a fuel pellet. It produced 3.15 MJ of fusion energy. A myriad of problems still remain, and this thesis hopes to make some non-negligible contribution towards solving them.

1.1 Laser-plasma instabilities in inertial confinement fusion

In the direct-drive approach illustrated in figure 1.1, virtually immediately after the laser beams first hit the surface of the pellet, its outer layer is rapidly ionised and turned into a plasma. It then expands to surround the target, and leads to the formation of the

[1]The following references contain fascinating accounts of ICF history: Nuckolls (2007); Grams (2021); Rosen (2024).

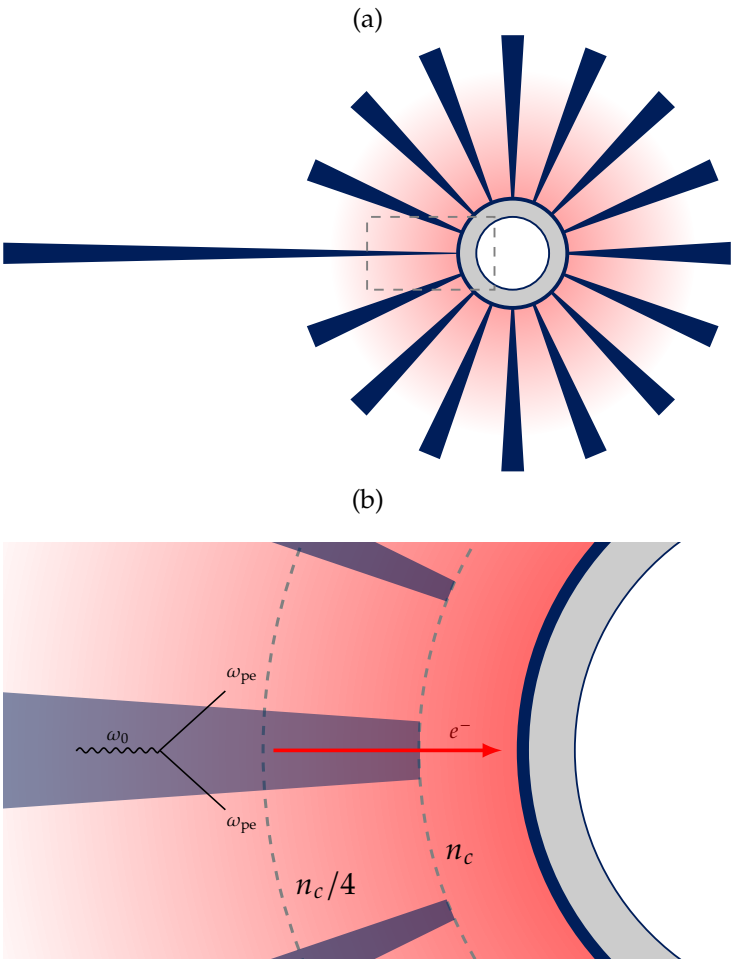


Figure 1.1: (a) An illustration of a spherical ICF fuel pellet, directly driven by multiple laser beams. (b) A zoom-in of the coronal plasma region surrounding the target, showing the laser beams propagating up to the critical density surface n_c, together with the two-plasmon decay instability near the quarter-critical ($n_c/4$) surface responsible for generating energetic (hot) electrons.

so-called *corona* through which the laser beams have to propagate in order to deposit their energy into the pellet. This turns out to be problematic.

The problem lies in the fact that a plasma supports a multitude of normal modes of oscillations (waves) which can non-linearly couple and start interacting provided their amplitude is sufficiently high. In the typically non-magnetised plasmas of ICF, these modes are: the electromagnetic one, along with the two electrostatic ones – the fast electron plasma oscillations (Langmuir modes), and the slow ion-acoustic oscillations. Once a resonance becomes possible between the powerful laser beam propagating through the coronal plasma and two of these normal modes, the laser beam becomes subject to a plethora of decay instabilities. The conditions under which a resonance is possible are determined by the wave number and frequency matching between the three waves:

$$\omega_1 = \omega_2 + \omega_3, \qquad \mathbf{k}_1 = \mathbf{k}_2 + \mathbf{k}_3, \tag{1.1}$$

Wave 1	Wave 2	Wave 3	Instability
EMW	LW	LW	Two-plasmon decay (TPD)
EMW	EMW	LW	Stimulated Raman scattering (SRS)
EMW	EMW	IAW	Stimulated Brillouin scattering (SBS)
EMW	EMW	IAW	Cross-beam energy transfer (CBET)

Table 1.1: A list of the most common three-wave decay instabilities occurring in the ICF coronal plasma which the incoming laser beams are subject to. Here EMW refers to electromagnetic waves; LW refers to Langmuir waves, and IAW to an ion-acoustic one.

with ω_j and $\mathbf{k}_j$ being the angular frequency and wave vector of the j-th wave respectively.

The case which we are concerned with at present is when $(\omega_1, \mathbf{k}_1)$ represents the laser pulses used for the compression of the ICF pellet. Depending on what waves 2 and 3 are, a summary of the most relevant instabilities is given in table 1.1.

Soon after the first high-power laser facilities capable of carrying out implosion experiments were constructed in the 1970s, it was found that these laser-plasma instabilities (LPI) were responsible for generating copious amounts of hot electrons and backscatter (Craxton *et al.*, 2015; Hurricane *et al.*, 2023; Michel, 2023). Hot electrons are highly energetic electrons originating in the coronal plasma and are correlated with experimental signatures of the instabilities involving Langmuir waves. They can propagate to the fusion fuel, heat it up prematurely, and hence prevent its efficient compression. Backscatter is laser light effectively reflected from the coronal plasma by the instabilities involving an electromagnetic mode as one of its products. The deleterious effects of LPI were so problematic that this era of ICF research is commonly referred to as the *infrared catastrophe*, in reference to the $> 1\,\mu$m wavelength of the laser light used at those early facilities (Froula *et al.*, 2025).

With the move to frequency tripled light at around $\sim 0.3\,\mu$m, LPI were partially tamed, at least in comparison to the infrared catastrophe days[2]. Nevertheless, the ablation pressures required for high gain direct-drive ICF necessitate laser intensities which are still prohibitive from an LPI standpoint. So the challenge still stands, and one promising approach actively being pursued currently is the use of broad bandwidth lasers.

Instead of the usual extremely narrow frequency spectrum a typical laser has, broad bandwidth lasers have power spectra with some appreciable frequency bandwidth $\Delta\omega$. A simple argument can be made which shows why bandwidth may be beneficial for LPI mitigation. A broadband laser pulse will maintain coherence over times of order

[2]Shorter wavelength lasers were seen as beneficial for a variety of reasons. An oft-cited one is that the oscillation velocity of an electron in the presence of the electric field of a laser – to which LPI growth rates are generally proportional to – is $v_{\mathrm{os}} \propto \sqrt{I_{\mathrm{L}}\lambda_{\mathrm{L}}^2}$, where I_{L} and λ_{L} are the laser intensity and wavelength. Shorter wavelengths also lead to more favourable conditions in the coronal plasma such as decreased scale length and temperature (Schmitt & Obenschain, 2023*a*).

$\tau_c \sim 1/\Delta\omega$ (the coherence time). Suppose the amplitudes of the product waves in an LPI grow exponentially with some typical growth rate γ_0 (under a monochromatic laser of the same intensity), the relevant time scale of this growth is γ_0^{-1}. Therefore, one can imagine how, if the coherence time of the broadband pulse is substantially shorter than the typical growth time scale, i.e. $\gamma_0\tau_c \ll 1$, the resonance that must be maintained between the three waves involved in the instability will be spoiled and the growth rate will be reduced. It turns out that the typical reduction in the growth rate is roughly by a factor of $\gamma_0\tau_c$, or equivalently – the growth rate becomes $\gamma_0 \to \gamma_0^2/\Delta\omega$. Simulations have shown that fractional bandwidths $\Delta\omega/\omega_0$ for third harmonic light of around 2 % may be enough to suppress most LPI of concern to direct-drive ICF (Follett *et al.*, 2019, 2021; Bates *et al.*, 2023). Such bandwidths will soon become experimentally accessible.

The argument above outlines why bandwidth may lead to a reduction in the growth rate of an LPI in some average sense but misses out important details. For example, the growth rate is generally a function of wave number $\gamma_{\mathbf{k}}$ – certain modes grow faster than others. Some questions one might pose are: how does bandwidth change this spectrum? Is the growth rate reduced at every wave number? How important is the shape of the laser spectrum? The challenge in producing a theory of an instability under a broadband driving laser field which may answer these questions, is that such a field is random in some sense – meaning we lack complete information about the minute details of its space-time dependence, and it is possible to specify only, say, a power spectrum of its fluctuations.

1.2 Turbulence and saturation

The detrimental hot electron production process due to the electronic instabilities involving Langmuir waves such as the two-plasmon decay (TPD) and stimulated Raman scattering (SRS), is understood to occur when the instabilities are driven to non-linear saturation where linear damping mechanisms such as collisional and Landau damping, or convection out of resonance due to inhomogeneity, are insufficient to halt instability growth. Characterising this saturated state is essential for developing effective mitigation strategies, and informing accurate reduced modelling.

Particle-in-cell simulations and numerical solutions of the Zakharov model (see sections 2.3 and 3.2), show a saturated turbulent state characterised by a broad k-space spectrum of Langmuir modes extending to the Landau cut-off ($k\lambda_{\mathrm{De}} \simeq 0.3$ with λ_{De} being the Debye length) (Vu *et al.*, 2012*a*,*b*, 2014; Myatt *et al.*, 2013, 2014). By definition, for non-linear saturation to occur, modes excited during the linear stage experience insufficient damping (collisional or Landau). Therefore non-linear processes must be responsible for

the transport of energy from where it is injected by the instability, to where it is dissipated at high k. This is the conceptual framework of the Kolmogorov phenomenological theory of fluid turbulence describing a cascade of energy due to stirring at the large scales, towards viscous dissipation at the small (Kolmogorov, 1941; Frisch, 1995).

For neutral fluids, the non-linear "object" responsible for this energy transport across scales is the turbulent eddy. In strong Langmuir turbulence (SLT) it is the caviton: a Langmuir wave packet localised in a self-consistent density depression that ponderomotively deepens until it reaches scales small enough for Landau damping (or, more accurately, some strongly non-linear version of it) to become strong enough to dissipate the electrostatic energy contained in it (see figure 2.4) (Zakharov, 1972)[3]. A steady state is achieved when the power injected by the external stirring is balanced by the power dissipated by the sea of cavities in the SLT state.

How is such a balance realised? Strong Langmuir turbulence has been studied extensively, and its fundamental characteristics are well-understood—ranging from the micro-physics of individual caviton dynamics, to global properties such as fluctuation spectra and caviton number density in the SLT state (for a review, see Robinson, 1997). Typically, these properties are defined for a prescribed rate of external driving, such as a linear instability or an external field. However, when Langmuir turbulence is excited by wave-wave coupling instabilities like the two-plasmon decay, the question of power injection becomes more complex.

As explained in the previous section, a wave-wave coupling instability occurs via resonances between waves. It is well-known that wave propagation is substantially modified in a strongly turbulent system. A principal effect is that of turbulent damping, or turbulent decorrelation, which causes individual Fourier modes in a turbulent system to decohere (Krommes, 2002, 2015; Diamond *et al.*, 2010). Parallel to the previous discussion regarding the effect of a laser with short coherence time on wave-wave coupling, if the turbulent decorrelation rate exceeds the coherent instability growth rate, one should expect a similar modification. This has indeed been explored by Sagdeev *et al.* (1982), via a similarly heuristic argument.

While exact analytical solutions are rare in plasma turbulence, rigorous theory provides the explanatory framework necessary to navigate the inconsistencies of less systematic treatments. Statistical closure theories – specifically the Direct-Interaction Approximation (DIA) – offer a robust methodology for capturing these strong turbulence effects systematically.

[3]Caviton collapse is an effect analogous to self-focusing of intense laser beams in non-linear Kerr media (Michel, 2023).

1.3 Outline of the thesis

The problems outlined in the previous two sections – understanding the influence of laser bandwidth on the two-plasmon decay growth rate, and describing its non-linear saturation – are intimately related. Both demand modelling the instability in which one or more of the modes evolve highly stochastically (i.e. turbulently). And indeed such a unified description exists.

Chapter 2 provides the necessary background on: the two-plasmon decay instability, the direct-interaction approximation used to study TPD in a strongly turbulent background, and the fundamentals of Langmuir collapse, which characterises this turbulent state.

Chapter 3 then applies the direct-interaction approximation to an extended Zakharov system, incorporating the non-linear term which couples the externally imposed laser electric field to the Langmuir waves. Using the Markovianisation procedure of Bowman *et al.* (1993), I derive a non-linear growth rate for the TPD instability to quantify the energy injection rate in the turbulent steady state. The influence of the turbulent background on TPD is explained through the concept of the *triad interaction time* – a measure of the duration over which the three modes involved in the TPD resonance maintain coherence. This interaction time incorporates both the laser coherence time and the turbulent decorrelation rate of the Langmuir modes. By balancing the power dissipated by cavitons with the energy injection rate calculated within the DIA, I derive scalings for the overall fluctuation level (total Langmuir wave energy density), and total power absorbed from the laser. The resulting scalings appear consistent with numerical work which reports a constant hot electron fraction, and constant laser anomalous absorption.

Chapter 4 examines the linear regime of the TPD instability, specifically: the growth rate under a single temporally incoherent laser beam. Laser bandwidth leads to the "smearing" of the TPD growth rate in wave number space: so although peak values are indeed generally reduced, the broadening effect implies that the growth rate of other modes in fact increases. That chapter also addresses the practically important problem of achieving broad laser bandwidth using a number of discrete spectral lines, and evaluates their quenching effect on parametric instabilities in general.

Chapter 5 summarises and discusses these results, outlining directions for ongoing and future work.

"Contradictions do not exist. Whenever you think that you are facing a contradiction, check your premises. You will find that one of them is wrong."

"If you don't know, the thing to do is not to get scared, but to learn."

— Ayn Rand *Atlas Shrugged*

2 Background

Contents

2.1 The two-plasmon decay 7
2.2 Plasma turbulence in the direct-interaction approximation 10
2.2.1 Wave propagation in a turbulent medium 10
2.2.2 Derivation of the DIA 15
2.2.3 Single-field DIA 19
2.2.4 Markovianisation 20
2.2.5 Energy conservation, realizability, and the random-coupling model 23
2.3 Langmuir collapse 24
2.4 Summary 26

2.1 The two-plasmon decay

The two-plasmon decay instability is a three-wave decay instability in which an electromagnetic mode resonantly interacts with two Langmuir modes in a plasma. In the presence of an externally imposed plane-wave field $\mathbf{E}_L$[1]:

$$\mathbf{E}_L(t,\mathbf{x}) = \tfrac{1}{2}\mathbf{E}_0 e^{-i\omega_0 t + i\mathbf{k}_0\cdot\mathbf{x}} + \text{c.c.} \tag{2.1}$$

an electron will execute oscillatory motion at the same frequency, with its *quiver velocity* being:

$$\mathbf{v}_{os}(t,\mathbf{x}) = -i\frac{e\mathbf{E}_0}{m_e\omega_0}\, e^{-i\omega_0 t} + \text{c.c.} \tag{2.2}$$

An analysis of the motion of the electron fluid under such a perturbation is carried out in section 3.2 where I derive the general equations I will use to study the turbulence

[1] *c.c.* stands for *complex conjugate*.

excited by the two-plasmon decay. But for the present purposes, it is enough to note that a standard perturbation procedure applied to the equations of motion for the electron fluid will produce couplings such as $\mathbf{v}_{\text{os}} \cdot \boldsymbol{\nabla} \delta n_e$, where δn_e is the density perturbation associated with a Langmuir mode. This allows for the resonant interaction between the externally imposed laser, and the plasma.

Resonance demands that frequency and wave number matching be satisfied between the three modes:

$$\omega_0 = \omega_1 + \omega_2, \qquad \mathbf{k}_0 = \mathbf{k}_1 + \mathbf{k}_2. \tag{2.3}$$

The Langmuir dispersion relation[2]:

$$\omega_{\mathbf{k}} = \omega_{\text{pe}} \left(1 + \tfrac{3}{2} k^2 \lambda_{\text{De}}^2\right), \tag{2.4}$$

implies that Langmuir waves always have frequencies near, and only slightly above ω_{pe}, due to strong Landau damping for modes with $k\lambda_{\text{De}} > 0.3$ (Nicholson, 1983). This confines the TPD instability spatially to a narrow region near the density at which $\omega_0 \simeq 2\omega_{\text{pe}}$, i.e. the quarter-critical density $n_c/4$ (see figure 1.1). Here $\omega_{\text{pe}} = \sqrt{n_e e^2/(\epsilon_0 m_e)}$ is the plasma frequency; $\lambda_{\text{De}} = v_{\text{the}}/\omega_{\text{pe}}$ is the electron Debye length, with $v_{\text{the}} = \sqrt{T_e/m_e}$ being the electron thermal speed; the critical density is given by $n_c = \omega_0^2 \epsilon_0 m_e/e^2$. The inhomogeneity of the coronal plasma has important consequences for the laser intensity *threshold* above which the instability is excited, but let us first consider the problem of examining the growth rate in a homogeneous plasma.

For a plane wave laser field such as (2.1), the growth rate can be derived by standard methods (Michel, 2023)[3]:

$$\gamma_{0\mathbf{k}} = \gamma_0 \left| \frac{(\mathbf{k} \cdot \mathbf{e}_0)}{k_0} \frac{(k^2 - p^2)}{kp} \right|. \tag{2.5}$$

Here $\gamma_0 = k_0 v_{\text{os}}/4$ is the maximum value the growth rate attains over all wave numbers; $\mathbf{e}_0$ is a unit vector denoting the laser polarisation such that $\mathbf{E}_0 = E_0 \mathbf{e}_0$; and $\mathbf{p} = \mathbf{k}_0 - \mathbf{k}$ is the wave number of the second resonant Langmuir mode. (2.5) applies under the assumption that frequency matching between the Langmuir modes $\mathbf{k}$ and $\mathbf{p}$, and the laser $\mathbf{k}_0$ is satisfied:

$$\omega_0 = \omega_{\mathbf{k}} + \omega_{\mathbf{p}}. \tag{2.6}$$

[2]This is valid for long wavelengths $k\lambda_{\text{De}} \ll 1$ but as noted later on, short-wavelength Langmuir modes are heavily Landau-damped.

[3]In chapter 4, I derive this growth rate from a more general result which allows for a broadband laser electric field with an arbitrary power spectrum. A standard derivation can also be provided by ignoring the ion terms in (3.48) and (3.50) assuming a plane wave electromagnetic mode.

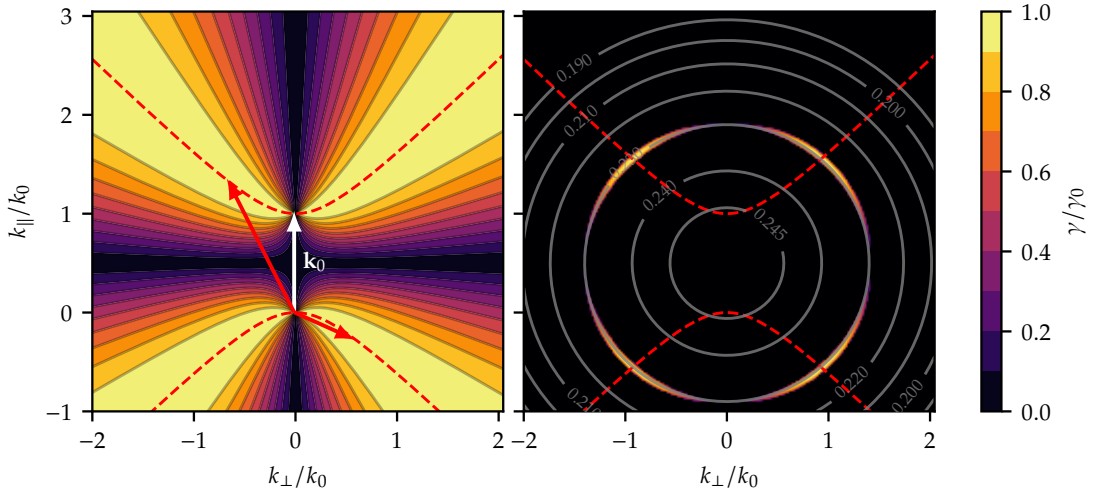


Figure 2.1: Plot of the TPD growth rate $\gamma_{0\mathbf{k}}$ overlaid with the wave-vector diagram showing the laser wave vector $\mathbf{k}_0$ in white, together with the two Langmuir wave vectors in red (left panel). The red dashed hyperbolas satisfy $k_\perp^2 = k_\parallel\left(k_\parallel - k_0\right)$, and are the locations along which the growth rate is maximised. The normalisation is $\gamma_0 = k_0 v_{\mathrm{os}}/4$.

The growth rate $\gamma_{0\mathbf{k}}$ is shown in the left panel of figure 2.1. The dimensionless factor inside of the absolute value operator in (2.5) has a maximum value of 1 which it attains on two hyperbolas satisfying $k_\perp^2 = k_\parallel(k_\parallel - k_0)$. Here the perpendicular and parallel directions are in reference to the wave vector $\mathbf{k}_0$, and so $k_\parallel = \mathbf{k}\cdot\mathbf{k}_0/k_0$ and $k_\perp = \mathbf{k}\cdot\mathbf{e}_0$.

The frequency matching condition implies that at a given plasma density (and hence a given ω_{pe}) the magnitude of the allowed resonant wave numbers k and p is rather narrow. This is illustrated in the right panel of figure 2.1 which is a plot of:

$$\gamma_{0\mathbf{k}}\delta(\omega_0 - \omega_{\mathbf{k}} - \omega_{\mathbf{p}}) \tag{2.7}$$

for $n_e = 0.23 n_c$, and the delta function is understood as a Lorentzian of width $\gamma_{0\mathbf{k}}$ (i.e. the instability resonance). Each density defines a circle in k-space for which the resonance condition is satisfied. These circles are given by:

$$\left(\frac{k_\perp}{k_0}\right)^2 + \left(\frac{k_\parallel}{k_0} - \frac{1}{2}\right)^2 = \frac{c^2}{12 v_{\mathrm{the}}^2}\frac{1 - 4n_e/n_c}{1 - n_e/n_c} - \frac{1}{4}. \tag{2.8}$$

A number of them are shown in figure 2.1 for $T_e = 2\,\mathrm{keV}$. The Landau cut-off $k\lambda_{\mathrm{De}} = 0.3$ is near the $n_e/n_c = 0.21$ circle. The implication is that at each point along the density gradient, TPD excites Langmuir waves of quite specific scale – at lower densities, one needs higher wave numbers in order to frequency match to the laser. As $n_e \to n_c/4$ the wave number of one of the Langmuir modes tends to vanish: $\mathbf{k} \to \mathbf{0}$ and $\mathbf{p} \to \mathbf{k}_0$. As we shall see in chapter 4, this will change under a broadband laser.

The presence of the density gradient has the important consequence that waves born at a given location along it, will tend to convect out of resonance, and hence only achieve a finite amount of amplification. Modes generated at lower densities have higher group velocities and have this convective character. This is to be contrasted with absolute modes, which have small k, and are generated very near the quarter-critical (Simon *et al.*, 1983; Yan *et al.*, 2010; Myatt *et al.*, 2014). There exists a threshold intensity for the excitation of absolute modes which is approximately given by (Vu *et al.*, 2012*a*):

$$I_{\mathrm{thr},14} = \frac{230\, T_{e,\mathrm{keV}}}{L_{n,\mu\mathrm{m}}}, \tag{2.9}$$

with the threshold intensity $I_{\mathrm{thr},14}$ being in units of $10^{14}\,\mathrm{W/cm^2}$, the temperature in keV, and $L_{n,\mu\mathrm{m}}$ is the density scale length at the quarter-critical in microns. Once this threshold is exceeded, and absolute modes excited, their saturation can only come from non-linear mechanisms, resulting in a state of Langmuir turbulence (Kline *et al.*, 2006). Strong Langmuir turbulence dominated by Langmuir collapse has been unambiguously observed in both Zakharov and particle-in-cell simulations of the saturated state of the two-plasmon decay instability (Vu *et al.*, 2012*a*,*b*, 2014; Myatt *et al.*, 2013, 2014).

2.2 Plasma turbulence in the direct-interaction approximation

2.2.1 Wave propagation in a turbulent medium

I have explained how one of the central problems tackled in this thesis is that of the modification of the TPD instability due to the turbulence it itself has excited. With TPD being a wave-wave coupling, in order to quantitatively address this issue, we need a way of studying wave propagation in a turbulent medium.

How does one study wave propagation in a non-turbulent medium? The usual procedure by which one finds the linear waves supported by a plasma, is to start with some equilibrium background, perturb around it, and study the evolution of those perturbations (Nicholson, 1983). These linear wave solutions then obey[4]:

$$\varphi(t,\mathbf{x}) = \varphi_0 e^{-\mathrm{i}\omega_{\mathbf{k}} t + \mathrm{i}\mathbf{k}\cdot\mathbf{x}} + \text{c.c.} \tag{2.10}$$

where the wave frequency $\omega_{\mathbf{k}}$ is obtained by solving for the zeros of the dispersion function $D_{\mathbf{k}}(\omega)$ derived from the underlying equation governing φ. Consider a system in which many of these modes are excited:

$$\varphi(t,\mathbf{x}) = \sum_{\mathbf{k}} \varphi_{\mathbf{k}} e^{-\mathrm{i}\omega_{\mathbf{k}} t + \mathrm{i}\mathbf{k}\cdot\mathbf{x}} = \sum_{\mathbf{k}} \varphi_{\mathbf{k}}(t) e^{\mathrm{i}\mathbf{k}\cdot\mathbf{x}}. \tag{2.11}$$

[4] I follow the Fourier conventions of Krommes (1984) and Krommes (2002) where quantities are assumed to be periodic inside a finite box and spatial Fourier modes are discrete.

If the Fourier amplitudes $\varphi_{\mathbf{k}}$ evolve under the linearised equations of motion:

$$\left(\frac{\partial}{\partial t} + \mathrm{i}\omega_{\mathbf{k}}\right)\varphi_{\mathbf{k}}(t) = 0, \tag{2.12}$$

nothing really interesting happens – each mode evolves independently of the others. But as amplitudes are increased, we will need to consider non-linearities in the governing equations leading to the amplitudes obeying:

$$\left(\frac{\partial}{\partial t} + \mathrm{i}\omega_{\mathbf{k}}\right)\varphi_{\mathbf{k}}(t) = \sum_{\Delta} M_{\mathbf{kpq}}\,\varphi^*_{\mathbf{p}}(t)\,\varphi^*_{\mathbf{q}}(t), \tag{2.13}$$

where $\sum_{\Delta}$ denotes a sum over wave numbers $\mathbf{p}$ and $\mathbf{q}$ which satisfy $\mathbf{k}+\mathbf{p}+\mathbf{q} = \mathbf{0}$; $M_{\mathbf{kpq}}$ are the mode-coupling coefficients which are generally functions of wave number[5], and I have assumed that the field is real, thus $\varphi_{\mathbf{k}}(t) = [\varphi_{-\mathbf{k}}(t)]^*$. If there were only three modes in the system: $\mathbf{k}$, $\mathbf{p}$ and $\mathbf{q}$, the above reduces to the familiar three wave coupled mode equations:

$$\left(\frac{\partial}{\partial t} + \mathrm{i}\omega_{\mathbf{k}}\right)\varphi_{\mathbf{k}}(t) = M_{\mathbf{kpq}}\,\varphi^*_{\mathbf{p}}(t)\,\varphi^*_{\mathbf{q}}(t), \tag{2.14}$$

$$\left(\frac{\partial}{\partial t} + \mathrm{i}\omega_{\mathbf{q}}\right)\varphi_{\mathbf{q}}(t) = M_{\mathbf{qkp}}\,\varphi^*_{\mathbf{k}}(t)\,\varphi^*_{\mathbf{p}}(t) \tag{2.15}$$

$$\left(\frac{\partial}{\partial t} + \mathrm{i}\omega_{\mathbf{p}}\right)\varphi_{\mathbf{p}}(t) = M_{\mathbf{pqk}}\,\varphi^*_{\mathbf{q}}(t)\,\varphi^*_{\mathbf{k}}(t), \tag{2.16}$$

which typically represent *coherent* interactions between the three modes, and are ubiquitous in the study of laser-plasma instabilities. In that context, the effect of the non-linearity is to introduce some small imaginary correction to the dispersion function leading to the slow damping or growth of the amplitude of a given mode:

$$D_{\mathbf{k}}(\omega) = -\mathrm{i}\omega + \mathrm{i}\omega_{\mathbf{k}} \quad \longrightarrow \quad D_{\mathbf{k}}(\omega) = -\mathrm{i}\omega + \mathrm{i}\omega_{\mathbf{k}} + \gamma_{\mathbf{k}}. \tag{2.17}$$

The nature of the system can turn from coherent to stochastic, i.e. turbulent, in the presence of a large number of modes. The sum in the non-linear term represents interactions between mode $\mathbf{k}$ and the rest of the modes in the system. Even for small non-linearity, this may cause the rapid decoherence between the modal phases – an

[5]For example consider the ion non-linearity appearing in one of the Zakharov equations (see section 2.3 and 3.2). After a Fourier transformation in $\mathbf{x}$ and using the convolution theorem $[A(\mathbf{x})B(\mathbf{x})]_{\mathbf{k}} = \sum_{\mathbf{q}} A_{\mathbf{k}-\mathbf{q}} B_{\mathbf{q}}$, we have:

$$\boldsymbol{\nabla}\cdot[n(\mathbf{x})\boldsymbol{\nabla}\psi(\mathbf{x})] \xrightarrow{\mathrm{FT}} -\sum_{\mathbf{p},\mathbf{q}} \delta_{\mathbf{k},\mathbf{p}+\mathbf{q}}\,(\mathbf{k}\cdot\mathbf{q})\,n_{\mathbf{p}}\psi_{\mathbf{q}}.$$

For real fields this can be written as:

$$\sum_{\Delta} (\mathbf{k}\cdot\mathbf{q})\,n^*_{\mathbf{p}}\psi^*_{\mathbf{q}},$$

leading to $M_{\mathbf{kpq}} = (\mathbf{k}\cdot\mathbf{q})$.

example of phase mixing – and thus allow for (or even demand) a statistical description[6]. The situation remains mostly similar to before, except now one generally focuses on the evolution of the spectra of the fluctuations:

$$C_{\mathbf{k}} = \overline{|\varphi_{\mathbf{k}}|^2}. \tag{2.18}$$

The over-line represents an ensemble average, or a suitable time average (e.g. over the fast oscillations of the waves), and the amplitudes $\varphi_{\mathbf{k}}$ are assumed to be random quantities with zero mean $\overline{\varphi_{\mathbf{k}}} = 0$. Again, if the non-linearity is weak, its effect on the spectra will amount to a slow growth or damping at each $\mathbf{k}$ – i.e. energy is shuffled around the system by the non-linearity, but the waves present in it are still the linear waves. This can be made more concrete if we write for the spectrum (also referred to as the *covariance*):

$$C_{\mathbf{k}}(t, t') = \overline{\varphi_{\mathbf{k}}(t)\varphi^*_{\mathbf{k}}(t')}, \tag{2.19}$$

and assume that the Fourier amplitudes evolve as:

$$\varphi_{\mathbf{k}}(t) = \widehat{\varphi}_{\mathbf{k}}(t)\, e^{-\mathrm{i}\omega_{\mathbf{k}} t}, \tag{2.20}$$

with $\widehat{\varphi}_{\mathbf{k}}(t)$ being some slowly evolving amplitude of the linear mode $\omega_{\mathbf{k}}$. Then, we can write the covariance in a way in which we can clearly separate out its variation on the slow, and fast time scales:

$$C_{\mathbf{k}}(T|\tau) = C_{\mathbf{k}}(T) e^{-\mathrm{i}\omega_{\mathbf{k}}\tau}. \tag{2.21}$$

Here $C_{\mathbf{k}}(T|\tau)$ is just the covariance reexpressed in terms of the centre time $T = (t + t')/2$, which represents the slow evolution; and the difference $\tau = t - t'$, which represents the fast evolution:

$$C_{\mathbf{k}}(T|\tau) \equiv C_{\mathbf{k}}\left(T + \tau/2, T - \tau/2\right). \tag{2.22}$$

A Fourier transformation in τ:

$$C_{\mathbf{k}}(T|\omega) = C_{\mathbf{k}}(T)\, \delta(\omega - \omega_{\mathbf{k}}), \tag{2.23}$$

shows a slowly-evolving frequency spectrum at each $\mathbf{k}$ which is delta-shaped at the linear frequency $\omega_{\mathbf{k}}$. This picture of linear waves, whose spectra are slowly modulated due to the non-linearity, is weak-turbulence theory (Kadomtsev, 1965; Sagdeev & Galeev, 1969; Tsytovich, 1970; Schekochihin, 2026). The equation governing $C_{\mathbf{k}}(T)$ is referred to as the *wave kinetic equation*.

[6] Stochasticity criteria for this system have been given by Zaslavskii & Sagdeev (1967).

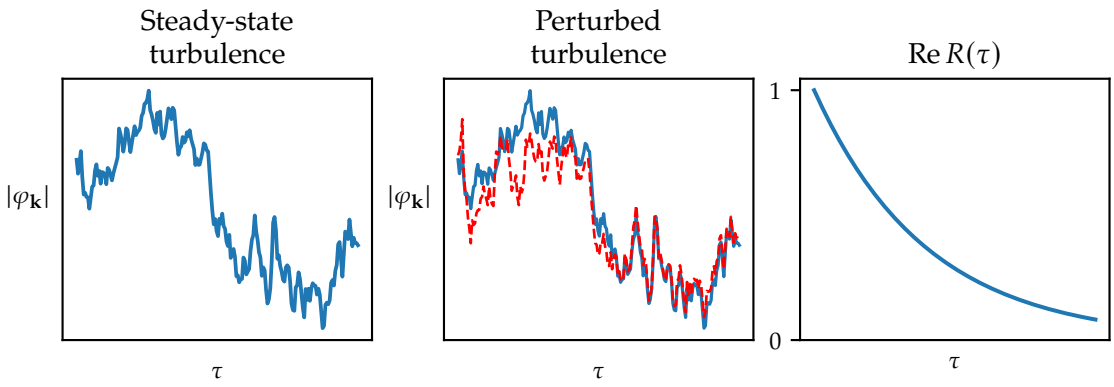


Figure 2.2: Perturbations of the turbulent medium. For a steady-state to exist, the response R must be a decaying function of time.

As wave amplitudes are increased even further, we can expect the non-linearity to start modifying the properties of the "linear waves" as well. This is the strongly turbulent regime. We saw in (2.17) that for weak non-linearity we get some small correction to the dispersion function. The generalisation of this in a strongly turbulent system is to introduce the turbulent corrections $\Sigma_{\mathbf{k}}(\omega)$:

$$D_{\mathbf{k}}(\omega) \quad \longrightarrow \quad \mathscr{D}_{\mathbf{k}}(\omega) = D_{\mathbf{k}}(\omega) + \Sigma_{\mathbf{k}}(\omega), \tag{2.24}$$

which are now comparable in magnitude to the terms in the linear $D_{\mathbf{k}}(\omega)$, and which we expect to be functionals of the fluctuation spectrum, as well as the modified dispersion function $\Sigma[C, \mathscr{D}]$.

$\mathscr{D}_{\mathbf{k}}(\omega)$ describes how perturbations of the turbulent medium evolve. This is illustrated in figure 2.2. It is useful to shift focus from the dispersion function, to what is referred to as the *response* function. This is the Green's function for the differential equation satisfied by the field, and is what propagates forward in time any perturbation in the system.

Consider first the response of the amplitudes in the absence of non-linearity:

$$\left(\frac{\partial}{\partial t} + \mathrm{i}\omega_{\mathbf{k}}\right) \varphi_{\mathbf{k}}(t) = s_{\mathbf{k}}(t), \tag{2.25}$$

which we may investigate by adding an infinitesimal source $s_{\mathbf{k}}$ to the equation. The response $R_{\mathbf{k}}(t; t')$ is then defined as:

$$R_{\mathbf{k}}(t; t') = \left.\frac{\delta \varphi_{\mathbf{k}}(t)}{\delta s_{\mathbf{k}}(t')}\right|_{s=0}, \tag{2.26}$$

and satisfies:

$$\left(\frac{\partial}{\partial t} + \mathrm{i}\omega_{\mathbf{k}}\right) R_{\mathbf{k}}(t; t') = \delta(t - t'), \tag{2.27}$$

which follows directly from taking the functional derivative $\boldsymbol{\delta}/\boldsymbol{\delta}s_{\mathbf{k}}(t')$ of (2.25), and noting that $\boldsymbol{\delta}s_{\mathbf{k}}(t)/\boldsymbol{\delta}s_{\mathbf{k}}(t') = \delta(t-t')$. The semi-colon represents the causality condition $R_{\mathbf{k}}(t;t') = 0$ for $t' > t$; the bold-face $\boldsymbol{\delta}$ stands for the functional derivative. In a steady state, we can set $\tau = t - t'$, and Fourier transform:

$$(-\mathrm{i}\omega + \mathrm{i}\omega_{\mathbf{k}})\, R_{\mathbf{k}}(\omega) = 1, \tag{2.28}$$

and we see that the response is simply related to the dispersion function through $[R_{\mathbf{k}}(\omega)]^{-1} = D_{\mathbf{k}}(\omega)$. The solution of (2.27) is:

$$R_{\mathbf{k}}(t;t') = H(t-t')\, e^{-\mathrm{i}\omega_{\mathbf{k}}(t-t')}, \tag{2.29}$$

with the Heaviside step function being $H(t) = 1$ for $t > 0$ and zero otherwise. If $\varphi_{\mathbf{k}}(t)$ evolves from an initial condition of $\varphi_{\mathbf{k}}(t_0)$ at $t = t_0$, we have that:

$$\varphi_{\mathbf{k}}(t) = \varphi_{\mathbf{k}}(t_0)\, R_{\mathbf{k}}(t;t_0). \tag{2.30}$$

Turning now to the turbulent case, we can carry out a similar procedure. Since the amplitudes $\varphi_{\mathbf{k}}$ are considered random, we will need to make a distinction between the exact random response $\tilde{R}$, and its average $R = \overline{\tilde{R}}$. Adding a source to (2.13) and taking the functional derivative with respect to it, we have:

$$\left(\frac{\partial}{\partial t} + \mathrm{i}\omega_{\mathbf{k}}\right)\overline{\tilde{R}}_{\mathbf{k}}(t;t') - \sum_{\Delta} M_{\mathbf{kpq}}\, \frac{\boldsymbol{\delta}}{\boldsymbol{\delta}s_{\mathbf{k}}(t')}\left[\overline{\varphi^*_{\mathbf{p}}(t)\,\varphi^*_{\mathbf{q}}(t)}\right] = \delta(t-t'). \tag{2.31}$$

The turbulent correction Σ to the dispersion function will eventually emerge from approximating this new term due to the non-linearity. Note that it contains a quantity quadratic in the field, which may easily be represented in terms of the covariance of the fluctuations (the spectrum) $C_{\mathbf{k}}(t,t')$, and we are enquiring about its response to the source. This should hopefully make it apparent why Σ is expected to be functionally dependent on both the spectrum and the new response.

We are inevitably faced with the closure problem. If we derive an equation for the covariance (quadratic in the field), the non-linearity will necessarily introduce terms which will be cubic, then quartic, and so on:

$$\overline{\varphi\varphi} \leftarrow \overline{\varphi\varphi\varphi} \leftarrow \overline{\varphi\varphi\varphi\varphi} \leftarrow \dots \tag{2.32}$$

The goal of statistical closure is not to merely truncate the hierarchy, but to express higher order moments in terms of lower order ones in a self-consistent manner. One such closure is the direct-interaction approximation (DIA) first put forward by Robert Kraichnan for fluid turbulence (Kraichnan, 1959). The DIA provides a particular form for Σ.

Before moving on to describing a derivation of the DIA, it is worth mentioning that the problem of wave propagation in a turbulent medium which I have just outlined, is highly analogous to problems concerning *renormalisation* in quantum field theory (QFT). The propagators in QFT are akin to the dispersion functions describing classical waves, and mass renormalisation is the procedure which introduces a quantity called the self-energy in those propagators – analogous to the turbulent corrections. The self-energies describe the interactions of the bare particles with the background of quantum fluctuations, which plays the role of the turbulent background. There is a highly systematic procedure translating QFT techniques to classical systems known as the Martin, Siggia, Rose (MSR) formalism (Martin *et al.*, 1973). The DIA is the lowest-order approximation in an expansion in a quantity which measures the deviation away from Gaussianity of the statistical fluctuations. On the subject of applying formal statistical closure methods to plasma turbulence, the following references have been particularly useful: Krommes (2015, 2002, 1984); Diamond *et al.* (2010); Bowman (1992); Bowman *et al.* (1993).

2.2.2 Derivation of the DIA

This section presents a heuristic derivation of the direct-interaction approximation. The approach takes inspiration from DuBois & Espedal (1978) and Krommes (2015), as it helps make a few important points about the DIA rather clear. These are:

- the procedure is coordinate-free – it does not depend on the choice of variables.

  This will become important since for the TPD problem, there are many fields coupled together through multiple equations, and this can be handled by introducing an additional field species index variable on which some generalised field depends.

- The DIA assumes that the statistics of the fluctuations are nearly Gaussian, which has implications for the physical content of the model.

- It also shows how the DIA's principle approximation is one of ignoring the vertex corrections of the general MSR formalism.

Consider quadratically non-linear systems of the form:

$$\partial_{t_1}\varphi_1 = L_{12}\varphi_2 + \tfrac{1}{2}M_{123}\varphi_2\varphi_3. \tag{2.33}$$

This is a generalised version of (2.13). The subscripts refer to generalised indices which may contain any number of continuous or discrete variables needed to describe the problem. For example $1 \equiv (t_1, \mathbf{x}_1)$ for a single field which is a function of space and time only:

$\varphi(t, \mathbf{x})$. Multiple fields (or components of a vector field) may be represented by a discrete variable index so that $1 \equiv (t_1, \mathbf{x}_1, \sigma_1)$. Repeated indices imply a summation-integration convention, with sums corresponding to the discrete ones, and integration corresponding to continuous ones. To illustrate how the notation works, consider a prototype equation designed to mimic the first of the Zakharov equations in form (see section 2.3):

$$\left(\partial_t - \nabla^2\right) \psi = \boldsymbol{\nabla} \cdot (n \boldsymbol{\nabla} \psi) \,. \tag{2.34}$$

This equation can be written in the general form of (2.33) by identifying the following coefficients. For the linear term we have:

$$L_{12} \equiv L^{\sigma_1 \sigma_2}(t_1, \mathbf{x}_1, t_2, \mathbf{x}_2), \tag{2.35}$$

which for $\sigma_1 = \psi$ implies $L^{\psi n} = 0$ (no terms linear in n in the equation for $\partial_t \psi$), and:

$$L^{\psi\psi} = \nabla^2_{\mathbf{x}_1} \delta(\mathbf{x}_1 - \mathbf{x}_2) \delta(t_1 - t_2). \tag{2.36}$$

The $\sigma_1 = \psi$ component of $L_{12}\varphi_2$ can be written out explicitly as:

$$[L_{12}\varphi_2](t_1, \mathbf{x}_1, \sigma_1 = \psi) = \sum_{\sigma_2} \int \mathrm{d}t_2 \mathrm{d}\mathbf{x}_2 \; L^{\psi\sigma_2}(t_1, \mathbf{x}_1, t_2, \mathbf{x}_2) \, \varphi^{\sigma_2}(t_2, \mathbf{x}_2) \tag{2.37}$$

$$= \int \mathrm{d}t_2 \mathrm{d}\mathbf{x}_2 \; \nabla^2_{\mathbf{x}_1} \delta(\mathbf{x}_1 - \mathbf{x}_2) \delta(t_1 - t_2) \, \psi(t_2, \mathbf{x}_2) \tag{2.38}$$

$$= \nabla^2_{\mathbf{x}_1} \psi(t_1, \mathbf{x}_1). \tag{2.39}$$

In a similar fashion, the couplings for the non-linear terms:

$$M_{123} \equiv M^{\sigma_1 \sigma_2 \sigma_3}(t_1, \mathbf{x}_1, t_2, \mathbf{x}_2, t_3, \mathbf{x}_3), \tag{2.40}$$

are given by:

$$M^{\psi n \psi} = \tfrac{1}{2} \boldsymbol{\nabla}_{\mathbf{x}_1} \cdot \boldsymbol{\nabla}_{\mathbf{x}_3} \, \delta(\mathbf{x}_1 - \mathbf{x}_2) \delta(\mathbf{x}_1 - \mathbf{x}_3) \delta(t_1 - t_2) \delta(t_1 - t_3), \tag{2.41}$$

$$M^{\psi \psi n} = \tfrac{1}{2} \boldsymbol{\nabla}_{\mathbf{x}_1} \cdot \boldsymbol{\nabla}_{\mathbf{x}_2} \, \delta(\mathbf{x}_1 - \mathbf{x}_2) \delta(\mathbf{x}_1 - \mathbf{x}_3) \delta(t_1 - t_2) \delta(t_1 - t_3). \tag{2.42}$$

The couplings are symmetric in the second two indices: $M_{123} = M_{132}$. As a final note: an evolution equation for n would provide the $L^{n\sigma_2}$ and $M^{n\sigma_2\sigma_3}$ coefficients for a self-consistent description of the problem. Otherwise the quantity n would need to be prescribed.

Consider then the random response $\tilde{R}_{11'} \doteq \boldsymbol{\delta}\varphi_1 / \boldsymbol{\delta} s_{1'}$ of the system to an infinitesimal source s_1 added to it:

$$\partial_{t_1} \varphi_1 = L_{12}\varphi_2 + \tfrac{1}{2} M_{123} \varphi_2 \varphi_3 + s_1. \tag{2.43}$$

Upon taking the functional derivative of the equation:

$$\frac{\boldsymbol{\delta}}{\boldsymbol{\delta} s_{1'}}\dot{\varphi}_1 = L_{12}\frac{\boldsymbol{\delta}\varphi_2}{\boldsymbol{\delta} s_{1'}} + \tfrac{1}{2}M_{123}\frac{\boldsymbol{\delta}}{\boldsymbol{\delta} s_{1'}}[\varphi_2\varphi_3] + \frac{\boldsymbol{\delta} s_1}{\boldsymbol{\delta} s_{1'}}, \tag{2.44}$$

and after ensemble averaging, we get an equation for $R_{11'} \doteq \overline{\tilde{R}_{11'}}$:

$$\dot{R}_{11'} - L_{12}R_{21'} + \Sigma_{12}R_{21'} = \delta_{11'}, \tag{2.45}$$

where we have introduced the turbulent corrections (or self-energies) Σ which are the objects describing how the time evolution (propagation) of fluctuations is modified in a turbulent system:

$$\Sigma_{12} \doteq \tfrac{1}{2}M_{134}R^{-1}_{2'2}\frac{\boldsymbol{\delta}}{\boldsymbol{\delta} s_{2'}}C_{34}. \tag{2.46}$$

Here R^{-1}_{12} is an operator, the inverse of the response function, which satisfies:

$$R^{-1}_{12}R_{21'} = \delta_{11'}, \tag{2.47}$$

and is explicitly given by:

$$R^{-1}_{12} = \delta_{12}\partial_{t_2} - L_{12} + \Sigma_{12}. \tag{2.48}$$

$C_{12} \doteq \overline{\varphi_1\varphi_2}$ is the covariance of the fluctuations. I shall also define the random version of this quantity $\tilde{C}_{12} \doteq \varphi_1\varphi_2$, and I will assume that there are no mean fields $\overline{\varphi}_1 = 0$.

In order to get an equation for the covariances C_{12} on which the self-energies Σ_{12} depend, consider writing the original equation in a form in which the fluctuations appear to be propagated forward in time not by the exact response, but by the averaged one:

$$\left(\delta_{12}\partial_{t_2} - L_{12} + \Sigma_{12}\right)\varphi_2 = \tfrac{1}{2}M_{123}\varphi_2\varphi_3, \tag{2.49}$$

and assume that the couplings M are unmodified. The so-called vertex corrections of the general MSR formalism involve "renormalisations" of the couplings M in addition to the renormalisation of the response by addition of the self-energy. The DIA ignores vertex corrections and keeps the couplings M unchanged. Then:

$$R^{-1}_{12}R^{-1}_{1'2'}\tilde{C}_{22'} = \tfrac{1}{4}M_{123}M_{1'2'3'}\tilde{C}_{23}\tilde{C}_{2'3'}. \tag{2.50}$$

Upon averaging:

$$R^{-1}_{12}R^{-1}_{1'2'}C_{22'} = \tfrac{1}{4}M_{123}M_{1'2'3'}\overline{\tilde{C}_{23}\tilde{C}_{2'3'}}. \tag{2.51}$$

Due to the assumption that the fluctuations are close to Gaussian, the fourth order correlator is factored in the Gaussian way:

$$\overline{\tilde{C}_{23}\tilde{C}_{2'3'}} = \overbrace{\varphi_2\varphi_3}\overbrace{\varphi_{2'}\varphi_{3'}} + \overbrace{\varphi_2\varphi_3}\overbrace{\varphi_{2'}\varphi_{3'}} + \overbrace{\varphi_2\varphi_3}\overbrace{\varphi_{2'}\varphi_{3'}} \tag{2.52}$$

$$= C_{23}C_{2'3'} + C_{22'}C_{33'} + C_{23'}C_{2'3}, \tag{2.53}$$

to produce:

$$R_{12}^{-1}R_{1'2'}^{-1}C_{22'} = \tfrac{1}{4}M_{123}M_{1'2'3'}C_{23}C_{2'3'} + \tfrac{1}{4}M_{123}M_{1'2'3'}C_{22'}C_{33'} + \tfrac{1}{4}M_{123}M_{1'2'3'}C_{23'}C_{2'3}. \tag{2.54}$$

The requirement that the mean field is zero demands $M_{123}C_{23} = 0$, which can be seen by averaging (2.33). The other two terms are identical due to the symmetry $M_{123} = M_{132}$, which follows from the governing equation (2.33). Thus:

$$R_{12}^{-1}R_{1'2'}^{-1}C_{22'} = F_{11'}, \qquad F_{11'} = \tfrac{1}{2}M_{123}M_{1'2'3'}C_{22'}C_{33'}. \tag{2.55}$$

The quantity F is referred to as the non-linear noise source. Armed with an equation for C we can now calculate the self-energies (2.46). Taking the derivative of the above with respect to the source gives:

$$\frac{\boldsymbol{\delta} R_{12}^{-1}}{\boldsymbol{\delta} s_4}R_{1'2'}^{-1}C_{22'} + R_{12}^{-1}\frac{\boldsymbol{\delta} R_{1'2'}^{-1}}{\boldsymbol{\delta} s_4}C_{22'} + R_{12}^{-1}R_{1'2'}^{-1}\frac{\boldsymbol{\delta} C_{22'}}{\boldsymbol{\delta} s_4} = \frac{\boldsymbol{\delta} F_{11'}}{\boldsymbol{\delta} s_4}, \tag{2.56}$$

To compute the derivative of the inverse response, take its unaveraged form:

$$\underbrace{(\delta_{12}\partial_{t_2} - L_{12} - M_{123}\varphi_3)}_{\tilde{R}_{12}^{-1}}\tilde{R}_{21'} = \delta_{11'}, \tag{2.57}$$

from which it follows that:

$$\frac{\boldsymbol{\delta}\tilde{R}_{12}^{-1}}{\boldsymbol{\delta} s_4} = M_{123}\tilde{R}_{34}. \tag{2.58}$$

Upon averaging, the same relationship will hold for R^{-1} and R. Ignoring the contribution of $\boldsymbol{\delta}F/\boldsymbol{\delta}s$ to (2.56) and after a short calculation, the self-energy is:

$$\Sigma_{11'} = -M_{123}M_{2'3'1'}R_{22'}C_{33'}. \tag{2.59}$$

This completes the derivation. In summary, we now have a self-consistent description of the average response of the system $R_{11'}$, including the turbulent corrections (or self-energies) $\Sigma_{11'}$, and the covariances $C_{11'}$. For convenience, I give the DIA equations below[7]:

$$\dot{R}_{11'} - L_{12}R_{21'} + \Sigma_{12}R_{21'} = \delta_{11'}, \tag{2.60}$$

$$\dot{C}_{11'} - L_{12}C_{21'} + \Sigma_{12}C_{21'} = F_{12}R_{1'2}, \tag{2.61}$$

$$\Sigma_{11'} = -M_{123}M_{2'3'1'}R_{22'}C_{33'}, \tag{2.62}$$

$$F_{11'} = \tfrac{1}{2}M_{123}M_{1'2'3'}C_{22'}C_{33'}. \tag{2.63}$$

[7]The second equation (for the covariance) is obtained by acting with R on both sides of (2.55), and substituting the explicit form of R_{12}^{-1}, i.e. (2.48).

In the present derivation, the crucial step appears to be (2.49) whose interpretation is that the physical content of the DIA consists of modifying the response of the fluctuations (by way of renormalising R), but not the couplings M, thus ignoring the vertex corrections of the general MSR formalism.

2.2.3 Single-field DIA

In order to make more sense of the equations just derived, let us return to the particular case of a single real-valued field obeying (2.13). It would be especially useful to show the form of the turbulent correction mentioned in (2.24). I will assume statistical homogeneity, under which all functions of the form $F(\mathbf{x}, \mathbf{x}')$ depend only on the difference $\mathbf{x} - \mathbf{x}'$. The general set of equations (2.60-2.63) reduces to the following[8]:

$$(\partial_t + \mathrm{i}\omega_{\mathbf{k}})\, R_{\mathbf{k}}(t;t') + \int_{t'}^{t} \mathrm{d}\bar{t}\; \Sigma_{\mathbf{k}}(t;\bar{t})\, R_{\mathbf{k}}(\bar{t};t') = \delta(t-t'), \tag{2.64}$$

$$(\partial_t + \mathrm{i}\omega_{\mathbf{k}})\, C_{\mathbf{k}}(t,t') + \int_{0}^{t} \mathrm{d}\bar{t}\; \Sigma_{\mathbf{k}}(t;\bar{t})\, C_{\mathbf{k}}(\bar{t},t') = \int_{0}^{t} \mathrm{d}\bar{t}\; F_{\mathbf{k}}(t,\bar{t})\, R^*_{\mathbf{k}}(t';\bar{t}), \tag{2.65}$$

with the self-energy Σ, and the non-linear noise source F being:

$$\Sigma_{\mathbf{k}}(t;t') = -\sum_{\Delta} M_{\mathbf{kpq}} M^*_{\mathbf{pqk}}\, R^*_{\mathbf{p}}(t;t')\, C^*_{\mathbf{q}}(t,t'), \tag{2.66}$$

$$F_{\mathbf{k}}(t,t') = \frac{1}{2}\sum_{\Delta} |M_{\mathbf{kpq}}|^2\, C^*_{\mathbf{p}}(t,t')\, C^*_{\mathbf{q}}(t,t'). \tag{2.67}$$

The lower bound on the integral in (2.65) is due to an initial condition at $t = 0$. In a steady state, all functions of time will depend only on the difference $\tau = t - t'$:

$$R_{\mathbf{k}}(t;t') = R_{\mathbf{k}}(t-t'), \quad C_{\mathbf{k}}(t,t') = C_{\mathbf{k}}(t-t'). \tag{2.68}$$

Thus (2.64) becomes:

$$(\partial_\tau + \mathrm{i}\omega_{\mathbf{k}})\, R_{\mathbf{k}}(\tau) + \int_{0}^{\tau} \mathrm{d}\overline{\tau}\; \Sigma_{\mathbf{k}}(\tau - \overline{\tau})\, R_{\mathbf{k}}(\overline{\tau}) = \delta(\tau). \tag{2.69}$$

A Laplace transformation in τ gives:

$$[-\mathrm{i}\omega + \mathrm{i}\omega_{\mathbf{k}} + \Sigma_{\mathbf{k}}(\omega)]\, R_{\mathbf{k}}(\omega) = 1. \tag{2.70}$$

And so we see that the equation for the response (2.64) is essentially a statement of (2.24) where:

$$\mathscr{D}_{\mathbf{k}}(\omega) = [R_{\mathbf{k}}(\omega)]^{-1}, \qquad \mathscr{D}_{\mathbf{k}}(\omega) = -\mathrm{i}\omega + \mathrm{i}\omega_{\mathbf{k}} + \Sigma_{\mathbf{k}}(\omega). \tag{2.70a,b}$$

[8] In appendix B.2 the statistically homogeneous DIA equations are derived for *multiple* fields. They are reduced to the present equations by further assuming diagonality in the field species index, and using the fact that the field is real. See also section 3.3.1.

The same procedure applied to (2.66) gives:

$$\Sigma_{\mathbf{k}}(\omega) = -\int \mathrm{d}\omega' \sum_{\Delta} M_{\mathbf{kpq}} M^*_{\mathbf{pqk}}\, R^*_{\mathbf{p}}(\omega')\, C^*_{\mathbf{q}}(\omega-\omega') \tag{2.71}$$

$$= -\int \mathrm{d}\omega' \sum_{\Delta} M_{\mathbf{kpq}} M^*_{\mathbf{pqk}}\, \frac{C^*_{\mathbf{q}}(\omega-\omega')}{\mathscr{D}^*_{\mathbf{p}}(\omega')} \tag{2.72}$$

$$= -\int \mathrm{d}\omega' \sum_{\Delta} M_{\mathbf{kpq}} M^*_{\mathbf{pqk}}\, \frac{C^*_{\mathbf{q}}(\omega-\omega')}{D^*_{\mathbf{p}}(\omega') + \Sigma^*_{\mathbf{p}}(\omega')}. \tag{2.73}$$

A couple of important things to note here are that: i. we see that the effect of the turbulent correction is to renormalise the resonance in (2.73) and that Σ is functionally dependent on itself; ii. the DIA equations reduce to the weak turbulence approximation by ignoring Σ in the denominator on the right-hand side of (2.73) which overall leads to a small correction to the dispersion representing the weak-turbulence growth/damping rates[9]. These corrections are computed with the *linear, unperturbed* dispersion functions.

The meaning of the covariance equation (2.65) is best elucidated in parallel with the procedure which will allow me to define the important concept of the *triad interaction time*, which will be crucial for the TPD problem. So I move on to that task.

2.2.4 Markovianisation

The DIA is a closure which evidently involves time history. Markovian closures are statistical closures involving only equal-time quantities. It is possible to construct a Markovianisation procedure for the DIA which will package up all of the time history into a quantity referred to as the *triad interaction time* (Bowman, 1992; Bowman *et al.*, 1993) and which will be integral to the physical interpretation of the influence of the turbulence on TPD.

Suppose we wished to derive an evolution equation for the equal time covariance:

$$C_{\mathbf{k}}(t) \doteq C_{\mathbf{k}}(t,t')|_{t'=t}\,. \tag{2.74}$$

The covariance is Hermitian:

$$C_{\mathbf{k}}(t,t') = \overline{\varphi_{\mathbf{k}}(t)\,\varphi^*_{\mathbf{k}}(t')} \quad \Longrightarrow \quad C_{\mathbf{k}}(t',t) = [C_{\mathbf{k}}(t,t')]^*\,, \tag{2.75}$$

which means we can write:

$$\partial_t C_{\mathbf{k}}(t) = \partial_t C_{\mathbf{k}}(t,t')|_{t'=t} + \partial_t C_{\mathbf{k}}(t',t)|_{t'=t} \tag{2.76}$$

$$= \partial_t C_{\mathbf{k}}(t,t')|_{t'=t} + \partial_t C^*_{\mathbf{k}}(t,t')\big|_{t'=t} \tag{2.77}$$

$$= 2\,\mathrm{Re}\;\partial_t C_{\mathbf{k}}(t,t')|_{t'=t}\,. \tag{2.78}$$

[9] For Langmuir turbulence this is shown in DuBois & Rose (1981).

Using (2.65):

$$\partial_t C_{\mathbf{k}}(t) = 2\gamma^{\text{lin}}_{\mathbf{k}} C_{\mathbf{k}}(t) + 2\,\text{Re}\int_0^t \mathrm{d}\bar{t}\,\left[F_{\mathbf{k}}(t,\bar{t})\,R^*_{\mathbf{k}}(t;\bar{t}) - \Sigma_{\mathbf{k}}(t;\bar{t})\,C^*_{\mathbf{k}}(t,\bar{t})\right]. \tag{2.79}$$

With $\gamma^{\text{lin}}_{\mathbf{k}} = \text{Im}\,\omega_{\mathbf{k}}$ I have assumed that the linear modes may contain some linear growth rate injecting energy into the system[10]. One of the key steps behind the Markovianisation procedure is to attempt to simplify the time dependence of the quantities involved. In general the response $R(t;t')$ and the covariance $C(t,t')$ can evolve in time independently, but it is not unreasonable to expect their time dependence to be closely related. In fact, in thermal equilibrium they are identical:

$$C_{\mathbf{k}}(t,t') = C_{\mathbf{k}}(t)\,R_{\mathbf{k}}(t;t'), \tag{2.80}$$

and Bowman *et al.* (1993) argue that this is not a poor approximation for turbulent systems out of equilibrium as well. Equation (2.80) is referred to as a fluctuation-dissipation ansatz. Applying it to (2.79), the two terms are:

$$\text{Re}\int_0^t \mathrm{d}\bar{t}\,F_{\mathbf{k}}(t,\bar{t})\,R^*_{\mathbf{k}}(t;\bar{t}) = \frac{1}{2}\sum_{\Delta}|M_{\mathbf{kpq}}|^2\,\text{Re}\int_0^t \mathrm{d}\bar{t}\;C^*_{\mathbf{p}}(t,\bar{t})\,C^*_{\mathbf{q}}(t,\bar{t})\,R^*_{\mathbf{k}}(t;\bar{t}) \tag{2.81}$$

$$= \frac{1}{2}\sum_{\Delta}|M_{\mathbf{kpq}}|^2\,C_{\mathbf{p}}(t)\,C_{\mathbf{q}}(t)\,\text{Re}\int_0^t \mathrm{d}\bar{t}\;R^*_{\mathbf{k}}(t;\bar{t})\,R^*_{\mathbf{p}}(t;\bar{t})\,R^*_{\mathbf{q}}(t;\bar{t}) \tag{2.82}$$

$$= \frac{1}{2}\sum_{\Delta}|M_{\mathbf{kpq}}|^2\,\text{Re}\left[\theta^*_{\mathbf{kpq}}(t)\right]\;C_{\mathbf{p}}(t)\,C_{\mathbf{q}}(t), \tag{2.83}$$

$$\doteq F_{\mathbf{k}}(t), \tag{2.84}$$

and

$$\text{Re}\int_0^t \mathrm{d}\bar{t}\,\Sigma_{\mathbf{k}}(t;\bar{t})\,C^*_{\mathbf{k}}(t,\bar{t}) = -\text{Re}\sum_{\Delta}M_{\mathbf{kpq}}M^*_{\mathbf{pqk}}\int_0^t \mathrm{d}\bar{t}\,R^*_{\mathbf{p}}(t;\bar{t})\,C^*_{\mathbf{q}}(t,\bar{t})\,C^*_{\mathbf{k}}(t,\bar{t}) \tag{2.85}$$

$$= -C_{\mathbf{k}}(t)\,\text{Re}\sum_{\Delta}M_{\mathbf{kpq}}M^*_{\mathbf{pqk}}C_{\mathbf{q}}(t)\int_0^t \mathrm{d}\bar{t}\;R^*_{\mathbf{k}}(t;\bar{t})\,R^*_{\mathbf{p}}(t;\bar{t})\,R^*_{\mathbf{q}}(t;\bar{t}) \tag{2.86}$$

$$= -C_{\mathbf{k}}(t)\,\text{Re}\sum_{\Delta}M_{\mathbf{kpq}}M^*_{\mathbf{pqk}}\,\theta^*_{\mathbf{kpq}}(t)\,C_{\mathbf{q}}(t) \tag{2.87}$$

$$\doteq -\text{Re}\,\eta_{\mathbf{k}}(t)\,C_{\mathbf{k}}(t). \tag{2.88}$$

And so the Markovian form of the equation for $C_{\mathbf{k}}(t)$ is:

$$\partial_t C_{\mathbf{k}}(t) = 2\gamma^{\text{lin}}_{\mathbf{k}} C_{\mathbf{k}}(t) - 2\,\text{Re}\,\eta_{\mathbf{k}}(t)\,C_{\mathbf{k}}(t) + 2F_{\mathbf{k}}(t), \tag{2.89}$$

[10] This is precisely the assumption I will *not* make in order to study the saturated TPD state. Prescribing $\gamma^{\text{lin}}_{\mathbf{k}}$ by say the linear TPD growth rate would miss any effect the turbulence might have on the energy injection rate.

with:

$$\eta_{\mathbf{k}}(t) = -\sum_{\Delta} M_{\mathbf{kpq}} M^*_{\mathbf{pqk}}\, \theta^*_{\mathbf{kpq}}(t)\, C_{\mathbf{q}}(t), \tag{2.90}$$

$$F_{\mathbf{k}}(t) = \frac{1}{2}\sum_{\Delta} |M_{\mathbf{kpq}}|^2\, \mathrm{Re}\left[\theta^*_{\mathbf{kpq}}(t)\right]\, C_{\mathbf{p}}(t)\, C_{\mathbf{q}}(t), \tag{2.91}$$

where $\theta_{\mathbf{kpq}}(t)$ is the triad interaction time:

$$\theta_{\mathbf{kpq}}(t) = \int_0^t \mathrm{d}\bar{t}\; R_{\mathbf{k}}(t;\bar{t})\, R_{\mathbf{p}}(t;\bar{t})\, R_{\mathbf{q}}(t;\bar{t}). \tag{2.92}$$

Remembering that the response function is what propagates an initial condition forward in time [see (2.30)], we can see that the interaction time predicts that if any of the responses at time t have decayed, the interaction between perturbations of modes $\mathbf{k}$, $\mathbf{p}$ and $\mathbf{q}$ which has begun at $t = 0$, will cease.

This is not yet a full Markovian approximation, since we need a Markovian version of the response equation (2.64) as well. This is constructed by noticing that the *form* of the Markovianised covariance equation (2.89) can be obtained by assuming:

$$\Sigma_{\mathbf{k}}(t;t') \to \eta_{\mathbf{k}}(t)\, \delta(t-t'), \tag{2.93}$$

$$F_{\mathbf{k}}(t,t') \to F_{\mathbf{k}}(t)\, \delta(t-t'), \tag{2.94}$$

which prompts one to apply the same reasoning to (2.64), and hence:

$$(\partial_t + \mathrm{i}\omega_{\mathbf{k}})\, R_{\mathbf{k}}(t;t') + \eta_{\mathbf{k}}(t)\, R_{\mathbf{k}}(t;t') = \delta(t-t'), \tag{2.95}$$

with $\eta_{\mathbf{k}}$ given by (2.90).

In a steady state, there are remarkably simple solutions for the response, and the interaction time. In that case all equal-time quantities such as $C_{\mathbf{k}}(t)$, $F_{\mathbf{k}}(t)$ or $\eta_{\mathbf{k}}(t)$ will be independent of time. And so for the response we will have:

$$R_{\mathbf{k}}(\tau) = H(\tau)\, e^{-\mathrm{i}\omega_{\mathbf{k}}\tau - \eta_{\mathbf{k}}\tau}. \tag{2.96}$$

Although $\eta_{\mathbf{k}}$ will in general have an imaginary part, and hence accommodate a frequency shift as well, its more important feature is to cause R to decay. This is why it is referred to as the *turbulent damping*. This was illustrated in figure 2.2. The interaction time in the steady state is then:

$$\theta_{\mathbf{kpq}} = \frac{1}{\mathrm{i}\left(\omega_{\mathbf{k}} + \omega_{\mathbf{p}} + \omega_{\mathbf{q}}\right) + \left(\eta_{\mathbf{k}} + \eta_{\mathbf{p}} + \eta_{\mathbf{q}}\right)}, \tag{2.97}$$



Figure 2.3: An illustration of the role of the two non-linear terms contributing to the spectral balance in (2.89) representing the forward decays *from* **k**, and the mergers *into* **k**. The solid lines are used to denote the covariances entering each term, and the dashed lines represent the responses which enter by way of the interaction time.

and if we assume real η, we can see that the real part of θ plays the role of a broadened resonance:

$$\operatorname{Re}\theta_{\mathbf{kpq}} = \frac{\eta_{\mathbf{k}} + \eta_{\mathbf{p}} + \eta_{\mathbf{q}}}{\left(\omega_{\mathbf{k}} + \omega_{\mathbf{p}} + \omega_{\mathbf{q}}\right)^2 + \left(\eta_{\mathbf{k}} + \eta_{\mathbf{p}} + \eta_{\mathbf{q}}\right)^2}. \tag{2.98}$$

If the turbulent damping is negligible $\eta \to 0$, this is just frequency matching between the three interacting modes:

$$\operatorname{Re}\theta_{\mathbf{kpq}} \to \pi\delta(\omega_{\mathbf{k}} + \omega_{\mathbf{p}} + \omega_{\mathbf{q}}), \tag{2.99}$$

and is another manifestation of the weak turbulence approximation: the responses tend to those for the linear unperturbed modes. The weak turbulence form of θ turns (2.89) into the wave-kinetic equation. In the opposite limit, with the turbulent damping being much larger than any frequency mismatch between the three modes:

$$\operatorname{Re}\theta_{\mathbf{kpq}} \to \frac{1}{\left(\eta_{\mathbf{k}} + \eta_{\mathbf{p}} + \eta_{\mathbf{q}}\right)}, \tag{2.100}$$

which is simply the inverse sum of the decorrelation rates for each mode.

Physically the terms related to $\eta_{\mathbf{k}}$ and $F_{\mathbf{k}}$ in (2.89) have the following interpretations: $\eta_{\mathbf{k}} C_{\mathbf{k}}$ represents the rate of decay of mode **k** into all other possible modes; $F_{\mathbf{k}}$ is a positive-definite source term which gives the net rate at which energy is injected *into* **k**, due to the decays of the other modes. This is illustrated in figure 2.3. The general covariance equation (2.65) has the same interpretation but is written in terms of the time history and the two-time quantities.

2.2.5 Energy conservation, realizability, and the random-coupling model

I will conclude the discussion on the DIA with a few more important remarks. First, the DIA can be shown to conserve energy. If the field φ is appropriately normalised,

such that the covariance $C_{\mathbf{k}}$ is the energy, and if the non-linearity is energy conserving (meaning it is not injecting energy into the system), then it can be shown that:

$$\sum_{\mathbf{k}} (-\eta_{\mathbf{k}} C_{\mathbf{k}} + F_{\mathbf{k}}) = 0, \tag{2.101}$$

and thus energy is conserved by the averaged quantities of the statistical closure as well. Statistical closures do not automatically have this property.

Realizability is another property of the DIA which guarantees the positive-definiteness of the covariance $C_{\mathbf{k}}$. It should be noted that the Markovian approximation made in the previous section is actually not realizable as shown by Bowman *et al.* (1993). In the same work they construct a realizable Markovian closure out of the DIA. These issues appear to matter more when one is concerned with evolving an initial value problem forward in time, and less so when one investigates the long-time steady state.

Finally, to further clarify the physical content of the DIA, it is worth noting the fact that the DIA is *exact* for a system obeying the following equation:

$$\left(\frac{\partial}{\partial t} + \mathrm{i}\omega_{\mathbf{k}}\right) \varphi_{\mathbf{k}}(t) = \sum_{\Delta} \tilde{\phi}_{\mathbf{kpq}} M_{\mathbf{kpq}}\, \varphi^*_{\mathbf{p}}(t)\, \varphi^*_{\mathbf{q}}(t), \tag{2.102}$$

which is almost exactly the same as the governing equation considered in the previous sections, but the couplings are multiplied by the factors $\tilde{\phi}_{\mathbf{kpq}}$ which are *random* quantities taking on the values of ±1 at random for each triad. Two conclusions follow from this:

- the DIA may have trouble capturing coherent structures, which are by definition objects with well defined phase correlations between Fourier amplitudes; averaging over the factors $\tilde{\phi}_{\mathbf{kpq}}$ is bound to erase any such information from the non-linear term in the governing equation;
- the DIA is adequate for a system in which the couplings between modes can be thought of as maximally random.

A large number of Fourier modes does not necessarily guarantee sufficiently random couplings (see Diamond *et al.*, 2010, 6.1.6 and 5.3.1).

2.3 Langmuir collapse

A state of strong Langmuir turbulence (SLT) is characterised by the phenomenon of Langmuir collapse. It was first theorised in Zakharov (1972), and occurs when a localised Langmuir wave packet begins to self-focus into a density depletion due to its own ponderomotive pressure. A fluid model of the non-linear interaction between the slow

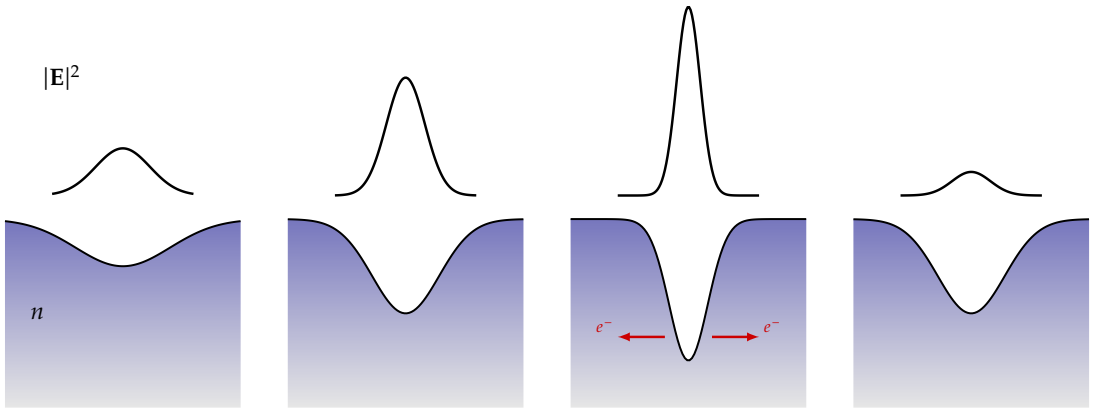


Figure 2.4: An illustration of a collapsing wave packet (a caviton) showing the four characteristic stages in the cycle.

quasi-neutral ion density perturbation n and the Langmuir field is derived in conjunction with the TPD non-linearity in section 3.2 but a heuristic discussion will suffice for now.

The plasma frequency $\omega_{\mathrm{pe}} = \sqrt{n_e e^2/m_e\epsilon_0}$ is a function of the electron number density. A local quasi-neutral perturbation in the ion density $\delta n_e = Z\delta n_i$ (with Z being the ion charge) will therefore result in a change in this frequency:

$$n_e = n_{0e} + \delta n_e, \qquad \frac{\delta\omega_{\mathrm{pe}}}{\omega_{\mathrm{pe}}} = \frac{\delta n_e}{2n_{0e}} \tag{2.102a,b}$$

and lead to the non-linear coupling between acoustic perturbations and Langmuir modes. The envelope of the electrostatic Langmuir field $\mathbf{E}$ then satisfies (Zakharov, 1972; Robinson, 1997):

$$\boldsymbol{\nabla}\cdot\left(\mathrm{i}\frac{\partial}{\partial t} + \frac{3v_{\mathrm{the}}^2}{2\omega_{\mathrm{pe}}}\nabla^2\right)\mathbf{E} = \boldsymbol{\nabla}\cdot\left(\frac{\omega_{\mathrm{pe}}\,\delta n_e}{2n_{0e}}\,\mathbf{E}\right). \tag{2.103}$$

This is known as the first, or electrostatic, Zakharov equation. For a self-consistent description, we need an equation for δn_e as well. We obtain it by taking into account the ponderomotive pressure $p \propto \boldsymbol{\nabla}|\mathbf{E}|^2$ that the Langmuir field exerts onto the electrons. This leads to an equation on the ion time scale:

$$\left(\frac{\partial^2}{\partial t^2} - c_s^2\nabla^2\right)\frac{\delta n_e}{n_{0e}} = c_s^2\nabla^2\left(\frac{\epsilon_0|\mathbf{E}|^2}{4n_{0e}T_e}\right), \tag{2.104}$$

which is the second Zakharov equation.

The phenomenon of Langmuir collapse can occur when the non-linear term on the right-hand-side of (2.103) starts to overwhelm the dispersion due to the linear term on the left. The equations admit self-similar collapsing solutions which exhibit a singularity

in finite time. The process is illustrated in figure 2.4, and these objects undergoing collapse are referred to as *cavitons*. There are four main characteristic stages of the caviton (wave packet) life-cycle, which I describe below.

The route to collapse begins with the *nucleation* of energy by modes trapped in density depressions which do not yet have enough energy to begin collapsing (Russell *et al.*, 1986). Notice that (2.103) can be thought of as a Schrödinger equation with some external potential in light of density well δn_e, which could be considered prescribed. It is well known that it supports bound, non-propagating solutions. These trapped modes can accumulate energy either directly from an external driver tuned to near the plasma frequency (known as a *clamp*), or from other freely propagating Langmuir modes in the system. The former is relevant to ionospheric modification experiments (DuBois *et al.*, 1990, 2001). Nucleation should be contrasted with the modulational instability of a plane Langmuir wave which is what was thought to be the main mechanism by which collapsing wave packets are formed. This appears to be less relevant to fully developed turbulence characterised by broad spectra which tend to be modulationally stable.

Once enough energy is accumulated in the packet and a threshold is crossed, it may proceed to collapse self-similarly[11]. Collapse may be sub-sonic or super-sonic, depending on which of the terms on the left-hand-side of (2.104) dominates. And it may be energy conserving (also called *strong* collapse) in which the collapsing cavity does not release any energy during its shrinking. Weak collapse is when energy is not conserved, and it may be radiated before collapse halts.

Once the cavity has shrunk to a size of order $10\,\lambda_{\mathrm{De}}$, collapse is *arrested* by the rapid dissipation of electrostatic energy. This is a strongly kinetic effect[12], and leads to the production of highly energetic electrons. The rate of linear Landau damping does not grow quickly enough in order to halt collapse (Russell *et al.*, 1986; DuBois *et al.*, 1990).

What is left after the electrostatic energy is dissipated is an unsupported cavity which begins to relax. It will do so until enough energy is re-nucleated inside it to begin the collapse process again. A state of strong Langmuir turbulence is one in which many of these cavities are continuously formed and dissipated.

2.4 Summary

We have seen some of the basic properties of the two-plasmon decay instability – it occurs due to the non-linear coupling of an electromagnetic mode to Langmuir waves and is

[11] Collapse also requires $D > 1$ spatial dimensions.
[12] See section V.F. in Robinson (1997), and Bingham *et al.* (1997).

spatially localised around the quarter-critical region of the coronal plasma. When it is driven above threshold to non-linear saturation, it leads to a state of strong Langmuir turbulence characterised by the continuous generation and collapse of cavitons – localised self-focusing Langmuir wave packets.

Studying power input due to TPD demands a description of the process in a turbulent background. When fluctuations are large, the response of a turbulent system to perturbations is altered: the usual dispersion functions describing linear waves of the medium are modified to include turbulent corrections. The direct-interaction approximation is a self-consistent description of the evolution of the fluctuations (the covariance) and the response. It generally involves time-history which may be approximated using the triad interaction time – a quantity measuring the effective "coherence time" for efficient non-linear interaction between any three modes in the system.

Study hard what interests you the most in the most undisciplined, irreverent, and original manner possible.

— Richard P. Feynman

3

Power injection by the two-plasmon decay into the turbulent steady state

Contents

3.1 Introduction **28**
3.2 The Zakharov system forced by the two-plasmon decay **30**
3.2.1 Relevant temporal and spatial scales 30
3.2.2 Derivation 31
3.2.3 Time-enveloping, normalisation, and Fourier decomposition . . 35
3.3 Application of the DIA to the ZakTPD system **39**
3.3.1 Statistical homogeneity and symmetries 39
3.3.2 Governing equations 43
3.3.3 Spectral balance and total power injected by TPD 47
3.4 Estimate of the non-linear growth rate and the injected power under a Markovian approximation **49**
3.5 Scalings of the injected power with laser intensity and bandwidth . **53**
3.6 Summary **58**

3.1 Introduction

Strong Langmuir turbulence dominated by Langmuir collapse has been unambiguously observed in both Zakharov and particle-in-cell simulations of the saturated state of the two-plasmon decay instability (Vu *et al.*, 2010, 2012*a*,*b*, 2014; Myatt *et al.*, 2013, 2014). The overall level of fluctuations, fraction of laser power absorbed, or hot electron flux generated, are all examples of quantities of acute practical interest, which are determined by the balance of injected power due to TPD and its eventual dissipation by the turbulence. Traditionally in studies of Langmuir turbulence (and in statistical turbulence theory

more generally) the forcing mechanism is assumed to be some linear growth rate $\gamma_{\mathbf{k}}$ present *a priori* in the linear dispersion functions in the same way as Landau damping is added in an ad hoc manner to fluid equations; or by an external source term s_{ext} added to the right-hand side of the governing equation[1]:

$$\boldsymbol{\nabla} \cdot \left(\mathrm{i} \frac{\partial}{\partial t} + \frac{3 v_{\text{the}}^2}{2 \omega_{\text{pe}}} \nabla^2 - \mathrm{i} \gamma_{\mathbf{k}} \circ \right) \mathbf{E} = \boldsymbol{\nabla} \cdot \left(\frac{\omega_{\text{pe}}}{2 n_{0e}} \delta n_e \, \mathbf{E} \right) + s_{\text{ext}}. \tag{3.1}$$

If $\gamma_{\mathbf{k}}$ is set to be the growth rate of the TPD instability in the linear regime[2] then this will be making the assumption that the instability is completely unaffected by the fluctuations it is exciting. This is reasonable for weakly turbulent plasmas (Silin & Tikhonchuk, 1986; Tikhonchuk, 2019), but knowing that once above threshold, TPD saturates in a strongly non-linear way, with a steady state dominated by Langmuir collapse, such an assumption would be dubious at best. As explained in section 2.2 wave propagation is substantially modified in a strongly turbulent medium. The very mechanism giving rise to such a prescribed $\gamma_{\mathbf{k}}$ involves a wave-wave resonance, and so it must also be modified.

Such a modification was first suggested by Sagdeev *et al.* (1982), who conjectured that the Fourier amplitudes of freely propagating Langmuir modes experience a finite auto-correlation time due to random phase jumps caused by the passing through the collapsing cavities:

$$\overline{\mathbf{E}_{\mathbf{k}}(t) \cdot \mathbf{E}_{\mathbf{k}}^*(t')} \propto e^{-\nu_{\text{corr}}(t-t')}. \tag{3.2}$$

Thus the *rate at which energy is injected* into the system is reduced to a value of $\gamma_0^2 / \nu_{\text{corr}}$. Here γ_0 is the growth rate of the instability in the linear regime under a plane wave laser electric field. The decorrelation rate ν_{corr} is said to be the rate of scattering of free Langmuir modes by the cavitons. One of the main results in this chapter is to present a systematic treatment of this effect from the point of view of statistical closure theory. This is achieved by applying the direct-interaction approximation to an extended version of the Zakharov system, which explicitly includes the non-linear terms giving rise to the TPD instability.

The DIA has been applied to the Zakharov system itself (excluding the TPD forcing) by DuBois & Rose (1981), with the main goal of studying the Langmuir modulational instability via the renormalised DIA equations. In later years, due to the difficulty of the DIA to capture the bound, coherent caviton structures of the SLT state, the statistical approach was abandoned in favour of direct numerical simulation of the Zakharov model

[1] Here $\gamma_{\mathbf{k}} \circ$ is a convolution operator whose Fourier transform when applied to $\mathbf{E}$ is $\gamma_{\mathbf{k}} \mathbf{E}_{\mathbf{k}}$.

[2] Either the well-known one (2.5) due to a plane wave laser electric field, or generalisations to broad bandwidth ones such as those considered in chapter 4 of this thesis, and in Ruskov *et al.* (2024).

(DuBois, 2000). Nevertheless, as I will explain later on, the DIA may be a completely adequate description of the TPD process amidst the SLT background, and thus accurately capture the power injected by the instability. The steady state properties can then be inferred by a separate, DIA-independent model of SLT dissipation.
This chapter presents the following advances:

1. I have applied the direct-interaction approximation to a version of the Zakharov system in which the forcing is not prescribed, but is represented by an additional non-linear term describing the TPD instability. This extends the results of DuBois & Rose (1981), and provides a fundamental description of TPD evolution amidst turbulence.

2. I then use the Markovianisation procedure of Bowman *et al.* (1993) to derive a turbulence-modified TPD power injection rate, which incorporates both laser incoherence as well as decorrelation due to turbulent damping.

3. This is subsequently combined with the SLT dissipation model of Robinson & Newman (1990) to derive scalings of the saturated fluctuation level and absorbed power with laser intensity and bandwidth.

3.2 The Zakharov system forced by the two-plasmon decay

This section gives a brief, physically motivated derivation of the governing system of equations, and then puts them in a form suitable for the application of the DIA. To the best of my knowledge, these equations were first derived in Sagdeev *et al.* (1982), and appear in DuBois *et al.* (1995*a*) who carried out seminal numerical work studying TPD saturation via Langmuir turbulence as it pertains to ICF conditions. Substantially more rigorous procedures obtaining the Zakharov equations from plasma kinetic theory are presented in DuBois *et al.* (1995*b*) and Schekochihin (2026).

3.2.1 Relevant temporal and spatial scales

The plasma period, $2\pi/\omega_{\mathrm{pe}}$, at the quarter critical density for a $\lambda = 351\,\mathrm{nm}$ laser is approximately 2 fs. The TPD growth rate is set by the laser intensity, which when taken to be $I_{\mathrm{L}} = 10^{15}\,\mathrm{W/cm^2}$, results in $\gamma_0 \simeq 13\,\mathrm{ps}^{-1}$. The ratio of this growth rate to the plasma frequency is therefore small $\gamma_0/\omega_{\mathrm{pe}} \simeq 3\times10^{-3}$. Other non-linear rates describing the interactions between the Langmuir and ion modes will be of similar order of magnitude at saturation since at that point they will need to balance the energy injection rate due to TPD.

Another important temporal time scale is the rate of electron-ion collisions. In typical ICF experiments with targets containing a plastic ablator, the ions in the plasma are a roughly equal mixture of carbon and hydrogen, leading to an average ion charge of $\overline{Z} = 3.5$. The temperature ratio is usually $T_e/T_i \simeq 2$. This results in a collision rate of approximately $\nu_{\mathrm{ei}} \simeq 1\,\mathrm{ps}^{-1}$, which is much slower than the TPD growth rate.

Finally, an ICF implosion evolves on time scales of order nanoseconds, and therefore there is sufficient time for LPIs such as TPD to reach a steady saturated state.

Concerning spatial scales, starting with the shortest one, the Debye length under these conditions is approximately $\lambda_{\mathrm{De}} \simeq 7{\times}10^{-3}\,\mu$m. Cavitons collapse down to sizes of roughly $15\lambda_{\mathrm{De}} \simeq 0.1\,\mu$m (Robinson, 1997). The plasma scale length for Omega-like implosions is roughly $L_n \simeq 200\,\mu$m. Since TPD is strongly localised near the quarter critical density, it is only active over densities n_0/n_c in the range of 0.20 to 0.25 which spans a length of about $40\,\mu$m. Ignition-scale plasmas can have scale lengths in the vicinity of $L_n = 600\,\mu$m.

3.2.2 Derivation

The Zakharov model applies in a regime in which both the electron and ion motions are well described in the fluid approximation. For the electrons, this implies that their typical motion occurs on scales large compared to the Debye length $k\lambda_{\mathrm{De}} \ll 1$[3]. The ion-sound motion will be Landau damped on the ions, and hence not fluid, unless:

$$\frac{v_{\mathrm{thi}}}{c_s} \sim \sqrt{\frac{T_i}{ZT_e + 3T_i}} \ll 1, \tag{3.3}$$

with $v_{\mathrm{thi}} = \sqrt{T_i/m_i}$ and $c_s = [(ZT_e + 3T_i)/m_i]^{1/2}$. The sound speed c_s as given here, corresponds to a plasma with a single species of ions with charge Z. As previously mentioned, the temperature ratio is $T_e/T_i \sim 2$, and so (3.3) is maybe only marginally satisfied. Kinetic modifications to the ion response are possible (c.f. DuBois *et al.*, 1995*b*), but I will not consider such complications here.

Another crucial assumption in the Zakharov model is that the interactions between the electrons and ions are weak and slow in the sense that they occur on time scales $t \gg \omega_{\mathrm{pe}}^{-1}$. This will manifest itself as a limitation on the typical amplitudes of the turbulent fluctuations beyond which the model will break. Providing precise validity criteria is difficult but a good rule of thumb is that the average electrostatic energy density in

[3]This is true for all times except the very final and brief stages of collapse. It has been argued that missing this kinetic physics makes little difference to the global turbulence properties (Robinson & Newman, 1990; DuBois *et al.*, 1990).

Langmuir fluctuations is small compared to the thermal energy density, and that the slow density fluctuations are small compared to the background:

$$\langle W \rangle = \frac{\frac{1}{2}\epsilon_0 \langle E^2 \rangle}{n_0 T_e} \ll 1, \qquad \frac{\delta n}{n_0} \ll 1. \tag{3.4}$$

where the average is taken over time and space in the steady state[4]. For parameters of interest to ICF research, these appear to be satisfied (Myatt *et al.*, 2013; Vu *et al.*, 2014).

With those restrictions in place, we may proceed with the derivation. The plasma is assumed to be subject to an externally applied laser field $\mathbf{E}_\mathrm{L}(t, \mathbf{x})$ which for the moment I will assume is not necessarily monochromatic, but may possess some relatively narrow power spectrum of width $\Delta\omega \ll \omega_0$ with ω_0 being its centre, which crucially is near $2\omega_\mathrm{pe}$. The electron motion in this system can be assumed to be composed of a slow evolution on the ion time scale, plus fast oscillations on top of this background: both, transverse – due to the laser field; as well as longitudinal – due to the Langmuir waves. And so we can perturbatively expand in a small parameter ϵ:

$$n_e = n_0 + \epsilon\delta n + \epsilon\delta\tilde{n}_e, \qquad \mathbf{v}_e = \epsilon\mathbf{v}_\mathrm{os} + \epsilon\tilde{\mathbf{u}}_e. \tag{3.5}$$

Here δn is the slow density modulation on the ion time scale (i.e. near $\omega \sim 0$), $\delta\tilde{n}_e$ is the fast modulation associated with Langmuir oscillations (near $\omega \sim \omega_\mathrm{pe}$), and of course the motion induced by the externally applied laser field is transverse and induces no density perturbation. There is a velocity perturbation due to the transverse wave though, which will be denoted by $\mathbf{v}_\mathrm{os}$ (near $\omega \sim \omega_0 \sim 2\omega_\mathrm{pe}$). Finally $\tilde{\mathbf{u}}_e$ is the velocity perturbation associated with Langmuir waves (again near $\omega \sim \omega_\mathrm{pe}$). The electric field is written similarly:

$$\mathbf{E} = \epsilon\mathbf{E}_\mathrm{L} + \epsilon\tilde{\mathbf{E}}_e, \tag{3.6}$$

with $\mathbf{E}_\mathrm{L}$ being transverse near $2\omega_\mathrm{pe}$, and $\tilde{\mathbf{E}}_e$ being longitudinal and near ω_pe, and so is the magnetic field $\mathbf{B} = \epsilon\mathbf{B}_\mathrm{L}$. The equations of motion for the electron fluid are (Michel, 2023):

$$\frac{\partial n_e}{\partial t} + \boldsymbol{\nabla} \cdot (n_e \mathbf{v}_e) = 0, \tag{3.7}$$

$$\frac{\partial \mathbf{v}_e}{\partial t} + (\mathbf{v}_e \cdot \boldsymbol{\nabla})\, \mathbf{v}_e = -\gamma_e v_\mathrm{the}^2 \frac{\boldsymbol{\nabla} n_e}{n_e} - \frac{e}{m_e}(\mathbf{E} + \mathbf{v}_e \times \mathbf{B}). \tag{3.8}$$

Here γ_e is the adiabatic index for the electrons (not to be confused with the growth rate of the TPD instability defined later on). For two quantities oscillating near some arbitrary

[4]One may wonder why this condition is given in terms of the space-time average since surely the validity of the model will be determined by the extreme values occurring at the collapse sites. This is certainly true, but what is also true is that the peak values of the fluctuations generally scale with $\langle W \rangle$. The validity conditions for the instantaneous values are less stringent than the ones quoted above (Robinson, 1997).

frequencies ω_1 and ω_2, a quadratic non-linearity results in a coupling oscillating near $\omega_1 \pm \omega_2$. And so one may effectively decompose the equations above into components near the relevant frequencies. This procedure amounts to enveloping the fields, although I choose not to introduce the envelope variables explicitly at this point. Thus for example, the only terms contributing near the laser frequency $\omega \sim \omega_0 \sim 2\omega_{\rm pe}$ are in the momentum equation:

$$\frac{\partial \mathbf{v}_{\rm os}}{\partial t} = -\frac{e}{m_e}\mathbf{E}_{\rm L} + O(\epsilon). \tag{3.9}$$

Higher order terms in this equation lead to effects such as pump depletion, or the stimulated Raman scattering instability, which are ignored in the present analysis. Pump depletion is related to the reduction in effective laser intensity due to power deposited in the plasma as the beam is propagating along the density gradient. I will be assuming that at a given point along the gradient, the system will be well represented by a local uniform description in which the external laser field is fixed[5]. The intensity threshold for the Raman instability can be higher than that for the TPD process and hence not relevant (Rosenberg *et al.*, 2018). This is the case for Omega-scale implosion experiments with third harmonic light, or also ignition scale designs with shorter wavelength lasers (Schmitt & Obenschain, 2023*a*,*b*).

Moving on, near $\omega_{\rm pe}$ we have for the equations of motion:

$$\frac{\partial \delta\tilde{n}_e}{\partial t} + n_0 \boldsymbol{\nabla}\cdot\tilde{\mathbf{u}}_e + \epsilon\left[\boldsymbol{\nabla}\cdot(\delta n\tilde{\mathbf{u}}_e) + \mathbf{v}_{\rm os}\cdot\boldsymbol{\nabla}\delta\tilde{n}_e\right] = 0, \tag{3.10}$$

$$\frac{\partial \tilde{\mathbf{u}}_e}{\partial t} + \epsilon\left[3v_{\rm the}^2\frac{\boldsymbol{\nabla}\delta\tilde{n}_e}{n_0} + (\tilde{\mathbf{u}}_e\cdot\boldsymbol{\nabla})\,\mathbf{v}_{\rm os} + (\mathbf{v}_{\rm os}\cdot\boldsymbol{\nabla})\,\tilde{\mathbf{u}}_e + \frac{e}{m_e}\tilde{\mathbf{u}}_e\times\mathbf{B}_{\rm L}\right] = -\frac{e}{m_e}\delta\tilde{\mathbf{E}}_e, \tag{3.11}$$

The correction from the electron pressure is also assumed to be $O(\epsilon)$ due to $k\lambda_{\rm De} \ll 1$[6]. Since perturbations are long wavelength and rapid, $\omega/k \gg v_{\rm the}$, and the electron motion can be taken to be adiabatic with the adiabatic index being $\gamma_e = 3$. (Nicholson, 1983). Poisson and Faraday's laws are:

$$\boldsymbol{\nabla}\cdot\delta\tilde{\mathbf{E}}_e = -\frac{e}{\epsilon_0}\delta\tilde{n}_e, \tag{3.12}$$

$$\boldsymbol{\nabla}\times\mathbf{E}_{\rm L} = -\frac{\partial \mathbf{B}_{\rm L}}{\partial t}. \tag{3.13}$$

Taking a time derivative of the density equation:

$$\frac{\partial^2\delta\tilde{n}_e}{\partial t^2} + n_0\boldsymbol{\nabla}\cdot\frac{\partial\tilde{\mathbf{u}}_e}{\partial t} + \epsilon\left[\boldsymbol{\nabla}\cdot\left(\delta n\frac{\partial\tilde{\mathbf{u}}_e}{\partial t}\right) + \frac{\partial}{\partial t}\left(\mathbf{v}_{\rm os}\cdot\boldsymbol{\nabla}\delta\tilde{n}_e\right)\right] = 0. \tag{3.14}$$

[5] See also sub-section 3.3.1.

[6] As a reminder, the "thermal correction" to the Langmuir dispersion relation $\omega^2 = \omega_{\rm pe}^2 + 3k^2v_{\rm the}^2$, comes from the electron thermal pressure term. The ratio of that term to the plasma frequency is $\sim k\lambda_{\rm De}$, which is assumed small. Perturbations with $k\lambda_{\rm De} \sim 1$, will involve kinetic physics outside of the scope of the Zakharov model. For example the physics of arrest of collapse.

Using the identity:

$$\boldsymbol{\nabla}\left(\mathbf{A}\cdot\mathbf{B}\right)=\left(\mathbf{A}\cdot\boldsymbol{\nabla}\right)\mathbf{B}+\left(\mathbf{B}\cdot\boldsymbol{\nabla}\right)\mathbf{A}+\mathbf{A}\times\boldsymbol{\nabla}\times\mathbf{B}+\mathbf{B}\times\boldsymbol{\nabla}\times\mathbf{A}, \tag{3.15}$$

Faraday's law, and (3.9), the non-linearity in the momentum equation can be written as

$$\left(\tilde{\mathbf{u}}_e\cdot\boldsymbol{\nabla}\right)\mathbf{v}_{\mathrm{os}}+\left(\mathbf{v}_{\mathrm{os}}\cdot\boldsymbol{\nabla}\right)\tilde{\mathbf{u}}_e+\frac{e}{m_e}\tilde{\mathbf{u}}_e\times\mathbf{B}_{\mathrm{L}}=\boldsymbol{\nabla}\left(\mathbf{v}_{\mathrm{os}}\cdot\tilde{\mathbf{u}}_e\right), \tag{3.16}$$

since from (3.11) $\boldsymbol{\nabla}\times\tilde{\mathbf{u}}_e=O(\epsilon^2)$. From (3.10) together with Poisson's equation, we have for $\tilde{\mathbf{u}}_e$ that:

$$\tilde{\mathbf{u}}_e=\frac{\epsilon_0}{en_0}\frac{\partial\delta\tilde{\mathbf{E}}_e}{\partial t}+O(\epsilon) \tag{3.17}$$

And so up to terms of order $O(\epsilon)$ we have,

$$\left[\frac{\partial^2}{\partial t^2}+\omega_{\mathrm{pe}}^2-3v_{\mathrm{the}}^2\nabla^2\right]\delta\tilde{n}_e=\boldsymbol{\nabla}\cdot\left(\delta n\frac{e\delta\tilde{\mathbf{E}}_e}{m_e}\right)+\frac{\epsilon_0}{e}\nabla^2\left(\mathbf{v}_{\mathrm{os}}\cdot\frac{\partial\tilde{\mathbf{E}}_e}{\partial t}\right)-\frac{\partial}{\partial t}\left(\mathbf{v}_{\mathrm{os}}\cdot\boldsymbol{\nabla}\delta\tilde{n}_e\right). \tag{3.18}$$

Expressing the density perturbation in terms of the electric potential defined by $\tilde{\mathbf{E}}_e=-\boldsymbol{\nabla}\tilde{\phi}_e$ results in:

$$\begin{aligned}\left[-\frac{\partial^2}{\partial t^2}-\omega_{\mathrm{pe}}^2+3v_{\mathrm{the}}^2\nabla^2\right]\nabla^2\tilde{\phi}_e&\\ =\omega_{\mathrm{pe}}^2\boldsymbol{\nabla}\cdot\left(\frac{\delta n}{n_0}\boldsymbol{\nabla}\tilde{\phi}_e\right)+\underbrace{\nabla^2\left(\mathbf{v}_{\mathrm{os}}\cdot\boldsymbol{\nabla}\frac{\partial\tilde{\phi}_e}{\partial t}\right)+\frac{\partial}{\partial t}\left[\left(\mathbf{v}_{\mathrm{os}}\cdot\boldsymbol{\nabla}\right)\nabla^2\tilde{\phi}_e\right]}_{\mathrm{TPD}}.&\end{aligned} \tag{3.19}$$

The left hand side of this equation describes the usual linear propagation of Langmuir waves. The first of the terms on the right represents the non-linear interactions between Langmuir waves and ion-sound, and is what appears in what is usually known as the Zakharov system (Zakharov, 1972). The last two terms represent the non-linear interaction between the externally imposed laser field and the Langmuir waves, giving rise to the two-plasmon instability.

In order to close (3.19) we need an equation for the evolution of the slow perturbation δn. The physics basis for the model which will follow is the idea that in addition to the electron thermal pressure providing the restoring force for the acoustic oscillations in the linear regime, there will also be a ponderomotive contribution associated with the energy density of the high frequency electron oscillations. So, if one considers the electron fluid momentum equation (3.8) near the zero frequency scale, for the slow perturbations $\delta\mathbf{v}_e$ we will have[7]:

$$\frac{\partial\delta\mathbf{v}_e}{\partial t}+\left(\tilde{\mathbf{u}}_e\cdot\boldsymbol{\nabla}\right)\tilde{\mathbf{u}}_e=-v_{\mathrm{the}}^2\frac{\boldsymbol{\nabla}\delta n}{n_0}-\frac{e}{m_e}\delta\mathbf{E}, \tag{3.20}$$

[7]In this case, $\omega/k\ll v_{\mathrm{the}}$, and isothermal equation of state with $\gamma_e=1$ has been assumed for the electron fluid (Nicholson, 1983).

where the ordering $\delta\mathbf{v}_e \sim O(\epsilon^2)$ has now been assumed, and only terms up to that order have been retained in the equation. From (3.15) the non-linear term can be expressed as:

$$(\tilde{\mathbf{u}}_e \cdot \boldsymbol{\nabla})\,\tilde{\mathbf{u}}_e = \tfrac{1}{2}\boldsymbol{\nabla}\left(|\tilde{\mathbf{u}}_e|^2\right) + O(\epsilon^3), \tag{3.21}$$

and so by demanding $\partial\delta\mathbf{v}_e/\partial t = 0$, i.e. that pressure forces on the electron fluid *must* balance otherwise they will cause motion on the $\omega_{\mathrm{pe}}^{-1}$ scale, we get that:

$$\frac{e}{m_e}\delta\mathbf{E} = -v_{\mathrm{the}}^2\frac{\boldsymbol{\nabla}\delta n}{n_0} - \tfrac{1}{2}\boldsymbol{\nabla}\left(|\tilde{\mathbf{u}}_e|^2\right). \tag{3.22}$$

This electric field induces a motion in the ions whose linearised fluid equations of motion are (neglecting the ion thermal pressure):

$$\frac{\partial\delta n_i}{\partial t} + n_{0i}\boldsymbol{\nabla}\cdot\delta\mathbf{v}_i = 0, \tag{3.23}$$

$$\frac{\partial\delta\mathbf{v}_i}{\partial t} = \frac{Ze}{m_i}\delta\mathbf{E}. \tag{3.24}$$

Taking a time derivative of the first equation, and substituting in the second, together with the result for $\delta\mathbf{E}$, one has:

$$\left(\frac{\partial^2}{\partial t^2} - c_s^2\nabla^2\right)\frac{\delta n}{n_0} = \frac{1}{2}\frac{Zm_e}{m_i}\nabla^2\left(|\tilde{\mathbf{u}}_e|^2\right), \tag{3.25}$$

where quasi-neutrality has been assumed, so both $Zn_{0i} = n_0$ and $Z\delta n_i = \delta n$, and $c_s = \sqrt{ZT_e/m_i}$ has been defined as the sound speed. Again, up to $O(\epsilon)$ we have that:

$$\tilde{\mathbf{u}}_e = \frac{\epsilon_0\omega_{\mathrm{pe}}}{en_0}\delta\tilde{\mathbf{E}}_e + O(\epsilon), \tag{3.26}$$

which implies:

$$\left(\frac{\partial^2}{\partial t^2} - c_s^2\nabla^2\right)\frac{\delta n}{n_0} = c_s^2\nabla^2\left(\frac{\epsilon_0|\boldsymbol{\nabla}\tilde{\phi}_e|^2}{2n_0T_e}\right). \tag{3.27}$$

This equation, together with (3.19), is a closed system and provides a self-consistent description of Langmuir turbulence forced through the TPD instability. The external forcing laser field $\mathbf{E}_{\mathrm{L}}$ is considered prescribed and enters through $\mathbf{v}_{\mathrm{os}}$ by way of (3.9).

3.2.3 Time-enveloping, normalisation, and Fourier decomposition

I will now introduce the complex slowly-varying envelopes for the electrostatic potential and the laser electric field, and write down the system of equations in Fourier space for ease of applying the DIA. The fast electrostatic potential $\tilde{\phi}_e(t,\mathbf{x})$ is written in terms of the complex envelope $\psi(t,\mathbf{x})$ as follows:

$$\tilde{\phi}_e(t,\mathbf{x}) = \tfrac{1}{2}\psi(t,\mathbf{x})e^{-\mathrm{i}\omega_{\mathrm{pe}}t} + \tfrac{1}{2}\psi^*(t,\mathbf{x})e^{\mathrm{i}\omega_{\mathrm{pe}}t}. \tag{3.28}$$

Similarly for the laser electric field:

$$\mathbf{E}_{\mathrm{L}}(t,\mathbf{x}) = \tfrac{1}{2}\boldsymbol{\xi}(t,\mathbf{x})e^{-\mathrm{i}\omega_0 t} + \tfrac{1}{2}\boldsymbol{\xi}^*(t,\mathbf{x})e^{\mathrm{i}\omega_0 t}. \tag{3.29}$$

In this approximation, up to the same order of the non-linear terms in (3.19) we can set:

$$\mathbf{v}_{\mathrm{os}}(t,\mathbf{x}) = -\mathrm{i}\frac{e}{m_e\omega_0}\boldsymbol{\xi}(t,\mathbf{x})\,e^{-\mathrm{i}\omega_0 t} + \text{c.c.} \tag{3.30}$$

In terms of the envelope, the second order derivative in (3.19) is:

$$\frac{\partial^2\tilde{\phi}_e}{\partial t^2} = \frac{1}{2}\left(\frac{\partial^2\psi}{\partial t^2} - 2\mathrm{i}\omega_{\mathrm{pe}}\frac{\partial\psi}{\partial t} - \omega_{\mathrm{pe}}^2\psi\right)e^{-\mathrm{i}\omega_{\mathrm{pe}}t} + \text{c.c.} \tag{3.31}$$

Since the envelope is assumed slowly varying $\partial_t^2\psi \ll \mathrm{i}\omega\partial_t\psi$ which makes the left hand side of (3.19):

$$\left[-\frac{\partial^2}{\partial t^2} - \omega_{\mathrm{pe}}^2 + 3v_{\mathrm{the}}^2\nabla^2\right]\nabla^2\tilde{\phi}_e \simeq \nabla^2\left[\mathrm{i}\omega_{\mathrm{pe}}\frac{\partial\psi}{\partial t} + \tfrac{3}{2}v_{\mathrm{the}}^2\nabla^2\psi\right]e^{-\mathrm{i}\omega_{\mathrm{pe}}t} + \text{c.c.} \tag{3.32}$$

On the right hand side, the ion non-linearity becomes simply:

$$\omega_{\mathrm{pe}}^2\boldsymbol{\nabla}\cdot\left(\frac{\delta n}{n_0}\boldsymbol{\nabla}\tilde{\phi}_e\right) = \tfrac{1}{2}\omega_{\mathrm{pe}}^2\boldsymbol{\nabla}\cdot\left(\frac{\delta n}{n_0}\boldsymbol{\nabla}\psi\right) + \text{c.c.} \tag{3.33}$$

while the terms which will contribute to the TPD non-linearity near the ω_{pe} frequency will come from the $\xi\psi^*$ products since we assume that the laser central frequency is very near twice the plasma frequency $\Omega = \omega_0 - 2\omega_{\mathrm{pe}} \ll \omega_{\mathrm{pe}}$. Ω will be referred to as the *detuning*, and is a parameter which effectively sets the local plasma density, since for fixed ω_0, a larger detuning implies a lower ω_{pe}. Thus for example, Ω sets the radii of the circles in figure 2.1. Therefore, substituting in the expressions for the envelopes, and similarly to before, ignoring the derivatives of the envelopes compared to the frequencies of the waves, for the TPD non-linear terms in (3.19) we get[8]:

$$\begin{aligned}\mathrm{TPD} &= -\mathrm{i}\frac{e}{4m_e\omega_0}e^{-\mathrm{i}\Omega t}\left[\mathrm{i}\omega_{\mathrm{pe}}\nabla^2\left(\boldsymbol{\xi}\cdot\boldsymbol{\nabla}\psi^*\right) - \mathrm{i}(\omega_{\mathrm{pe}}+\Omega)\left(\boldsymbol{\xi}\cdot\boldsymbol{\nabla}\right)\left(\nabla^2\psi^*\right)\right]e^{-\mathrm{i}\omega_{\mathrm{pe}}t} + \ldots &(3.34)\\ &\simeq \frac{e\omega_{\mathrm{pe}}}{4m_e\omega_0}e^{-\mathrm{i}\Omega t}\left[\nabla^2\left(\boldsymbol{\xi}\cdot\boldsymbol{\nabla}\psi^*\right) - \left(\boldsymbol{\xi}\cdot\boldsymbol{\nabla}\right)\left(\nabla^2\psi^*\right)\right]e^{-\mathrm{i}\omega_{\mathrm{pe}}t} + \ldots &(3.35)\end{aligned}$$

Hence the equation for the envelope $\psi(t,\mathbf{x})$ becomes:

$$\begin{aligned}\nabla^2\left(\mathrm{i}\omega_{\mathrm{pe}}\partial_t + \tfrac{3}{2}v_{\mathrm{the}}^2\nabla^2\right)\psi = \tfrac{1}{2}\omega_{\mathrm{pe}}^2\boldsymbol{\nabla}\cdot\left(\frac{\delta n}{n_0}\boldsymbol{\nabla}\psi\right)\\ + \frac{e\omega_{\mathrm{pe}}}{4m_e\omega_0}e^{-\mathrm{i}\Omega t}\left[\nabla^2\left(\boldsymbol{\xi}\cdot\boldsymbol{\nabla}\psi^*\right) - \left(\boldsymbol{\xi}\cdot\boldsymbol{\nabla}\right)\left(\nabla^2\psi^*\right)\right].\end{aligned} \tag{3.36}$$

[8]The dots "..." are used to denote additional terms oscillating at frequencies other than ω_{pe} which are not of interest.

By the same logic, the ion equation will only couple to the $\psi\psi^*$ terms, and so:

$$\left(\frac{\partial^2}{\partial t^2} - c_s^2\nabla^2\right)\frac{\delta n}{n_0} = c_s^2\nabla^2\left(\frac{\epsilon_0|\boldsymbol{\nabla}\psi|^2}{4n_0T_e}\right). \tag{3.37}$$

I will refer to this system of equations as the ZaKTPD system.

Let us now develop some convenient normalisations for all of the fields we are dealing with: δn, ψ and $\boldsymbol{\xi}$. The slow density perturbation is most naturally normalised to the background density n_0 so that we can work with a new variable n which measures the fractional deviation from it:

$$\frac{\delta n}{n_0} \mapsto n. \tag{3.38}$$

For the potential ψ it is most convenient to normalise so that the non-linear term in the ion equation becomes:

$$\frac{\epsilon_0|\boldsymbol{\nabla}\psi|^2}{4n_0T_e} \mapsto |\boldsymbol{\nabla}\psi|^2. \tag{3.39}$$

This transforms the electrostatic field $\mathbf{E} = \boldsymbol{\nabla}\psi$ into units such that its energy density is measured as a fraction of the thermal energy density n_0T_e. In these units:

$$\langle|\boldsymbol{\nabla}\psi|^2\rangle = \langle W\rangle, \tag{3.40}$$

where $\langle W\rangle$ is the parameter mentioned at the beginning of the section relating to the discussion of the validity conditions for the Zakharov model. It is particularly useful since $\langle W\rangle \sim (k\lambda_{\mathrm{De}})^2$ is a good estimate for the onset of strong turbulence effects. Finally, in a similar vein, a convenient normalisation for the laser electric field $\boldsymbol{\xi}$ is one in which its energy density is normalised to unity. Since I will be allowing for laser fields with arbitrary power spectra, it is most useful to relate the energy density to the average laser intensity I_{L} such that:

$$\frac{I_{\mathrm{L}}}{c} = \tfrac{1}{2}\epsilon_0\langle|\boldsymbol{\xi}|^2\rangle. \tag{3.41}$$

Hence:

$$\boldsymbol{\xi} \mapsto \frac{\boldsymbol{\xi}}{\sqrt{2I_{\mathrm{L}}/(c\epsilon_0)}}. \tag{3.42}$$

For a laser plane wave of intensity I_{L} the TPD growth rate maximises to a value of $\gamma_0 = k_0v_{\mathrm{os}}/4$ with $v_{\mathrm{os}} = e/(m_e\omega_0)\sqrt{2I_{\mathrm{L}}/(c\epsilon_0)}$. Expressing the laser electric field in these units makes the TPD non-linearity proportional to γ_0 – i.e. a measure of the coupling strength. With these three substitutions the equations become:

$$\nabla^2\left(\mathrm{i}\omega_{\mathrm{pe}}\partial_t + \tfrac{3}{2}v_{\mathrm{the}}^2\nabla^2\right)\psi = \tfrac{1}{2}\omega_{\mathrm{pe}}^2\boldsymbol{\nabla}\cdot(n\boldsymbol{\nabla}\psi) + \frac{\omega_{\mathrm{pe}}\gamma_0}{k_0}e^{-\mathrm{i}\Omega t}\left[\nabla^2\left(\boldsymbol{\xi}\cdot\boldsymbol{\nabla}\psi^*\right) - \left(\boldsymbol{\xi}\cdot\boldsymbol{\nabla}\right)\left(\nabla^2\psi^*\right)\right], \tag{3.43}$$

$$\left(\frac{\partial^2}{\partial t^2} - c_s^2\nabla^2\right) n = c_s^2\nabla^2\left(|\boldsymbol{\nabla}\psi|^2\right). \tag{3.44}$$

The final piece of bookkeeping left to be carried out is to put the equations in Fourier space as that allows for the most straight-forward application of the DIA. For that I will follow the slightly unorthodox but convenient notation of DuBois & Rose (1981). Let us first decompose ψ into Fourier modes:

$$\psi(t,\mathbf{x}) = \sum_{\mathbf{k}} e^{\mathrm{i}\mathbf{k}\cdot\mathbf{x}}\,\psi_{\mathbf{k}}(t). \tag{3.45}$$

The transform of its complex conjugate is therefore:

$$\psi^*(t,\mathbf{x}) = \sum_{\mathbf{k}} e^{-\mathrm{i}\mathbf{k}\cdot\mathbf{x}}\,\psi^*_{\mathbf{k}}(t) = \sum_{\mathbf{k}} e^{\mathrm{i}\mathbf{k}\cdot\mathbf{x}}\,\psi^*_{-\mathbf{k}}(t) \doteq \sum_{\mathbf{k}} e^{\mathrm{i}\mathbf{k}\cdot\mathbf{x}}\,\psi^\dagger_{\mathbf{k}}(t), \tag{3.46}$$

where the dagger notation here denotes $\psi^\dagger_{\mathbf{k}} = \psi^*_{-\mathbf{k}}$ as opposed to the usual Hermitian conjugate. Simply put: $\psi^\dagger_{\mathbf{k}}$ are the Fourier modes of $\psi^*(\mathbf{x})$. Equivalently for $\boldsymbol{\xi}$ and $\boldsymbol{\xi}^*$:

$$\boldsymbol{\xi}(t,\mathbf{x}) = \sum_{\mathbf{k}} e^{\mathrm{i}\mathbf{k}\cdot\mathbf{x}}\,\boldsymbol{\xi}_{\mathbf{k}}(t), \qquad \boldsymbol{\xi}^*(t,\mathbf{x}) = \sum_{\mathbf{k}} e^{\mathrm{i}\mathbf{k}\cdot\mathbf{x}}\,\boldsymbol{\xi}^\dagger_{\mathbf{k}}(t). \tag{3.46a,b}$$

The slow perturbation is un-enveloped and real, and therefore satisfies:

$$n^\dagger_{\mathbf{k}} = n^*_{-\mathbf{k}} = n_{\mathbf{k}}. \tag{3.47}$$

By the convolution theorem $[A(\mathbf{x})B(\mathbf{x})]_{\mathbf{k}} = \sum_{\mathbf{q}} A_{\mathbf{k}-\mathbf{q}}B_{\mathbf{q}}$, the Fourier transforms of the equations are readily written down:

$$(\partial_t + \mathrm{i}\delta\omega_{\mathbf{k}})\,\psi_{\mathbf{k}} = -\sum_{\mathbf{k}=\mathbf{p}+\mathbf{q}} \frac{\mathrm{i}\omega_{\mathrm{pe}}}{2}\frac{(\mathbf{k}\cdot\mathbf{q})}{k^2} n_{\mathbf{p}}\psi_{\mathbf{q}} - \sum_{\mathbf{k}=\mathbf{p}+\mathbf{q}} \mathrm{i}\gamma_0\frac{k_\mu}{k_0}\left(\frac{k^2-q^2}{k^2}\right) e^{-\mathrm{i}\Omega t}\,\xi^\mu_{\mathbf{p}}\psi^\dagger_{\mathbf{q}}, \tag{3.48}$$

where $\xi^\mu_{\mathbf{q}}$ and k_μ are the components of the vectors $\boldsymbol{\xi}_{\mathbf{q}}$ and $\mathbf{k}$; I have used the fact that $\boldsymbol{\xi}$ is transverse $\boldsymbol{\nabla}\cdot\boldsymbol{\xi} = 0$ which implies $q_\mu\xi^\mu_{\mathbf{q}} = 0$; the meaning of the sum is $\sum_{\mathbf{k}=\mathbf{p}+\mathbf{q}} = \sum_{\mathbf{p},\mathbf{q}}\delta_{\mathbf{k},\mathbf{p}+\mathbf{q}}$; and $\delta\omega_{\mathbf{k}} = 3k^2v^2_{\mathrm{the}}/(2\omega_{\mathrm{pe}})$ is the linear frequency of oscillation of the Langmuir envelope. The Fourier transform for the ion equation is:

$$\left(\frac{\partial^2}{\partial t^2} + c_s^2k^2\right) n_{\mathbf{k}} = c_s^2 \sum_{\mathbf{k}=\mathbf{p}+\mathbf{q}} k^2\,(\mathbf{p}\cdot\mathbf{q})\,\psi_{\mathbf{p}}\psi^\dagger_{\mathbf{q}}. \tag{3.49}$$

Equations (3.48) and (3.49) represent the ZakTPD system in Fourier space.

The last manipulation before proceeding with the derivation of the DIA equations for this system is to reduce the order of (3.49) and to provide an evolution equation for $\psi^\dagger_{\mathbf{k}}$. The latter is achieved by taking the complex conjugate of (3.48) and negating $\mathbf{k}$, $\mathbf{p}$ and $\mathbf{q}$:

$$(\partial_t - \mathrm{i}\delta\omega_{\mathbf{k}})\,\psi^\dagger_{\mathbf{k}} = \sum_{\mathbf{k}=\mathbf{p}+\mathbf{q}} \frac{\mathrm{i}\omega_{\mathrm{pe}}}{2}\frac{(\mathbf{k}\cdot\mathbf{q})}{k^2} n_{\mathbf{p}}\psi^\dagger_{\mathbf{q}} - \sum_{\mathbf{k}=\mathbf{p}+\mathbf{q}} \mathrm{i}\gamma_0\frac{k_\mu}{k_0}\left(\frac{k^2-q^2}{k^2}\right) e^{\mathrm{i}\Omega t}\,\xi^{\dagger\mu}_{\mathbf{p}}\psi_{\mathbf{q}}. \tag{3.50}$$

The order is reduced by defining the hydrodynamic flux potential u through $\partial_t n = c_s^2 \nabla^2 u$. Therefore (3.49) decomposes into:

$$\frac{\partial n_{\mathbf{k}}}{\partial t} = -c_s^2 k^2 u_{\mathbf{k}}, \tag{3.51}$$

$$\frac{\partial u_{\mathbf{k}}}{\partial t} = n_{\mathbf{k}} - \sum_{\mathbf{k}=\mathbf{p}+\mathbf{q}} (\mathbf{p}\cdot\mathbf{q})\, \psi_{\mathbf{p}} \psi^{\dagger}_{\mathbf{q}}. \tag{3.52}$$

3.3 Application of the DIA to the ZakTPD system

3.3.1 Statistical homogeneity and symmetries

Equations (3.48) and (3.50-3.52) describe the evolution of the generalised field φ_1 for which the variables are $1 \equiv (t, \mathbf{k}, \sigma)$ with the field index σ taking the values $\sigma = \{\psi, \psi^{\dagger}, n, u, \xi^{\mu}, \xi^{\dagger\mu}\}$. An evolution equation for the laser envelope $\xi^{\mu}_{\mathbf{k}}$ will not be needed as the field is considered prescribed[9].

The DIA equations (2.60-2.63) in their full generality describe all of the responses $R^{\sigma\sigma'}_{\mathbf{k}\mathbf{k}'}(t;t')$ (plus the associated turbulent corrections Σ) and covariances $C^{\sigma\sigma'}_{\mathbf{k}\mathbf{k}'}(t,t')$, constituting a prohibitively complicated system to study. The first, standard, and in fact well-applicable assumption leading to substantial simplifications, is that of statistical homogeneity – namely the dependence of all spatial quantities $F(\mathbf{x}, \mathbf{x}')$ only on the difference $\mathbf{x} - \mathbf{x}'$. For the covariances this leads to the relationship $C_{\mathbf{k}\mathbf{k}'} = C_{\mathbf{k}} \delta_{\mathbf{k}+\mathbf{k}',\mathbf{0}}$, while for the responses we have $R_{\mathbf{k}\mathbf{k}'} = R_{\mathbf{k}} \delta_{\mathbf{k}\mathbf{k}'}$[10]. This is reasonable to assume due to the large scale separation between the characteristic turbulence length scale and the scale over which the density varies near the quarter critical. The turbulence scale can be taken to be of order the size of a typical caviton, i.e. tens of Debye lengths, which for the relevant plasma conditions corresponds to roughly 0.1 μm. Since TPD is strongly localised near the quarter critical, it is only active over densities n_0/n_c in the range of 0.20 to 0.25 which span a length of about 40 μm[11]. Thus one can imagine the turbulence near each point along the density gradient to be well described by the uniform, statistically homogeneous solutions corresponding to that density. Experience with Zakharov simulations using the Laser Plasma Simulation Environment code (Follett *et al.*, 2017, 2019) also suggests that this is reasonable. An analogous problem exists in the modelling of strong Langmuir turbulence excited during ionospheric modification experiments, where this assumption seems to hold as well (DuBois *et al.*, 2001).

[9] Or, to complete the system, one could imagine providing an evolution equation for $\xi^{\mu}_{\mathbf{k}}$ in which there are no linear or non-linear couplings to the other fields. The situation will remain unchanged.

[10] The difference stems from the fact that the response functions of the $\mathbf{k}$-space equations are not simply the Fourier transforms of the $\mathbf{x}$-space responses. This is explained in Appendix A.

[11] This corresponds to a scale length of approximately $L_n = 200\,\mu$m which is relevant for an Omega-like implosion experiment. Ignition scale targets could have scale-lengths $L_n > 600\,\mu$m.

Another substantial simplification follows from a symmetry theorem that the DIA for the Zakharov system obeys (DuBois & Rose, 1981). It allows one to consider only two of the correlation functions and two of the responses – the Langmuir fluctuation spectrum $C^{\psi\psi^\dagger}$, the ion fluctuation spectrum C^{nn}, and the responses $R^{\psi\psi}$ and $\widehat{R}^{nn}$[12]. It states that if the system starts from an initial condition in which all other responses and covariances vanish, they will do so for all times. This has significant implications for the physical content of the DIA applied to the Zakharov system. Suppose Langmuir turbulence is excited by the TPD instability growing from thermal noise. It is entirely reasonable to assume that the fields n and ψ are uncorrelated in such a state, therefore making $C^{n\psi}$ vanish. But once strong Langmuir turbulence develops and exhibits the cavitation phenomenon, it would be questionable to assume no cross-correlations between the density perturbation and the Langmuir field: the trapped Langmuir eigenstates inside of the density depressions of n, must be correlated with n. For example, the so-called *caviton correlator*:

$$\frac{\langle n|\mathbf{E}|^2\rangle}{\langle n^2\rangle^{1/2}\langle|\mathbf{E}|^2\rangle}, \tag{3.53}$$

is frequently used to measure cavitation activity in simulations (DuBois *et al.*, 1995*a*, 1996; Vu *et al.*, 2012*a*). Nevertheless, as I have mentioned, we are principally interested in studying the physics of power injection by the TPD source terms into the turbulent state, and not with an *a priori* prediction of the saturated spectra, which is what the DIA fails at. This symmetry property has been stated but not explicitly proved by DuBois & Rose (1981). Given the importance of its implications just outlined, and the need to investigate an extended version of the system (i.e. ZAKTPD), it is worth examining it in more detail.

The symmetry property is related to the conditions under which the general set of the DIA equations (2.60-2.63) is diagonal in the indices. This may not be immediately obvious but the reasons why the symmetry property appears more complicated for the Zakharov system are twofold; one: the need to consider complex-valued fields; and two: to reduce the order of equation (3.49). To avoid both, consider a primitive equation of the form:

$$G_\alpha^{-1}\varphi_\alpha(t) = \sum_{\beta\gamma}\tfrac{1}{2}M_{\alpha\beta\gamma}\varphi_\beta^*\varphi_\gamma^*, \tag{3.54}$$

where the fields φ are assumed real[13]; the indices α correspond to Fourier modes *and* a field index, so $\alpha \equiv (\mathbf{k}, \sigma)$; the operators G_α^{-1} are allowed to contain higher order time derivatives

[12]Technically, since the second-order-in-time equation for n (3.49) was decomposed into two first order ones, this makes all of R^{uu}, R^{nu}, R^{nn} non-zero. But as shown in appendix B, they can be replaced by a single second-order-in-time equation for a new response denoted by $\widehat{R}^{nn}$.

[13]And therefore their Fourier modes obey $\varphi^*_{(\mathbf{k},\sigma)} = \varphi_{(-\mathbf{k},\sigma)}$.

but are assumed diagonal in the index which is true for translationally invariant systems and fields which are *not* linearly coupled. For example in (3.49), $G^{-1}_{(\mathbf{k},n)} = \partial_t^2 + c_s^2 k^2$. Sums will be explicit. Equations (3.19) and (3.27) describing the ZakTPD system before the introduction of the complex envelope and the order reduction procedure, is of this form.

The equations for the response functions are (Krommes, 2002)[14]:

$$G_\alpha^{-1} R_{\alpha\alpha'}(t;t') + \int \mathrm{d}\bar{t} \sum_{\bar{\alpha}} \Sigma_{\alpha\bar{\alpha}}(t;\bar{t})\, R_{\bar{\alpha}\alpha'}(\bar{t};t') = \delta_{\alpha\alpha'}\delta(t-t'), \tag{3.55}$$

$$\Sigma_{\alpha\bar{\alpha}}(t;\bar{t}) = -\sum_{\beta\bar{\beta}\gamma\bar{\gamma}} M_{\alpha\beta\gamma} R^*_{\beta\bar{\beta}}(t;\bar{t})\, C^*_{\gamma\bar{\gamma}}(t,\bar{t})\, M^*_{\bar{\beta}\bar{\gamma}\alpha}, \tag{3.56}$$

and for the covariances:

$$G_\alpha^{-1} C_{\alpha\alpha'}(t,t') + \int \mathrm{d}\bar{t} \sum_{\bar{\alpha}} \Sigma_{\alpha\bar{\alpha}}(t;\bar{t})\, C_{\bar{\alpha}\alpha'}(\bar{t},t') = \int \mathrm{d}\bar{t}\, F_{\alpha\bar{\alpha}}(t,\bar{t})\, R^*_{\bar{\alpha}\alpha'}(t';\bar{t}), \tag{3.57}$$

$$F_{\alpha\bar{\alpha}}(t,\bar{t}) = \frac{1}{2} \sum_{\beta\bar{\beta}\gamma\bar{\gamma}} M_{\alpha\beta\gamma} C^*_{\beta\bar{\beta}}(t;\bar{t})\, C^*_{\gamma\bar{\gamma}}(t,\bar{t})\, M^*_{\bar{\alpha}\bar{\beta}\bar{\gamma}}. \tag{3.58}$$

The covariances here are $C_{\alpha\alpha'}(t,t') = \overline{\varphi_\alpha(t)\varphi^*_{\alpha'}(t')}$, which makes statistical homogeneity for both R and C given by a proportionality to $\delta_{\mathbf{k}\mathbf{k}'}$. Therefore for a single field, diagonality in the index is equivalent to statistical homogeneity. For multiple fields, the diagonality condition $C_{\alpha\alpha'}(t,t') = C_{\alpha\alpha}(t,t')\delta_{\alpha\alpha'} \equiv C_\alpha \delta_{\alpha\alpha'}$ further implies that the correlations between the different field species vanish. Note that this does not imply that the fields do not interact.

Suppose we start from an initial condition in which both the responses and the covariances are diagonal. For the system to remain diagonal at all times, all terms in equations (3.55-3.58) must retain this diagonal form. Since the linear operators G_α^{-1} are diagonal, they introduce no mixing between any off-diagonal terms. The non-linear terms may introduce mixing if $\Sigma_{\alpha\bar{\alpha}}$ or $F_{\alpha\bar{\alpha}}$ contain off-diagonal elements. This places a restriction on the couplings $M_{\alpha\beta\gamma}$. Consider the self-energies:

$$\begin{aligned}\Sigma_{\alpha\bar{\alpha}}(t;\bar{t}) &= -\sum_{\beta\bar{\beta}\gamma\bar{\gamma}} M_{\alpha\beta\gamma}\delta_{\beta\bar{\beta}}\delta_{\gamma\bar{\gamma}} R^*_\beta(t;\bar{t})\, C^*_\gamma(t,\bar{t})\, M^*_{\bar{\beta}\bar{\gamma}\alpha} \\ &= -\sum_{\beta\gamma} M_{\alpha\beta\gamma} R^*_\beta(t;\bar{t})\, C^*_\gamma(t,\bar{t})\, M^*_{\beta\gamma\bar{\alpha}}\end{aligned}, \tag{3.59}$$

[14] These are most easily derived by starting from the general DIA equations in **x**-space and carrying out a Fourier transformation. The fact that the DIA can accommodate higher order time derivatives (e.g. second order) can also be shown by constructing the DIA for an extended set of fields which implement an order reduction procedure such as the one in (3.49).

and the non-linear source:

$$\begin{aligned} F_{\alpha\overline{\alpha}}(t,\overline{t}) &= \frac{1}{2}\sum_{\beta\overline{\beta}\gamma\overline{\gamma}} M_{\alpha\beta\gamma}\delta_{\beta\overline{\beta}}\delta_{\gamma\overline{\gamma}} C^*_{\beta}(t,\overline{t})\, C^*_{\gamma}(t,\overline{t})\, M^*_{\overline{\alpha}\overline{\beta}\overline{\gamma}} \\ &= \frac{1}{2}\sum_{\beta\gamma} M_{\alpha\beta\gamma} C^*_{\beta}(t,\overline{t})\, C^*_{\gamma}(t,\overline{t})\, M^*_{\overline{\alpha}\beta\gamma} \end{aligned} . \tag{3.60}$$

For $\Sigma_{\alpha\overline{\alpha}}$ to be diagonal we need the couplings to obey:

$$M_{\alpha\beta\gamma}M^*_{\beta\gamma\overline{\alpha}} = M_{\alpha\beta\gamma}M^*_{\beta\gamma\alpha}\delta_{\alpha\overline{\alpha}}. \tag{3.61}$$

For a translationally invariant system the couplings are proportional to:

$$M_{\alpha\beta\gamma} \propto \delta_{\mathbf{k}+\mathbf{p}+\mathbf{q},\mathbf{0}}, \tag{3.62}$$

and so that immediately implies the homogeneity of Σ, since we need both $\mathbf{k}+\mathbf{p}+\mathbf{q}=\mathbf{0}$ and $\mathbf{q}+\mathbf{p}+\overline{\mathbf{k}}=\mathbf{0}$ to be satisfied[15] ; the wave numbers correspond to the respective index, so $\alpha \equiv (\mathbf{k},\sigma)$, $\beta \equiv (\mathbf{p},\sigma_2)$, $\gamma \equiv (\mathbf{q},\sigma_3)$, $\overline{\alpha} \equiv (\overline{\mathbf{k}},\overline{\sigma})$. Therefore translational invariance satisfies the $\delta_{\mathbf{k}\overline{\mathbf{k}}}$ part of the $\delta_{\alpha\overline{\alpha}}$ restriction:

$$M_{\alpha\beta\gamma}M^*_{\beta\gamma\overline{\alpha}} \propto \delta_{\mathbf{k}+\mathbf{p}+\mathbf{q},\mathbf{0}}\,\delta_{\mathbf{p}+\mathbf{q}+\overline{\mathbf{k}},\mathbf{0}} \propto \delta_{\mathbf{k}+\mathbf{p}+\mathbf{q},\mathbf{0}}\,\delta_{\mathbf{k}\overline{\mathbf{k}}}. \tag{3.63}$$

The same property makes F homogeneous as well.

Diagonality in the field indices for Σ:

$$M^{\sigma\sigma_2\sigma_3}_{\mathbf{kpq}}\left(M^{\sigma_2\sigma_3\overline{\sigma}}_{\mathbf{pqk}}\right)^* \propto \delta_{\sigma\overline{\sigma}}, \tag{3.64}$$

and for F:

$$M^{\sigma\sigma_2\sigma_3}_{\mathbf{kpq}}\left(M^{\overline{\sigma}\sigma_2\sigma_3}_{\mathbf{kpq}}\right)^* \propto \delta_{\sigma\overline{\sigma}}, \tag{3.65}$$

demands selection rules for which fields couple to which. For example, $M^{\sigma\sigma_2\sigma_3}_{\mathbf{kpq}}$ describes the coupling of σ_2 and σ_3 into the equation for σ, so $\sigma \leftarrow \sigma_2+\sigma_3$. Analogously $M^{\sigma_2\sigma_3\overline{\sigma}}_{\mathbf{pqk}}$ describes $\sigma_2 \leftarrow \sigma_3+\overline{\sigma}$. A sufficient condition to satisfy both the diagonality of Σ and of F is: if the coupling $\sigma \leftarrow \sigma_2+\sigma_3$ is allowed, then $\sigma_2+\sigma_3$ must not be able to couple into any other fields; furthermore in any sources for σ_2 and σ_3 involving each other, the only other allowed field is the original σ. This is analogous to the wave-vector triad constraint $\mathbf{k}+\mathbf{p}+\mathbf{q}=\mathbf{0}$ and is illustrated in figure 3.1.

Consider our ZAKTPD equations before enveloping: (3.19) and (3.27). Without the TPD non-linearity, the non-zero coupling coefficients for that system will be:

$$M^{\phi n\phi}, M^{n\phi\phi}, \tag{3.66}$$

[15]The fact that all wave-vectors now enter symmetrically is due to the complex conjugates in the primitive equation. Contrast this against e.g. $\mathbf{k}=\mathbf{p}+\mathbf{q}$ which appears in (3.48).



(a) Wave-vector constraint (b) Field species constraint

Figure 3.1: Illustration of the wave-vector and field species coupling constraints leading to the diagonalisation of the DIA.

and their symmetric equivalents, representing the interactions:

$$\begin{aligned} \phi &\leftarrow n + \phi, \\ n &\leftarrow \phi + \phi, \end{aligned} \tag{3.67}$$

These obey the field species constraint and allow the DIA for this system to be diagonal leading to the two responses $R_{(\mathbf{k},\phi)}$, $R_{(\mathbf{k},n)}$, and two covariances $C_{(\mathbf{k},\phi)}$ and $C_{(\mathbf{k},n)}$ being the only non-zero ones. Introducing the complex envelope $\phi \rightarrow \psi$ implies a move from $C_{(\mathbf{k},\phi)}$ to $C_{\mathbf{k}}^{\psi\psi^\dagger}$ for the spectrum, and $R_{(\mathbf{k},\phi)} \rightarrow R_{\mathbf{k}}^{\psi\psi}$ for the response. All other quantities will still vanish due to the argument above. This is the symmetric ensemble of DuBois & Rose (1981).

Including the TPD source term introduces another coupling $M^{\phi v\phi}$ describing $\phi \leftarrow v + \phi$, which breaks the species interaction constraint and will lead to off-diagonal terms such as:

$$\Sigma_{\mathbf{k}}^{nv} = -\sum_{\mathbf{k}+\mathbf{p}+\mathbf{q}=\mathbf{0}} \tfrac{1}{2} M_{\mathbf{kpq}}^{n\phi\phi} \left(M_{\mathbf{pqk}}^{\phi\phi v}\right)^* R_{(\mathbf{p},\phi)}^* C_{(\mathbf{q},\phi)}^*. \tag{3.68}$$

The extent to which this will break the symmetry remains to be assessed. The term above is just one example of a non-zero off-diagonal term. It is doubtful this is important because if the turbulent decorrelation due to the large amount of SLT fluctuations is to be appreciable, then it must be so with respect to the typical non-linear rate of the TPD coupling. This implies that the contributions to Σ due to terms involving the TPD non-linearity must be small compared to those in the original Zakharov system. See section 3.4.

3.3.2 Governing equations

The symmetry arguments from the previous subsection allow us to consider only the covariances $C^{\psi\psi^\dagger}$, C^{nn}, together with the laser spectrum $C^{\xi^\mu\xi^{\dagger\nu}}$ which I denote by $I_{\mathbf{q}}^{\mu\nu} \doteq C_{\mathbf{q}}^{\xi^\mu\xi^{\dagger\nu}}$. Similarly, we need only the two responses $R^{\psi\psi}$, and $\widehat{R}^{nn}$[16]. The

[16]The hat is used to signify that this is a response different from the R^{nn} function in the usual DIA notation. $\widehat{R}^{nn}$ obeys a second-order in time equation. See footnote 12 and appendix B.

derivation of the equations is not particularly illuminating, but the calculations are given in appendix B. I state the results below.

For the Langmuir response and spectrum one has:

$$(\partial_t + \mathrm{i}\delta\omega_{\mathbf{k}})\, R^{\psi\psi}_{\mathbf{k}}(t;t') + \int_{t'}^{t} \mathrm{d}\bar{t}\; \Sigma^{\psi\psi}_{\mathbf{k}}(t;\bar{t})\, R^{\psi\psi}_{\mathbf{k}}(\bar{t};t') = \delta(t-t'), \tag{3.69}$$

$$\begin{aligned}(\partial_t + \mathrm{i}\delta\omega_{\mathbf{k}})\, C^{\psi\psi^\dagger}_{\mathbf{k}}(t,t') + \int_{-\infty}^{t} \mathrm{d}\bar{t}\; \Sigma^{\psi\psi}_{\mathbf{k}}(t;\bar{t})\, C^{\psi\psi^\dagger}_{\mathbf{k}}(\bar{t},t') \\ = \int_{-\infty}^{t'} \mathrm{d}\bar{t}\; F^{\psi\psi^\dagger}_{\mathbf{k}}(t,\bar{t})\, R^{\psi^\dagger\psi^\dagger}_{\mathbf{k}}(t';\bar{t}).\end{aligned} \tag{3.70}$$

The turbulent correction (or the self-energy) of the Langmuir response is:

$$\begin{aligned}\Sigma^{\psi\psi}_{\mathbf{k}}(t;t') = \sum_{\mathbf{k}=\mathbf{p}+\mathbf{q}} \Bigg\{ & \frac{\omega_{\mathrm{pe}}^2}{4} \frac{(\mathbf{k}\cdot\mathbf{p})^2}{k^2 p^2}\, R^{\psi\psi}_{\mathbf{p}}(t;t')\, C^{nn}_{\mathbf{q}}(t,t') \\ & - \frac{\mathrm{i}\omega_{\mathrm{pe}} c_s^2}{2} \frac{p^2(\mathbf{k}\cdot\mathbf{q})^2}{k^2} \widehat{R}^{nn}_{\mathbf{p}}(t;t')\, C^{\psi\psi^\dagger}_{\mathbf{q}}(t,t') \\ & - \gamma_0^2 \frac{\left(k^2-p^2\right)^2}{k^2 p^2} \frac{k_\mu k_\nu}{k_0^2} e^{-\mathrm{i}\Omega(t-t')}\, R^{\psi^\dagger\psi^\dagger}_{\mathbf{p}}(t;t')\, I^{\mu\nu}_{\mathbf{q}}(t,t') \Bigg\}.\end{aligned} \tag{3.71}$$

The first two terms arise from the ion non-linearity, and up to different normalisations and sign conventions, are identical to those of DuBois & Rose (1981). This is of course true for all other expressions which I am about to give. These terms contain the Langmuir modulational instability as well as the Langmuir decay instability. The last term is new, and is the contribution of the TPD non-linearity to the Langmuir turbulent correction. It is what gives rise to the usual TPD growth rate in the linear regime. The non-linear source $F^{\psi\psi^\dagger}$ in the covariance equation is:

$$\begin{aligned}F^{\psi\psi^\dagger}_{\mathbf{k}}(t,t') = \sum_{\mathbf{k}=\mathbf{p}+\mathbf{q}} \Bigg\{ & \frac{\omega_{\mathrm{pe}}^2}{4} \frac{(\mathbf{k}\cdot\mathbf{p})^2}{k^4}\, C^{\psi\psi^\dagger}_{\mathbf{p}}(t,t')\, C^{nn}_{\mathbf{q}}(t,t') \\ & + \gamma_0^2 \frac{\left(k^2-p^2\right)^2}{k^4} \frac{k_\mu k_\nu}{k_0^2} e^{-\mathrm{i}\Omega(t-t')}\, C^{\psi^\dagger\psi}_{\mathbf{p}}(t,t')\, I^{\mu\nu}_{\mathbf{q}}(t,t') \Bigg\},\end{aligned} \tag{3.72}$$

with the TPD contribution being the second term. Due to the property $\psi^\dagger_{\mathbf{k}} = \psi^*_{-\mathbf{k}}$ the quantities $R^{\psi^\dagger\psi^\dagger}$ and $C^{\psi^\dagger\psi}$ obey a simple relationship:

$$R^{\psi^\dagger\psi^\dagger}_{\mathbf{k}} = \left(R^{\psi\psi}_{-\mathbf{k}}\right)^*, \qquad C^{\psi^\dagger\psi}_{\mathbf{k}} = \left(C^{\psi\psi^\dagger}_{-\mathbf{k}}\right)^*, \tag{3.72a,b}$$

and are therefore determined by the equations given so far. The ion response and covariance are governed by:

$$\left(\partial_t^2 + c_s^2 k^2\right) \widehat{R}^{nn}_{\mathbf{k}}(t;t') + \int_{t'}^{t} \mathrm{d}\bar{t}\; \widehat{\Sigma}^{nn}_{\mathbf{k}}(t;\bar{t})\, \widehat{R}^{nn}_{\mathbf{k}}(\bar{t};t') = \delta(t-t'), \tag{3.73}$$

$$\left(\partial_t^2 + c_s^2 k^2\right) C^{nn}_{\mathbf{k}}(t,t') + \int_{-\infty}^{t} \mathrm{d}\bar{t}\; \widehat{\Sigma}^{nn}_{\mathbf{k}}(t;\bar{t})\, C^{nn}_{\mathbf{k}}(\bar{t},t') = \int_{-\infty}^{t'} \mathrm{d}\bar{t}\; \widehat{F}^{nn}_{\mathbf{k}}(t,\bar{t})\, \widehat{R}^{nn}_{\mathbf{k}}(t';\bar{t}), \tag{3.74}$$

with the turbulent correction:

$$\widehat{\Sigma}^{nn}_{\mathbf{k}}(t;t') = \sum_{\mathbf{k}=\mathbf{p}+\mathbf{q}} \frac{\mathrm{i}\omega_{\mathrm{pe}}c_s^2}{2}\frac{k^2\,(\mathbf{p}\cdot\mathbf{q})}{p^2}\left[R^{\psi^\dagger\psi^\dagger}_{\mathbf{p}}(t;t')\,C^{\psi\psi^\dagger}_{\mathbf{q}}(t,t') - R^{\psi\psi}_{\mathbf{p}}(t;t')\,C^{\psi^\dagger\psi}_{\mathbf{q}}(t,t')\right], \quad (3.75)$$

and non-linear source:

$$\widehat{F}^{nn}_{\mathbf{k}}(t,t') = \sum_{\mathbf{k}=\mathbf{p}+\mathbf{q}} c_s^4 k^4\,(\mathbf{p}\cdot\mathbf{q})^2\,C^{\psi\psi^\dagger}_{\mathbf{p}}(t,t')\,C^{\psi^\dagger\psi}_{\mathbf{q}}(t,t'). \quad (3.76)$$

Let me now discuss how the equations will be used. In principle, this is a full self-consistent description of the turbulence: energy enters through the TPD terms in the self-energy $\Sigma^{\psi\psi}$ and the non-linear source $F^{\psi\psi^\dagger}$, stirring up fluctuations. The responses of the two fields in the system $R^{\psi\psi}$ and $\widehat{R}^{nn}$ and the evolution of their fluctuations $C^{\psi\psi^\dagger}$ and C^{nn} have been determined in terms of each other, thereby completing the goal of the closure procedure. But in light of the inadequacy of the DIA to treat coherent phenomena such as Langmuir collapse, naturally one may question the purpose of the present exercise. The logic is as follows.

The goal here is to study the injection of power by the TPD terms, for which I will argue that the DIA is appropriate. In a similar way to how the fluid equations we started from work well for the system apart from the latest stages of collapse, it is possible for the present DIA equations to be an appropriate description for those modes which are involved in the TPD interaction. Suppose then that one is not overly concerned with trying to *predict* the detailed properties of the fluctuation spectra $C^{\psi\psi^\dagger}$ and C^{nn} which the DIA is in theory meant to provide, but instead considers these as a prescribed *turbulent background* on top of which the TPD process occurs – either specifying those details oneself using physical insight and/or simulation, or ignoring them altogether[17]. The primary effect we are looking for is the modification of the response of the modes involved in TPD by the turbulent background. So the question of the appropriateness of the DIA in studying power injection has two components: (i.) are the TPD terms accurate, and (ii.) are the responses entering the TPD terms accurate as predicted by the DIA. Answering in the affirmative to the first is argued on the basis that the three modes involved in TPD should all evolve in a highly stochastic manner – the incoming laser field is broadband and fluctuating, and similarly for the two propagating Langmuir modes due to their interaction with the background turbulence, i.e. the sea of density depressions and trapped modes. (ii.) is more subtle: it is essentially asking whether *given* the spectra of the sea of coherent structures (the cavitons), such as the one shown in figure 3.2, are the

[17] I shall not necessarily pursue this here but one may formalise this by splitting the fluctuations into two components – one which is indeed prescribed, and one which is actually evolved self-consistently.

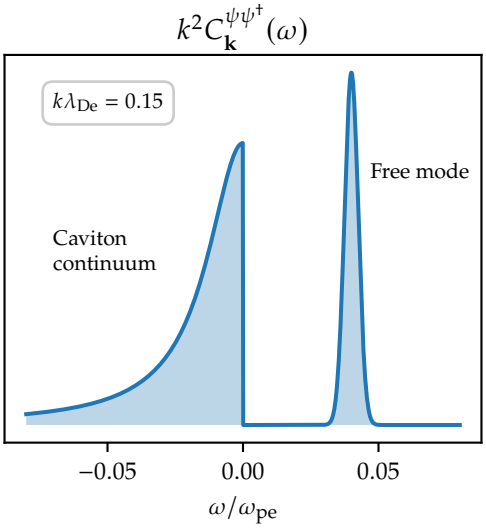


Figure 3.2: An illustration of a typical Langmuir frequency spectrum observed in simulations of the SLT state showing a free mode near $\delta\omega_{\mathbf{k}}$ as well as a *caviton continuum* of bound states having $\omega < \omega_{pe}$ (which because of enveloping corresponds to $\omega < 0$).

responses predicted by the DIA accurate for modes interacting with that sea. It is difficult to give a definitive answer, but it has been argued that the DIA may be appropriate in such cases (see 5.2 and 10.5 of Krommes, 2002). I will proceed with that assumption.

As illustrated in figure 3.2, a typical SLT state consists of bound Langmuir modes trapped in cavities having frequencies less than the local plasma frequency, as well as freely propagating Langmuir modes. I will be working under the assumption that TPD couples the external laser field predominantly to the freely propagating modes for which the sea of cavities indeed represents a *turbulent background*. Simulations show strong spectral signatures at the wave numbers for which linear theory predicts strongest TPD growth (Vu *et al.*, 2010, 2012*a*,*b*, 2014; Myatt *et al.*, 2013, 2014). These are by definition freely propagating.

The possibility of TPD coupling to bound states (Russell *et al.*, 1986) should not be dismissed easily though. Consider first a monochromatic laser with a well-defined frequency ω_0. At low densities (further away from the quarter critical), the detuning Ω grows, and so Langmuir modes need to have frequencies larger than the plasma frequency in order to couple to the laser. Therefore coupling from the laser to two bound modes will not be possible, except maybe very near $n_c/4$. It might be possible that TPD can couple to a bound mode, plus a freely propagating one. Laser bandwidth will change all of this since it will also allow a broader range of Langmuir modes to frequency match to it.

3.3.3 Spectral balance and total power injected by TPD

Power input will be captured by the evolution of the energy density $\mathscr{E}_{\mathbf{k}}(t) \doteq \overline{|\mathbf{E}_{\mathbf{k}}(t)|^2}$, which in terms of the quantities appearing in the DIA equations, is given by:

$$\mathscr{E}_{\mathbf{k}}(t) = C_{\mathbf{k}}^{EE^\dagger}(t,t) = k^2 C_{\mathbf{k}}^{\psi\psi^\dagger}(t,t), \tag{3.77}$$

where $\mathbf{E} = -\boldsymbol{\nabla}\psi$ is the Langmuir electric field envelope. The time evolution of this quantity can be expressed as follows:

$$\partial_t C_{\mathbf{k}}^{\psi\psi^\dagger}(t,t) = \partial_t C_{\mathbf{k}}^{\psi\psi^\dagger}(t,t')\Big|_{t'=t} + \partial_t C_{\mathbf{k}}^{\psi\psi^\dagger}(t',t)\Big|_{t'=t}. \tag{3.78}$$

By definition:

$$C_{\mathbf{k}}^{\psi\psi^\dagger}(t',t) = \overline{\psi_{\mathbf{k}}(t')\psi_{-\mathbf{k}}^\dagger(t)} = \overline{\psi_{-\mathbf{k}}^\dagger(t)\psi_{\mathbf{k}}(t')} = C_{-\mathbf{k}}^{\psi^\dagger\psi}(t,t') = \left[C_{\mathbf{k}}^{\psi\psi^\dagger}(t,t')\right]^*. \tag{3.79}$$

Therefore:

$$\partial_t C_{\mathbf{k}}^{\psi\psi^\dagger}(t,t) = 2\,\mathrm{Re}\left[\partial_t C_{\mathbf{k}}^{\psi\psi^\dagger}(t,t')\Big|_{t'=t}\right]. \tag{3.80}$$

In light of the discussion regarding not being overly concerned with minute details of the spectra, a step in that direction is to consider separating the time dependence of the covariances from the equal time intensities:

$$C_{\mathbf{k}}^{\psi\psi^\dagger}(t,t') = C_{\mathbf{k}}^{\psi\psi^\dagger}(t,t)\, G_{\mathbf{k}}^{\psi\psi}(t,t') = k^{-2}\mathscr{E}_{\mathbf{k}}(t)\, G_{\mathbf{k}}^{\psi\psi}(t,t'), \tag{3.81}$$

$$C_{\mathbf{k}}^{nn}(t,t') = C_{\mathbf{k}}^{nn}(t,t)\, G_{\mathbf{k}}^{nn}(t,t') \quad = \mathscr{N}_{\mathbf{k}}(t)\, G_{\mathbf{k}}^{nn}(t,t'), \tag{3.82}$$

$$I_{\mathbf{k}}^{\mu\nu}(t,t') = I_{\mathbf{k}}^{\mu\nu}\, G_{\mathbf{k}}^{\xi\xi}(t,t'), \tag{3.83}$$

where the equal time density covariance has been defined to be $\mathscr{N}_{\mathbf{k}}(t) \doteq C_{\mathbf{k}}^{nn}(t,t)$. This anticipates an approximation I will make later on in which I will set the time dependence of the Langmuir spectrum to be equal to the time dependence of the response function: $G_{\mathbf{k}}^{\psi\psi}(t,t') = R_{\mathbf{k}}^{\psi\psi}(t,t')$. This is part of the procedure which Markovianises the DIA and is referred to as a fluctuation-dissipation ansatz due to it holding true in thermal equilibrium (Bowman *et al.*, 1993)[18]. A useful idea to keep in mind is that the functions G give the frequency part of the power spectrum. In a steady state where quantities depend only on $\tau = t - t'$ a Fourier transformation gives for example:

$$C_{\mathbf{k}}^{\psi\psi^\dagger}(\omega) = k^{-2}\mathscr{E}_{\mathbf{k}}\, G_{\mathbf{k}}^{\psi\psi}(\omega). \tag{3.84}$$

The covariance equation (3.70) then turns into the spectral balance equation:

$$\partial_t \mathscr{E}_{\mathbf{k}}(t) + 2\eta_{\mathbf{k}}(t)\,\mathscr{E}_{\mathbf{k}}(t) - 2\Gamma_{\mathbf{k}}^{\mathrm{tpd}}(t)\,\mathscr{E}_{\mathbf{k}}(t) = 2\mathscr{F}_{\mathbf{k}}^{\mathrm{ion}}(t) + 2\mathscr{F}_{\mathbf{k}}^{\mathrm{tpd}}(t), \tag{3.85}$$

[18] See sub-section 2.2.4.

where $\eta_{\mathbf{k}}$ is the turbulent damping of Langmuir modes:

$$\eta_{\mathbf{k}}(t) = \mathrm{Re} \sum_{\mathbf{k}=\mathbf{p}+\mathbf{q}} \left\{ \frac{\omega_{\mathrm{pe}}^2}{4} \frac{(\mathbf{k}\cdot\mathbf{p})^2}{k^2 p^2} \Theta_{\mathbf{pqk}}^{\psi n \psi}(t)\, \mathscr{N}_{\mathbf{q}}(t) - \frac{\mathrm{i}\omega_{\mathrm{pe}} c_s^2}{2} \frac{p^2 (\mathbf{k}\cdot\mathbf{q})^2}{k^2 q^2} \Theta_{\mathbf{pqk}}^{n\psi\psi}(t)\, \mathscr{E}_{\mathbf{q}}(t) \right\}, \quad (3.86)$$

and $\Gamma_{\mathbf{k}}^{\mathrm{tpd}}(t)$ is a quantity which may be interpreted as the non-linear TPD growth rate:

$$\Gamma_{\mathbf{k}}^{\mathrm{tpd}}(t) = \sum_{\mathbf{k}=\mathbf{q}-\mathbf{p}} \gamma_0^2 \frac{\left(k^2 - p^2\right)^2}{k^2 p^2} \frac{k_\mu k_\nu}{k_0^2} I_{\mathbf{q}}^{\mu\nu}\, \mathrm{Re}\, \Theta_{\mathbf{pqk}}^{\mathrm{tpd}}(t). \quad (3.87)$$

The source function related to the ion non-linearity is denoted by $\mathscr{F}_{\mathbf{k}}^{\mathrm{ion}}$ and to the TPD one by $\mathscr{F}_{\mathbf{k}}^{\mathrm{tpd}}$:

$$\mathscr{F}_{\mathbf{k}}^{\mathrm{ion}}(t) = \mathrm{Re} \sum_{\mathbf{k}=\mathbf{q}-\mathbf{p}} \frac{\omega_{\mathrm{pe}}^2}{4} \frac{(\mathbf{k}\cdot\mathbf{q})^2}{k^2 q^2} \Theta_{\mathbf{kqp}}^{\psi^\dagger n \psi^\dagger}(t)\, \mathscr{N}_{\mathbf{p}}(t)\, \mathscr{E}_{\mathbf{q}}(t) \quad (3.88)$$

$$\mathscr{F}_{\mathbf{k}}^{\mathrm{tpd}}(t) = \mathrm{Re} \sum_{\mathbf{q}=\mathbf{k}+\mathbf{p}} \gamma_0^2 \frac{\left(k^2 - p^2\right)^2}{k^2 p^2} \frac{k_\mu k_\nu}{k_0^2} I_{\mathbf{q}}^{\mu\nu}\, \Theta_{\mathbf{kqp}}^{\mathrm{tpd}}(t)\, \mathscr{E}_{\mathbf{p}}(t). \quad (3.89)$$

Notice that now all of the time history captured by the DIA is packaged up into the Θ functions which can be interpreted as measuring the *triad interaction time* between the modes involved in each interaction. For the TPD process, this is:

$$\Theta_{\mathbf{pqk}}^{\mathrm{tpd}}(t) = \int_{-\infty}^{t} \mathrm{d}\bar{t}\; e^{-\mathrm{i}\Omega(t-\bar{t})} \left[R_{\mathbf{p}}^{\psi\psi}(t;\bar{t}) \right]^* G_{\mathbf{q}}^{\xi\xi}(t,\bar{t}) \left[G_{\mathbf{k}}^{\psi\psi}(t,\bar{t}) \right]^*, \quad (3.90)$$

while for the others I have adopted the following convention:

$$\Theta_{\mathbf{pqk}}^{\sigma_1\sigma_2\sigma_3}(t) = \int_{-\infty}^{t} \mathrm{d}\bar{t}\; R_{\mathbf{p}}^{\sigma_1\sigma_1}(t;\bar{t})\, G_{\mathbf{q}}^{\sigma_2\sigma_2}(t,\bar{t}) \left[G_{\mathbf{k}}^{\sigma_3\sigma_3}(t,\bar{t}) \right]^*. \quad (3.91)$$

It's good to emphasise that no approximations have been made thus far.

From the spectral balance equation we can compute the total power injected by TPD. A crucial fact is that the DIA is a closure which conserves energy. Since the ion non-linear term only serves to shuffle energy around the system, it can be shown that:

$$\sum_{\mathbf{k}} \left\{ \eta_{\mathbf{k}}(t)\, \mathscr{E}_{\mathbf{k}}(t) - \mathscr{F}_{\mathbf{k}}^{\mathrm{ion}}(t) \right\} = 0. \quad (3.92)$$

Therefore:

$$\sum_{\mathbf{k}} \partial_t \mathscr{E}_{\mathbf{k}} = 2 \sum_{\mathbf{k}} \left\{ \Gamma_{\mathbf{k}}^{\mathrm{tpd}}(t)\, \mathscr{E}_{\mathbf{k}}(t) + \mathscr{F}_{\mathbf{k}}^{\mathrm{tpd}}(t) \right\} \doteq \mathscr{P}_{\mathrm{tpd}}, \quad (3.93)$$

with $\mathscr{P}_{\mathrm{tpd}}$ being the total (space averaged) power injected by the two-plasmon decay. Strictly speaking, no steady state exists under this spectral balance equation ($\sum_{\mathbf{k}} \partial_t \mathscr{E}_{\mathbf{k}} > 0$) since we have not included any dissipation physics – neither linear damping mechanisms

(collisional or Landau), nor some exotic kinetic physics associated with the arrest of collapse. But that is immaterial as to whether $\mathscr{P}_{\text{tpd}}$ is accurate, which as I have argued, there are good reasons to believe it is. Note that upon performing the $\mathbf{k}$ sums, the non-linear TPD source function term would be almost identical to the coherent one:

$$\sum_{\mathbf{k}} \Gamma^{\text{tpd}}_{\mathbf{k}}(t)\, \mathscr{E}_{\mathbf{k}}(t) = \sum_{\mathbf{k},\mathbf{p},\mathbf{q}} \delta_{\mathbf{q},\mathbf{k}+\mathbf{p}}\, \gamma_0^2 \frac{\left(k^2-p^2\right)^2}{k^2p^2} \frac{k_\mu k_\nu}{k_0^2}\, I^{\mu\nu}_{\mathbf{q}}\, \mathscr{E}_{\mathbf{k}}(t)\, \text{Re}\, \Theta^{\text{tpd}}_{\mathbf{pqk}}(t), \tag{3.94}$$

$$\sum_{\mathbf{k}} \mathscr{F}^{\text{tpd}}_{\mathbf{k}}(t) = \sum_{\mathbf{k},\mathbf{p},\mathbf{q}} \delta_{\mathbf{q},\mathbf{k}+\mathbf{p}}\, \gamma_0^2 \frac{\left(k^2-p^2\right)^2}{k^2p^2} \frac{k_\mu k_\nu}{k_0^2}\, I^{\mu\nu}_{\mathbf{q}}\, \mathscr{E}_{\mathbf{p}}(t)\, \text{Re}\, \Theta^{\text{tpd}}_{\mathbf{kqp}}(t), \tag{3.95}$$

were it not for the fact that the current exact form of the interaction time is not symmetric under the swap of $\mathbf{k} \leftrightarrow \mathbf{p}$, i.e. the wave numbers of the two Langmuir modes involved in the decay. Under the approximation $G^{\psi\psi}_{\mathbf{k}} = R^{\psi\psi}_{\mathbf{k}}$, it will be.

A key conclusion from this discussion is that the central problem is one of determining the interaction time for the modes involved in the TPD interaction. This is the task which I shall take up now.

3.4 Estimate of the non-linear growth rate and the injected power under a Markovian approximation

The approximation $G^{\psi\psi}_{\mathbf{k}} = R^{\psi\psi}_{\mathbf{k}}$ allows us to develop a useful result for the triad interaction time. As previously mentioned, what this means is that we assume that the covariance decays in the same way as the response function. This can be used to develop a Markovian approximation derived from the DIA as shown by Bowman *et al.* (1993). The procedure works as follows.

Notice that the spectral balance equation (3.85) is an equation involving quantities evaluated at a single time t. The interaction history has been packaged up into the interaction time. This looks like a Markovian approximation, and in fact, an equation of the exact same form can be derived if one makes the substitutions:

$$\Sigma^{\psi\psi}_{\mathbf{k}}(t;t') = \widehat{\eta}_{\mathbf{k}}(t)\, \delta(t-t'), \tag{3.96}$$

$$F^{\psi\psi^\dagger}_{\mathbf{k}}(t,t') = \widehat{\mathscr{F}}_{\mathbf{k}}(t)\, \delta(t-t'), \tag{3.97}$$

into the covariance equation (3.70). To then obtain an equation for the response, i.e. equation (3.69), which does not involve time history, we chose to apply the first of those relations to it, resulting in:

$$\left(\partial_t + \mathrm{i}\delta\omega_{\mathbf{k}}\right) R^{\psi\psi}_{\mathbf{k}}(t;t') + \widehat{\eta}_{\mathbf{k}}(t)\, R^{\psi\psi}_{\mathbf{k}}(t;t') = \delta(t-t'), \tag{3.98}$$

where[19]

$$\mathrm{Re}\,\widehat{\eta}_{\mathbf{k}}(t) = \eta_{\mathbf{k}}(t) - \Gamma^{\mathrm{tpd}}_{\mathbf{k}}(t). \tag{3.99}$$

Suppose now that we are strictly investigating the steady state, so all quantities of the form $f(t,t')$ are functions of $t-t'$ only, and those evaluated at a single time $f(t)$ are constant. For a steady state to exist at all, all modes must be damped, and hence $\widehat{\eta}_{\mathbf{k}} > 0$. Let us also further assume that $\eta_{\mathbf{k}} \gg \Gamma^{\mathrm{tpd}}_{\mathbf{k}}$, and ignore any frequency shift which might arise from the imaginary parts of the defining expression for $\eta_{\mathbf{k}}$. The equation for the response is easily solved:

$$R^{\psi\psi}_{\mathbf{k}}(t;t') = H(t-t')e^{-\mathrm{i}\delta\omega_{\mathbf{k}}(t-t')-\eta_{\mathbf{k}}(t-t')}. \tag{3.100}$$

The fact that $\eta_{\mathbf{k}} \gg \Gamma^{\mathrm{tpd}}_{\mathbf{k}}$ is possible and likely to hold well is an important point. In a strongly turbulent system, the damping $\eta_{\mathbf{k}}$ must be significant. If that damping overwhelms the TPD growth rate, how could it be that there is a steady state at all? The response function measures the evolution of a test perturbation in time. But whether that decays or grows does not determine whether the overall fluctuation level at that wave number decays or grows. This is evident from the spectral balance equation, where one can see that in order to maintain the fluctuation level, the ion source $\mathscr{F}^{\mathrm{ion}}_{\mathbf{k}}$ must be such that it (mostly) balances the strong damping arising from $\eta_{\mathbf{k}}$. Finally, the form of (3.100), which describes a damped, freely propagating Langmuir mode, suggests that this Markovian approximation should be applicable to the respective freely propagating part of the spectrum, and not the trapped modes inside the cavities. Therefore even though we are proceeding with the Markov version of the responses in the evaluation of $\Gamma^{\mathrm{tpd}}_{\mathbf{k}}$, to the extent that one is concerned with features in the spectra arising from the caviton background, the damping that enters them, $\eta_{\mathbf{k}}$, should not be evaluated with those Markovian responses.

In any case, the TPD triad interaction time now becomes remarkably simple[20]:

$$\Theta^{\mathrm{tpd}}_{\mathbf{pqk}} = \int_0^\infty \mathrm{d}\tau\, e^{-\mathrm{i}\Omega\tau} \left[R^{\psi\psi}_{\mathbf{p}}(\tau)\right]^* G^{\xi\xi}_{\mathbf{q}}(\tau) \left[R^{\psi\psi}_{\mathbf{k}}(\tau)\right]^*, \tag{3.101}$$

If one defines $\delta\omega^{\mathrm{em}}_{\mathbf{q}}$ to be the deviation from the central laser envelope ω_0 frequency, then the response $R^{\xi\xi}$ is:

$$R^{\xi\xi}_{\mathbf{q}}(\tau) = H(\tau)\, e^{-\mathrm{i}\delta\omega^{\mathrm{em}}_{\mathbf{q}}\tau}. \tag{3.102}$$

[19] There are operators for taking the real part inside of the definitions for $\eta_{\mathbf{k}}$ and $\Gamma^{\mathrm{tpd}}_{\mathbf{k}}$. $\widehat{\eta}_{\mathbf{k}}$ is defined by the same expressions but excluding those operators.

[20] In a steady state, $R(\tau)$ can be taken to mean $R(\tau;0)$.

It is easy to show that $G^{\xi\xi}_{\mathbf{q}} = R^{\xi\xi}_{\mathbf{q}}$ holds exactly for the laser envelope due to it obeying its linear equation of motion. The interaction time is then:

$$\begin{aligned}\Theta^{\text{tpd}}_{\mathbf{pqk}} &= \int_0^\infty \mathrm{d}\tau\; e^{-\mathrm{i}\left(\delta\omega^{\text{em}}_{\mathbf{q}} - \delta\omega_{\mathbf{p}} - \delta\omega_{\mathbf{k}} + \Omega\right)\tau - \left(\eta_{\mathbf{p}} + \eta_{\mathbf{k}}\right)\tau} \\ &= \frac{1}{\mathrm{i}\left(\delta\omega^{\text{em}}_{\mathbf{q}} - \delta\omega_{\mathbf{p}} - \delta\omega_{\mathbf{k}} + \Omega\right) + \left(\eta_{\mathbf{p}} + \eta_{\mathbf{k}}\right)}.\end{aligned} \tag{3.103}$$

This makes the non-linear TPD growth rate equal to:

$$\Gamma^{\text{tpd}}_{\mathbf{k}} = \sum_{\mathbf{k}=\mathbf{q}-\mathbf{p}} \gamma_0^2 \frac{\left(k^2 - p^2\right)^2}{k^2 p^2} \frac{k_\mu k_\nu}{k_0^2} I^{\mu\nu}_{\mathbf{q}} \frac{\eta_{\mathbf{p}} + \eta_{\mathbf{k}}}{\left(\delta\omega^{\text{em}}_{\mathbf{q}} - \delta\omega_{\mathbf{p}} - \delta\omega_{\mathbf{k}} + \Omega\right)^2 + \left(\eta_{\mathbf{p}} + \eta_{\mathbf{k}}\right)^2}. \tag{3.104}$$

So we see that the interaction time plays the role of a broadened resonance function. In the limit of no turbulent damping $\eta \to 0$, the growth rate tends to:

$$\Gamma^{\text{tpd}}_{\mathbf{k}} = \sum_{\mathbf{k}=\mathbf{q}-\mathbf{p}} \gamma_0^2 \frac{\left(k^2 - p^2\right)^2}{k^2 p^2} \frac{k_\mu k_\nu}{k_0^2} I^{\mu\nu}_{\mathbf{q}}\, \pi\delta\left(\delta\omega^{\text{em}}_{\mathbf{q}} - \delta\omega_{\mathbf{p}} - \delta\omega_{\mathbf{k}} + \Omega\right). \tag{3.105}$$

The delta function serves to enforce frequency matching between the three modes involved in TPD. This is essentially the broadband TPD growth rate reported in Ruskov *et al.* (2024), and is relevant to the linear regime of the instability when driven by a broad bandwidth laser field. I will explore interesting aspects of the linear problem in the next chapter.

Suppose the laser field is comprised of a single temporally incoherent beam (Goodman, 2015). This is usually described in terms of a frequency spectrum, which for the purposes of a scaling estimate can be taken to be, say, a Lorentzian:

$$\hat{I}(\omega) = \frac{1}{\pi} \frac{\Delta\omega/2}{\omega^2 + (\Delta\omega/2)^2}. \tag{3.106}$$

If the beam is propagating along $\mathbf{k}_0$ and is polarised along some direction $\mathbf{e}_0$, then the spread in $\mathbf{q}$ of the spectrum is entirely in the direction of propagation $\mathbf{k}_0$, and so we then have:

$$I^{\mu\nu}_{\mathbf{q}} = e_0^\mu e_0^\nu\, \hat{I}\left(\delta\omega^{\text{em}}_{\mathbf{q}}\right)\, \delta_{\mathbf{q}_\perp,\mathbf{0}}, \tag{3.107}$$

with $\mathbf{q}_\perp = \mathbf{q} - (\mathbf{q}\cdot\mathbf{k}_0)/k_0$. Again, for the purposes of a scaling estimate, details of the wave number dependence of the growth rate are unimportant. The wave number factors in the non-linear growth rate only serve to modulate it with the usual hyperbola shapes familiar from linear theory (see section 2.1). The laser spectrum obviously peaks at $\delta\omega^{\text{em}}_{\mathbf{q}} = 0$. For any given wave number of one of the Langmuir modes $\mathbf{k}$ there exists a $\mathbf{p}$, the wave number of the second Langmuir mode, which maximises the resonance

function. This occurs for $\delta\omega_{\mathbf{p}} + \delta\omega_{\mathbf{k}} = \Omega$. This factor is then convolved with the laser spectrum (see for example figure 4.1). Therefore the peak growth rates are[21]:

$$\bar{\Gamma} \sim \gamma_0^2 \sum_{\mathbf{q}} \frac{1}{\pi} \frac{\Delta\omega/2}{\left(\delta\omega_{\mathbf{q}}^{\mathrm{em}}\right)^2 + (\Delta\omega/2)^2} \frac{2\eta}{\left(\delta\omega_{\mathbf{q}}^{\mathrm{em}}\right)^2 + (2\eta)^2} \tag{3.108}$$

$$\simeq \gamma_0^2 \int_{-\infty}^{\infty} \mathrm{d}\omega \, \frac{1}{\pi} \frac{\Delta\omega/2}{\omega^2 + (\Delta\omega/2)^2} \frac{2\eta}{\omega^2 + (2\eta)^2} \tag{3.109}$$

$$= \frac{2\gamma_0^2}{\Delta\omega + 4\eta}. \tag{3.110}$$

Note that this has the form of:

$$\bar{\Gamma} = \tau_{\mathrm{eff}} \gamma_0^2, \qquad \tau_{\mathrm{eff}}^{-1} = \tau_{\mathrm{laser}}^{-1} + \eta + \eta, \tag{3.110a,b}$$

with $\tau_{\mathrm{laser}} = 2/\Delta\omega$ being the auto-correlation time for the Lorentzian spectrum. Note that τ_{eff} has the form of the inverse sum of the coherence times for each mode involved in the interaction. The scaling of the growth rate of a parametric instability with the bandwidth (or the coherence time) of the driver $\sim \gamma_0^2/\Delta\omega$ is well known (Thomson & Karush, 1974; Thomson, 1975; Laval *et al.*, 1976, 1977; DuBois *et al.*, 1992; Pesme *et al.*, 1992). We see that in a strongly turbulent system, since the modes involved experience decoherence due to the turbulent background, that effective interaction time is further reduced by the turbulent damping rates.

Finally we can estimate the total injected power by:

$$\mathscr{P}_{\mathrm{tpd}} = 2 \sum_{\mathbf{k}} \left\{ \Gamma_{\mathbf{k}}^{\mathrm{tpd}} \mathscr{E}_{\mathbf{k}} + \mathscr{F}_{\mathbf{k}}^{\mathrm{tpd}} \right\} \tag{3.111}$$

$$= 4\bar{\Gamma} \sum_{\mathbf{k}} \mathscr{E}_{\mathbf{k}} \tag{3.112}$$

$$= 4\bar{\Gamma} \langle W \rangle \tag{3.113}$$

$$= \frac{8\gamma_0^2}{\Delta\omega + 4\eta} \langle W \rangle. \tag{3.114}$$

The second line follows from the fact that the interaction time $\Theta_{\mathbf{pqk}}^{\mathrm{tpd}}$ becomes symmetric in the first and last indices under the Markovian approximation, making the two terms equal to each other; see (3.94) and (3.95). Strictly speaking, the modes which contribute the most to the sum over wave number will be those for which the growth rate is significant. So technically $\langle W \rangle$ should be the space averaged energy of the free modes. Under the assumption that the free modes dominate the total energy content of the system, the distinction is of little consequence.

[21] With the sum being only over parallel $\mathbf{q}$, i.e. $\mathbf{q}_\perp = \mathbf{0}$.

3.5 Scalings of the injected power with laser intensity and bandwidth

In the case when all of the power injected by TPD (or at least some significant fraction of it) eventually ends up inside the collapsing caviton states, then $\mathscr{P}_{\text{tpd}}$ will be a good proxy for the total power going into hot electron production. This is due to the fact that the arrest of collapse is a strongly kinetic process in which all of the electrostatic energy contained in the caviton ends up being transferred to the electron population[22]. Hence obtaining scaling relations of $\mathscr{P}_{\text{tpd}}$ with the parameters of interest, which in this case would be the laser intensity I_{L} and bandwidth $\Delta\omega$, could potentially prove very useful.

The problem involves two parts. First, we need a model of how power is dissipated in order to provide the balance $\mathscr{P}_{\text{tpd}} = \mathscr{P}_{\text{out}}$. The dissipated power $\mathscr{P}_{\text{out}}$ will also be some function of the fluctuation level $\langle W \rangle$. Second, the dependence of $\mathscr{P}_{\text{tpd}}$ on the fluctuation level is non-trivial due to the turbulent damping η. Determining how η scales with $\langle W \rangle$ and then using the balance $\mathscr{P}_{\text{tpd}} = \mathscr{P}_{\text{out}}$ will set the overall scaling of the fluctuation level, and thus of the total injected power.

Let me address $\mathscr{P}_{\text{out}}$ first. I will employ the phenomenological model described in Robinson & Newman (1990) and later reviewed by Robinson (1997), which has found remarkable agreement with Zakharov simulations of strong Langmuir turbulence. The dissipated power is assumed to be of the form:

$$\mathscr{P}_{\text{out}} = N_c U / T_c, \tag{3.115}$$

where N_c is the number density of cavitons, U is the energy dissipated in each collapse event, and T_c is the time between collapses. The goal is to determine the scaling of these three quantities with the fluctuation level $\langle W \rangle$.

The number density of the cavitons is estimated as follows. In D spatial dimensions, $N_c \propto \ell^{-D}$, where ℓ is a typical separation between cavitons. One then assumes that individual collapse sites are relatively closely packed, and so the typical distance between them is of order their typical size ℓ_i at which collapse commences. Suppose the energy density inside such a site is W_i. Balancing the linear term with the non-linear one in the first Zakharov equation (see section 2.3), i.e. a rough condition for the onset of collapse, gives the typical initial size in terms of W_i:

$$\ell_i \propto W_i^{-1/2}. \tag{3.116}$$

[22] Virtually all of the energy in a caviton is contained in the fast electrostatic field associated with the electron motion. Research indicates that the damping mechanism responsible for the arrest of collapse is essentially a non-linear version of Landau damping, whereby electrons can be resonantly accelerated by the fields in the cavity (see Robinson, 1997, Section V.F).

The initial energy density at a given site is assumed to scale with the average energy $W_i \sim \langle W \rangle$, leading to:

$$\ell \propto \ell_i \propto W_i^{-1/2} \propto \langle W \rangle^{-1/2}. \tag{3.117}$$

Thus:

$$N_c \propto \langle W \rangle^{D/2}. \tag{3.118}$$

An argument based on the wave number which maximises the coherent modulational instability $k_{\max} \propto \langle W \rangle^{1/2}$ also gives the same result. The time between collapses can be estimated from a balance between the time derivative in the first Zakharov equation and the non-linearity, leading to:

$$T_c \propto \ell_i^{-2} \propto \langle W \rangle^{-1}. \tag{3.119}$$

Finally, U is assumed constant. This is based upon the assumption that collapse proceeds mostly subsonically. Combining all three gives:

$$\mathscr{P}_{\text{out}} \propto \langle W \rangle^{1+D/2}. \tag{3.120}$$

The physics of collapse is dimension dependent leading to the dissipated power being a function D. The dimension has been kept general since due to computational cost, it is common to perform simulations of TPD saturation in two, rather than three, dimensions potentially leading to different scalings of the measured quantities.

Another useful relation which may be obtained is to relate the average density fluctuation level $\langle n^2 \rangle$:

$$\langle n^2 \rangle = \sum_{\mathbf{k}} \mathcal{N}_{\mathbf{k}}, \tag{3.121}$$

to $\langle W \rangle$. A theoretical estimate can be obtained by averaging n^2 of a single collapsing caviton and multiplying by the number density of collapse sites N, resulting in:

$$\langle n^2 \rangle \propto \langle W \rangle^2. \tag{3.122}$$

In $3D$, numerically it was found that $\langle n^2 \rangle \simeq 0.4 \langle W \rangle^2$ (Robinson, 1997). In $2D$ there is a factor $\log(W_f / \langle W \rangle)$ involving the final energy density at arrest W_f for a single collapsing caviton.

Robinson & Newman (1990) have performed a detailed numerical study of Langmuir turbulence in which the Zakharov system was forced by a negative-damping driver, i.e. a specified linear growth rate $\Gamma_{\mathbf{k}}$ applied to each Langmuir mode. Their injected power

was then $\mathscr{P}_{\rm in} = \sum_{\mathbf{k}} \Gamma_{\mathbf{k}} \mathscr{E}_{\mathbf{k}} \sim \overline{\Gamma} \langle W \rangle$, which is identical in form to $\mathscr{P}_{\rm tpd}$ but with the crucial difference their $\overline{\Gamma}$ is independent of the turbulence. The resulting scalings they derive for how $\langle W \rangle$ scales with $\overline{\Gamma}$ are then obviously different, but their remarkable agreement with simulation gives us confidence that the scalings one obtains by substituting $\mathscr{P}_{\rm in} \to \mathscr{P}_{\rm tpd}$ might hold equally well, to the extent to which the model for $\mathscr{P}_{\rm tpd}$ is accurate.

I will now explore the scalings that follow from this substitution. Most importantly, we need to address the question of the scaling of the turbulent damping η with $\langle W \rangle$. Recall (3.86):

$$\eta_{\mathbf{k}}(t) = \sum_{\mathbf{k}=\mathbf{p}+\mathbf{q}} \left\{ \underbrace{\frac{\omega_{\rm pe}^2}{4} \frac{(\mathbf{k}\cdot\mathbf{p})^2}{k^2 p^2} \Theta^{\psi n \psi}_{\mathbf{pqk}}(t)\, \mathscr{N}_{\mathbf{q}}(t)}_{①} - \underbrace{\frac{\mathrm{i}\omega_{\rm pe} c_s^2}{2} \frac{p^2 (\mathbf{k}\cdot\mathbf{q})^2}{k^2 q^2} \Theta^{n\psi\psi}_{\mathbf{pqk}}(t)\, \mathscr{E}_{\mathbf{q}}(t)}_{②} \right\}, \tag{3.123}$$

and consider the scalings of the two terms:

$$① \propto \Theta \langle n^2 \rangle \propto \Theta \langle W \rangle^2, \tag{3.124}$$

$$② \propto \Theta p^2 \langle W \rangle \propto \Theta \ell_i^{-2} \langle W \rangle \propto \Theta \langle W \rangle^2, \tag{3.125}$$

where I have made use of the phenomenological scalings of Robinson & Newman (1990), relating the average square density fluctuation $\langle n^2 \rangle$ to $\langle W \rangle$, as well as the fact that the typical wave number scale at which the interaction between the free modes and the bound states in the cavitons is most efficient is near the nucleation scale $p \propto \ell_i^{-1} \propto \langle W \rangle^{1/2}$. In both cases the deviation from the usual linear scaling of the turbulent damping with the fluctuation level is due to the fact that here the preferred scale of the interactions described by η (i.e. between Langmuir and ion modes) changes with the fluctuation level.

I have also quietly assumed that the two interaction times are of similar order[23]. A reasonable candidate is $\Theta \sim T_c \propto \langle W \rangle^{-1}$, i.e. the interaction time is of order the collapse time. Another possibility is $\Theta \sim \eta^{-1}$. In reality, it is likely that the interaction time would be some combination of the two, such as $\Theta^{-1} \sim T_c^{-1} + \eta$, but both cases lead to the same overall scaling for η. This is:

$$\eta \propto \langle W \rangle, \tag{3.126}$$

[23] The observant reader may have noticed that $\Theta^{n\psi\psi}$ carries units of [time]^2. This is due to the ion response $\widehat{R}^{nn}$ which enters its defining expression (3.91) satisfying the second order in time equation (3.73). Therefore $\widehat{R}^{nn}$ is not dimensionless, but has $[\widehat{R}^{nn}] = [\text{time}]^{-1}$. The dimensional constants in ② take care of that obviously, but one may question the interpretation of that factor as an interaction time. Attempts to resolve that have led to some uninspiring technical complications which only seem to muddle the point. The point is that the Θ factor captures the time history in the DIA, and in the case of $\Theta^{n\psi\psi}$ should result in an overall term which characterises the typical time scales associated with that time history.

which is to be contrasted with the more common $\eta \propto C^{1/2}$ scaling for strong turbulence derived from $\eta \propto \theta C$ with $\theta \sim 1/\eta$ and C being the fluctuation level (see Krommes, 2002, section 4.2.6).

We can now explore the balance $\mathscr{P}_{\text{tpd}} = \mathscr{P}_{\text{out}}$:

$$\frac{I_{\text{L}}}{\Delta\omega + 4\eta}\langle W\rangle \propto \langle W\rangle^{1+D/2}. \tag{3.127}$$

Consider first the regime in which the bandwidth is negligible, so $\eta \gg \Delta\omega$. This would be the situation for TPD excited by a single monochromatic laser beam. Using the scaling for η we get for the fluctuation level:

$$\langle W\rangle \propto (I_{\text{L}})^{2/(2+D)} = \begin{cases} I_{\text{L}}^{1/2} & D = 2 \\ I_{\text{L}}^{2/5} & D = 3 \end{cases}. \tag{3.128}$$

Turning to the total injected power, notice that it does not depend on the fluctuation level in this regime, and is directly proportional to the intensity:

$$\mathscr{P}_{\text{tpd}} \propto \frac{I_{\text{L}}}{\eta}\langle W\rangle \propto I_{\text{L}}. \tag{3.129}$$

This interestingly does not depend on the specifics of the dissipation model, i.e. $\mathscr{P}_{\text{out}}$! It depends on SLT physics through the fact that the turbulent damping scales linearly with the fluctuation level.

Both particle-in-cell (Vu *et al.*, 2012*a*) and Zakharov simulations incorporating kinetic effects (Rovere *et al.*, 2023) report a linear scaling of the total hot electron flux with laser intensity when TPD is driven strongly above the inhomogeneity threshold, or equivalently a constant hot electron fraction (i.e. the fraction of laser power converted into hot electron flux). This is in agreement with (3.129). Simulations at ICF-relevant conditions also show a significant amount of collisional damping, and so $\mathscr{P}_{\text{tpd}}$ is balanced not just with $\mathscr{P}_{\text{out}}$ but also with a term $\nu_{ei}\langle W\rangle$ added to it[24]. Rovere *et al.* (2023) for example, report a roughly even split between collisional and Landau damping (i.e. $\mathscr{P}_{\text{out}}$) of the power injected by TPD. This does not invalidate the reasoning that the hot electron flux scales linearly with intensity due to the fact that $\mathscr{P}_{\text{out}} \propto \langle W\rangle^{1+D/2}$ scales much more strongly with the fluctuation level than does collisional damping. If at some given intensity they are comparable in magnitude, an increase in the injected power is predominantly supported by an increase in $\mathscr{P}_{\text{out}}$, i.e. the hot electron flux. Thus the overall "anomalous absorption" fraction of the laser power inclusive of collisional damping is also expected to be constant. That it is the turbulent damping that is responsible for these effects is far from conclusive,

[24] ν_{ei} being the electron-ion collision frequency.

but it is at least encouraging that the resulting scalings are consistent with simulation. It is important to note that those simulations included a density gradient. I have argued that there are good reasons to believe the properties of the turbulence are determined locally, and so this is not expected to make a difference, but a more thorough analysis is needed.

In a simpler model in which TPD is unaffected by the turbulence, the injected power is $\mathscr{P}_{\text{tpd}} \propto \gamma_0 \langle W \rangle$. If it saturates via a *coherent* Langmuir decay instability (LDI) cascade, then dissipation will be given by $\mathscr{P}_{\text{out}} \propto \langle W \rangle^{1/2} \langle W \rangle$ due to the fact that the growth rate of the coherent LDI instability is proportional to the Langmuir wave electric field amplitude $\langle W \rangle^{1/2}$, not its intensity. These lead to $\langle W \rangle \propto I_{\text{L}}$ and $\mathscr{P}_{\text{tpd}} \propto I_{\text{L}}^{3/2}$, which is distinct from the linear scaling.

Let us now consider the case where the interaction time is dominated by the (in)coherence of the laser: $\Delta\omega \gg \eta$. The power balance:

$$\frac{I_{\text{L}}}{\Delta\omega} \langle W \rangle \propto \langle W \rangle^{1+D/2}, \tag{3.130}$$

implies:

$$\langle W \rangle \propto \left(\frac{I_{\text{L}}}{\Delta\omega} \right)^{2/D} = \begin{cases} (I_{\text{L}}/\Delta\omega) & D = 2 \\ (I_{\text{L}}/\Delta\omega)^{2/3} & D = 3 \end{cases}, \tag{3.131}$$

and subsequently:

$$\mathscr{P}_{\text{tpd}} \propto \left(\frac{I_{\text{L}}}{\Delta\omega} \right)^{1+2/D} = \begin{cases} (I_{\text{L}}/\Delta\omega)^{2} & D = 2 \\ (I_{\text{L}}/\Delta\omega)^{5/3} & D = 3 \end{cases}. \tag{3.132}$$

We observe a more sensitive dependence on the intensity compared to the monochromatic case ($\Delta\omega \ll \eta$), but with that comes a sensitivity to bandwidth as well, which allows for a reduction in the injected power at a fixed laser intensity.

One can imagine a situation in which a laser of a given intensity is used to drive TPD to saturation and whose bandwidth is gradually increased. The dependence of the injected power on laser bandwidth is illustrated in figure 3.3. The two curves represent lasers of different intensities. The injected power is independent of bandwidth until the threshold $\eta \simeq \Delta\omega$ is met and the scaling transitions from (3.129) to (3.132). The transition depends on the turbulent damping, and hence on the fluctuation level through $\eta \propto \langle W \rangle$. Therefore the bandwidth required for the transition will scale as $\Delta\omega \propto (I_{\text{L}})^{2/(2+D)}$.

The question then is – can we estimate the bandwidth needed to provide this suppression? The turbulent damping can be estimated by assuming it is of order the collapse time: $\eta \simeq T_c^{-1}$, i.e. the characteristic non-linear time scale associated with strong Langmuir turbulence. Typical values of $\langle W \rangle$ are of order $\langle W \rangle \sim 10^{-2}$ for laser intensities near $I_{\text{L}} = 10^{15}\,\text{W/cm}^2$ as inferred from reduced particle-in-cell or Zakharov

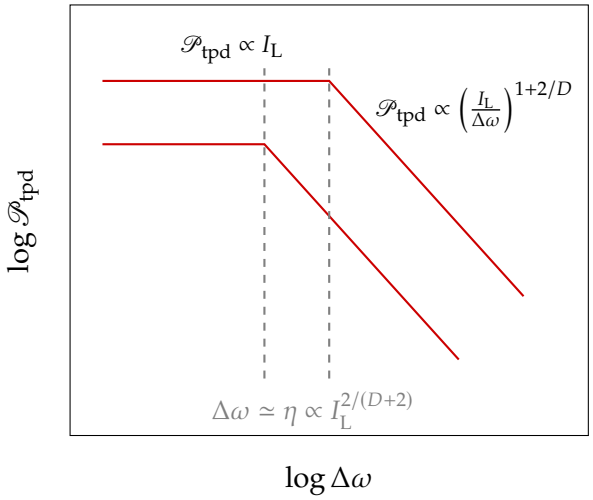


Figure 3.3: An illustration of the scaling laws for the power injected by the two-plasmon decay into the saturated state as a function of laser bandwidth.

simulations of TPD saturation (Vu *et al.*, 2012*b*; Myatt *et al.*, 2013; Rovere *et al.*, 2023). If one estimates $T_c \sim \omega_{\rm pe}\langle W\rangle$, then $\eta/\omega_{\rm pe} \sim \langle W\rangle \sim 10^{-2}$, which would imply that fractional laser bandwidths $\Delta\omega/\omega_0$ of the same order might be a good estimate for the bandwidth required to affect the TPD saturated state for intensities near $I_{\rm L} = 10^{15}\,{\rm W/cm^2}$. Of course these are very rough estimates and numerical factors could conspire to produce a different result, but it is unlikely to be orders of magnitude away.

3.6 Summary

The direct-interaction approximation was applied to the ZakTPD system: an extension of the Zakharov system including the non-linear interaction between the externally imposed laser electric field, and Langmuir modes. The TPD non-linearity produced additional terms in the renormalised Langmuir response and non-linear source, describing the injection of power in the turbulent system. The primary purpose of the DIA was to study power injection via those terms, and not to provide a full self-consistent description of the SLT state. Having derived the spectral balance equation, we saw that the problem was one of determining the time-history contained in the triad interaction time of the modes in the TPD resonance. A useful result for it was obtained via the Markovianisation procedure which approximates the time dependence of the Langmuir covariance to be identical to that of the Langmuir response. A particularly simple form for the non-linear growth rate and injected power was derived for a single broadband laser beam. It showed that in addition to the finite coherence time of the laser, the turbulent decorrelation that the Langmuir modes experience, further reduces the effective interaction time.

Scaling laws of the total injected power and fluctuation level as a function of the laser parameters were derived by the power balance between TPD forcing and dissipation via caviton collapse. Supplying the dissipation model was done via a phenomenological model outside of the direct-interaction approximation. For a monochromatic laser, the scalings predict that the total power injected by TPD scales linearly with the laser intensity, which appears consistent with numerical work reporting a constant hot electron fraction, and constant laser anomalous absorption. If the interaction time is instead dominated by the bandwidth of the laser, the fluctuation level and the absorbed power become more sensitive to the laser parameters.

I may be wrong and you may be right, and by an effort, we may get nearer to the truth.

— Karl Popper, *The Open Society and Its Enemies (Volume II: The High Tide of Prophecy: Hegel, Marx, and the Aftermath)*

4

Linear regime of the two-plasmon decay driven by broad bandwidth laser fields

Contents

4.1 Introduction **60**
4.2 Dependence of the growth rate on the laser spectrum **62**
4.2.1 Dispersion relation 62
4.2.2 Single temporally incoherent beam 63
4.2.3 Relation of the DIA to other statistical approximations 67
4.3 Parametric instabilities driven by a discrete N-line spectrum **67**
4.4 Summary **69**

4.1 Introduction

The previous chapter presented a general theory of the two-plasmon decay instability in a turbulent medium, and focused on the global (i.e. space-averaged) scaling properties of the saturated state with the laser parameters. A first step towards exploring for example the wave number dependence of the turbulent spectra, is to consider in more detail the influence of laser bandwidth on the growth rate of the instability in the linear stage. As we saw in (3.110), in the absence of turbulent damping, laser bandwidth will generally serve to reduce the growth rate of the instability from its coherent value of γ_0 to roughly $\gamma_0^2/\Delta\omega$ under the assumption $\gamma_0 \ll \Delta\omega$[1]. This property is quite generic, and was first studied in the context of the coupled mode equations which are more or less agnostic

[1]This assumption was made implicitly in (3.110) when the size of the non-linear TPD growth rate was ignored compared to the turbulent damping, i.e. $\eta_{\mathbf{k}} \gg \Gamma_{\mathbf{k}}^{\mathrm{tpd}}$ in (3.99).

to the type of three-wave instability under study (Thomson & Karush, 1974; Thomson, 1975; Laval *et al.*, 1976, 1977; DuBois *et al.*, 1992; Pesme *et al.*, 1992). Hence most work has generally ignored detailed wave number dependence of the resulting growth rates, and how the laser spectral shape might influence those.

Deriving dispersion relations and growth rates for specific broadband laser-plasma instabilities of interest has grown out of applications and generalisations of the wave-kinetic approach (Bingham *et al.*, 2005; Santos & Silva, 2005; Santos *et al.*, 2007; Trines *et al.*, 2009; Silva & Bingham, 2013; Brandão *et al.*, 2021). Wave-kinetics describes an incoherent bath of waves (such as a broadband laser) by a weakly inhomogeneous distribution function $N_{\mathbf{k}}(\mathbf{x})$ obeying a Vlasov-like equation. This usually assumes scale separation between the spatial inhomogeneity of the distribution and typical wave numbers of the waves it describes. Relaxing this assumption leads one to the so-called Wigner-Moyal formalism where the distribution function becomes the Wigner distribution of the underlying field. The ultimate generalisation of this approach stems from employing the full theory of the Wigner-Weyl transform – the Weyl symbol calculus – and allows for a systematic study of wave propagation in inhomogeneous media (Tracy *et al.*, 2014; Dodin, 2022).

That was the approach I pursued in Ruskov *et al.* (2024) to derive a dispersion relation for the broadband two-plasmon decay instability in the linear stage – the broadband laser was described in terms of its Wigner function, and the Weyl symbol calculus was used to analyse a system of equations essentially equivalent to (3.19) but excluding the ion non-linearity. The resulting growth rate that one derives from said dispersion relation, also follows rather straightforwardly from the theory presented in the previous chapter. And so I will not explore the Wigner-Moyal formalism in this thesis except to mention the following references which have examined the connection between wave-kinetics and the statistical closure methods that the thesis employs: see Appendix F. of Krommes (2002) and Krommes & Kim (2000).

In any case, the main purpose of this chapter is to investigate the $\mathbf{k}$-dependence of the growth rate in the linear regime due to spectral shape of the laser $I_{\mathbf{q}}$. I will consider only the case of a single temporally incoherent laser beam, with several different shapes of interest – the flat-top, the Lorentzian, and a spectrum comprised of a discrete set of N lines spread over bandwidth $\Delta\omega$. A notable feature would be a substantial modification in the *shape* of the growth rate, i.e. the spectrum of waves excited by the instability. I will also give conditions under which the discrete spectrum is a good approximation to the continuous flat-top one and is expected to have the same LPI quenching properties.

These results were reported in Ruskov *et al.* (2024) in which I was responsible for carrying out the analytical derivations and numerical evaluations, with scientific input and discussion from my coauthors. One of the co-authors – M. Harper – provided the initial version of the code used to numerically evaluate the broadband TPD growth rate.

4.2 Dependence of the growth rate on the laser spectrum

4.2.1 Dispersion relation

In the linear regime the system is unstable by definition (it is not in a steady state), and this appears to cause some trouble in attempting to reduce what I have called the non-linear TPD growth rate (equation 3.104) to its value for either a monochromatic laser with $\Delta\omega = 0$ (i.e. for when the laser spectrum contains just a single mode $\mathbf{k}_0$, so $I_{\mathbf{q}} = \delta_{\mathbf{q},\mathbf{k}_0}$), or one for which the bandwidth is comparable to the resonance width ($\gamma_0 \sim \Delta\omega$)[2]. Both cases are important, and a cure for these issues seems to be to extract a growth rate from the unstable root of the renormalised response function $R^{\psi\psi}$. This works as follows.

We keep only the TPD term in the self-energy (3.71), and use $I^{\mu\nu}_{\mathbf{q}}(t,t') = I^{\mu\nu}_{\mathbf{q}} e^{-\mathrm{i}\delta\omega^{\mathrm{em}}_{\mathbf{q}}(t-t')}$, to get:

$$\Sigma^{\psi\psi}_{\mathbf{k}}(t;t') = -\sum_{\mathbf{k}=\mathbf{q}-\mathbf{p}} \gamma_0^2 \frac{\left(k^2-p^2\right)^2}{k^2p^2}\frac{k_\mu k_\nu}{k_0^2} e^{-\mathrm{i}(\Omega+\delta\omega^{\mathrm{em}}_{\mathbf{q}})(t-t')} \left[R^{\psi\psi}_{\mathbf{p}}(t;t')\right]^* I^{\mu\nu}_{\mathbf{q}}. \tag{4.1}$$

Setting $\tau = t - t'$, a Laplace transformation in τ of (3.69) gives:

$$\left[-\mathrm{i}\omega + \mathrm{i}\delta\omega_{\mathbf{k}} + \Sigma^{\psi\psi}_{\mathbf{k}}(\omega)\right] R^{\psi\psi}_{\mathbf{k}}(\omega) = 1, \tag{4.2}$$

with

$$\Sigma^{\psi\psi}_{\mathbf{k}}(\omega) = -\sum_{\mathbf{k}=\mathbf{q}-\mathbf{p}} \gamma_0^2 \frac{\left(k^2-p^2\right)^2}{k^2p^2}\frac{k_\mu k_\nu}{k_0^2} I^{\mu\nu}_{\mathbf{q}} \left[R^{\psi\psi}_{\mathbf{p}}(\omega - \delta\omega^{\mathrm{em}}_{\mathbf{q}} - \Omega)\right]^*. \tag{4.3}$$

Defining the linear Langmuir dispersion function $D_{\mathbf{k}}(\omega) \doteq -\mathrm{i}\omega + \mathrm{i}\delta\omega_{\mathbf{k}}$, and setting $\omega_- \doteq \omega - \delta\omega^{\mathrm{em}}_{\mathbf{q}} - \Omega$ results in the dispersion relation:

$$D_{\mathbf{k}}(\omega) = \sum_{\mathbf{k}=\mathbf{q}-\mathbf{p}} \gamma_0^2 \frac{\left(k^2-p^2\right)^2}{k^2p^2}\frac{k_\mu k_\nu}{k_0^2} I^{\mu\nu}_{\mathbf{q}} \frac{1}{D^*_{\mathbf{p}}(\omega_-) + \Sigma^*_{\mathbf{p}}(\omega_-)}. \tag{4.4}$$

From a renormalisation point of view, these manipulations so far have been exact. Ignoring the self-energy in the denominator on the right-hand-side $\Sigma_{\mathbf{p}}(\omega_-) \to 0$, requires the growth rates to be smaller than the frequency $\gamma_0 \ll \delta\omega_{\mathbf{k}}$, which under the enveloped

[2]Notice that if we set $\eta_{\mathbf{k}} \to -\Gamma^{\mathrm{tpd}}_{\mathbf{k}}$ in (3.104) as one might expect if the assumption $\eta_{\mathbf{k}} \gg \Gamma^{\mathrm{tpd}}_{\mathbf{k}}$ was dropped, for frequency matched modes, the resonance becomes $(-1)/\Gamma^{\mathrm{tpd}}_{\mathbf{k}}$, leading to a negative growth rate.

equations is somewhat questionable since TPD can excite modes with $\mathbf{k} \to 0$ for which $\delta\omega_{\mathbf{k}} \to 0$. If one replaces these dispersion functions relating to the envelope, with the un-enveloped ones $D_{\mathbf{k}}(\omega) \to \widehat{D}_{\mathbf{k}}(\omega) = -\omega^2 + \omega_{\mathrm{pe}}^2 + 3k^2 v_{\mathrm{the}}^2$, this is no longer a problem, and in fact turns (4.4) into the result reported in Ruskov *et al.* (2024). Looking for solutions of the form $\omega = \delta\omega_{\mathbf{k}} + \mathrm{i}\gamma_{\mathbf{k}}$, results in:

$$\gamma_{\mathbf{k}} = \mathrm{Re} \sum_{\mathbf{k}=\mathbf{q}-\mathbf{p}} \gamma_0^2 \frac{\left(k^2-p^2\right)^2}{k^2p^2} \frac{k_\mu k_\nu}{k_0^2} I_{\mathbf{q}}^{\mu\nu} \frac{1}{-\mathrm{i}\left(\delta\omega_{\mathbf{q}}^{\mathrm{em}} - \delta\omega_{\mathbf{p}} - \delta\omega_{\mathbf{k}} + \Omega\right) + \gamma_{\mathbf{k}}} \tag{4.5}$$

$$= \sum_{\mathbf{k}=\mathbf{q}-\mathbf{p}} \gamma_0^2 \frac{\left(k^2-p^2\right)^2}{k^2p^2} \frac{k_\mu k_\nu}{k_0^2} I_{\mathbf{q}}^{\mu\nu} \frac{\gamma_{\mathbf{k}}}{\left(\delta\omega_{\mathbf{q}}^{\mathrm{em}} - \delta\omega_{\mathbf{p}} - \delta\omega_{\mathbf{k}} + \Omega\right)^2 + \gamma_{\mathbf{k}}^2}. \tag{4.6}$$

The well-known monochromatic growth rate is recovered for a single mode laser spectrum $I_{\mathbf{q}}^{\mu\nu} = e_0^\mu e_0^\nu \delta_{\mathbf{q},\mathbf{k}_0}$ where the wave number is $\mathbf{k}_0$ and the polarisation is $\mathbf{e}_0$.

$$\gamma_{0\mathbf{k}} = \gamma_0 \left| \frac{(\mathbf{k}\cdot\mathbf{e}_0)}{k_0} \frac{\left(k^2-p^2\right)}{kp} \right|, \tag{4.7}$$

with $\mathbf{p} = \mathbf{k}_0 - \mathbf{k}$ being the solution to the frequency matching condition $\delta\omega_{\mathbf{k}_0-\mathbf{k}} + \delta\omega_{\mathbf{k}} = \Omega$.

4.2.2 Single temporally incoherent beam

Let us consider again the case of a single beam of a temporally incoherent laser, with the spectrum[3]:

$$I_{\mathbf{q}}^{\mu\nu} = e_0^\mu e_0^\nu \, \hat{I}\left(\delta\omega_{\mathbf{q}}^{\mathrm{em}}\right) \, \delta_{\mathbf{q}_\perp,\mathbf{0}}, \tag{4.8}$$

If the typical spread of the frequency spectrum $\Delta\omega$ is much larger than the growth rate $\Delta\omega \gg \gamma_{\mathbf{k}}$, then the sum over wave numbers will ensure that the frequency detuning will dominate the resonance in (4.6), i.e.

$$\frac{\gamma_{\mathbf{k}}}{\left(\delta\omega_{\mathbf{q}}^{\mathrm{em}} - \delta\omega_{\mathbf{p}} - \delta\omega_{\mathbf{k}} + \Omega\right)^2 + \gamma_{\mathbf{k}}^2} \to \pi\delta\left(\delta\omega_{\mathbf{q}}^{\mathrm{em}} - \delta\omega_{\mathbf{p}} - \delta\omega_{\mathbf{k}} + \Omega\right), \tag{4.9}$$

resulting in a growth rate

$$\gamma_{\mathbf{k}} = \sum_{\mathbf{k}=\mathbf{q}_\parallel-\mathbf{p}} \pi\gamma_0^2 \left| \frac{(\mathbf{k}\cdot\mathbf{e}_0)}{k_0} \frac{\left(k^2-p^2\right)}{kp} \right|^2 \hat{I}\left(\delta\omega_{\mathbf{q}_\parallel}^{\mathrm{em}}\right) \, \delta\left(\delta\omega_{\mathbf{q}}^{\mathrm{em}} - \delta\omega_{\mathbf{p}} - \delta\omega_{\mathbf{k}} + \Omega\right). \tag{4.10}$$

For a given $\mathbf{k}$, the frequency matching condition results in a unique $q_\parallel = Q_{\mathbf{k}}$, and so the sum over $\mathbf{q}_\parallel$ reduces to a single evaluation at $Q_{\mathbf{k}}$:

$$\gamma_{\mathbf{k}} = \pi\gamma_0^2 \left| \frac{(\mathbf{k}\cdot\mathbf{e}_0)}{k_0} \frac{\left(k^2-p^2\right)}{kp} \right|^2 \hat{I}\left(\delta\omega_{Q_{\mathbf{k}}}^{\mathrm{em}}\right), \tag{4.11}$$

[3] As a reminder, $\mathbf{k}_0$ is the central wave number, $\mathbf{e}_0$ is the polarisation, and the delta ensures that the $\mathbf{q}$-spread is only in the direction of propagation, i.e. $\mathbf{q}_\perp = \mathbf{q} - (\mathbf{q}\cdot\mathbf{k}_0)/k_0 = \mathbf{0}$.

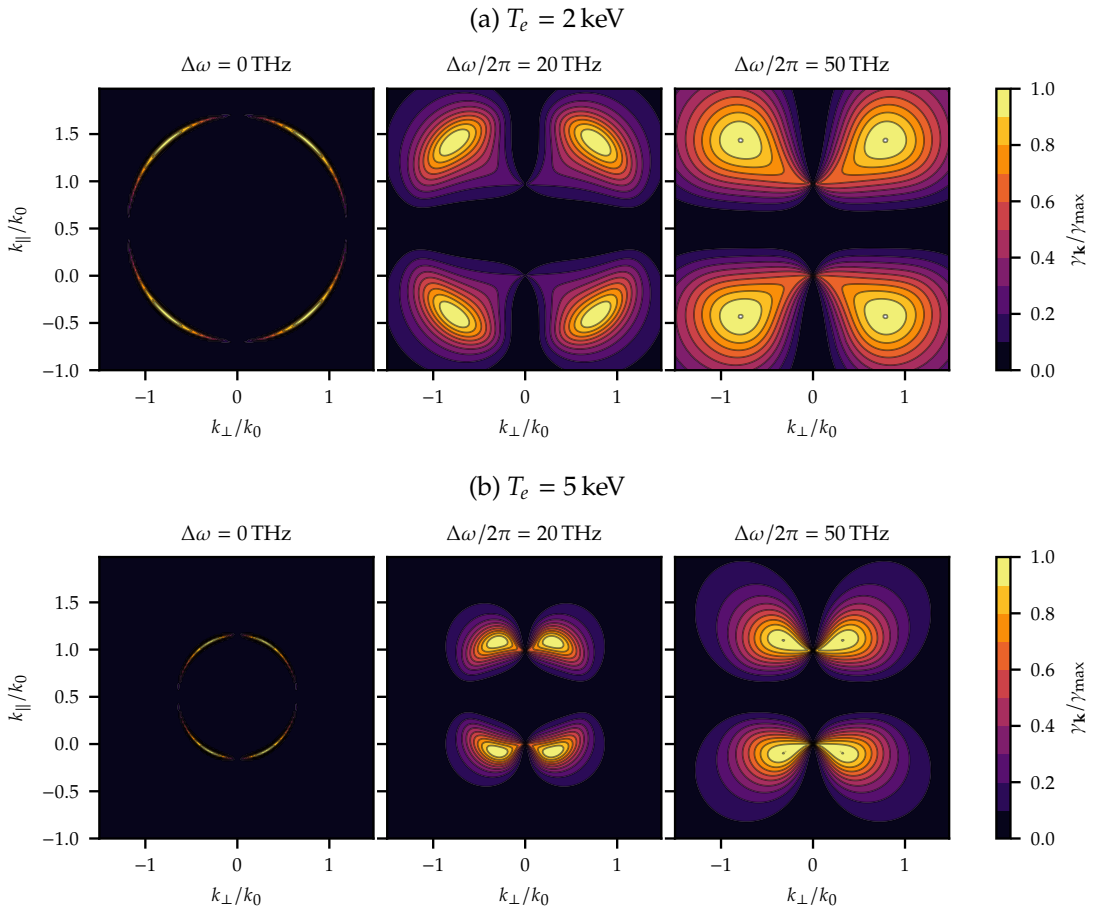


Figure 4.1: Plot of the growth rate of the TPD instability for different laser bandwidths. The laser has an intensity of $I_\mathrm{L} = 10^{15}\,\mathrm{W/cm^2}$, a wavelength $\lambda_\mathrm{L} = 351\,\mathrm{nm}$, and a Lorentzian power spectrum; the plasma conditions are $n_{0e}/n_c = 0.235$ and $T_e = 2\,\mathrm{keV}$ in (a), and $T_e = 5\,\mathrm{keV}$ in (b). The left panels show the monochromatic growth rates from the direct numerical solution of (4.6) for a single mode spectrum, and are normalised to γ_0. The middle and right panels show the analytic broadband growth rate $\gamma_{\mathbf{k}}$ (4.11) normalised to $\gamma_{\max} = 2\gamma_0^2/\Delta\omega$. $k_\perp$ and $k_\parallel$ refer to wave numbers perpendicular or parallel to the direction of propagation of the laser.

with $\mathbf{p} = Q_{\mathbf{k}}(\mathbf{k}_0/k_0) - \mathbf{k}$. The principal effect of the spectrum is to smear the monochromatic growth rate, thus leading to a general reduction of the growth rate magnitude, and a substantial broadening of the range of modes excited at each density.

I will explore the broadening first as that will make it clearer how the maximum of (4.11) is evaluated. The left panels of figure 4.1 show the monochromatic growth rate for the relevant plasma conditions, which results in a very narrow spectrum of modes due to the constraint of the frequency matching condition. The middle and right panels of figure 4.1 show the growth rate $\gamma_{\mathbf{k}}$ plotted for different bandwidths. As may be anticipated, the broad frequency spectrum of the laser allows a broader range of plasma waves to become resonant with it, hence the observed broadening in $\gamma_{\mathbf{k}}$. The middle panel corresponds to what might be reasonably expected from an

upcoming broadband ICF implosion facility. For example 20 THz corresponds to roughly $\Delta\omega/\omega_0 = 2\,\%$ for frequency tripled light ($\lambda_\mathrm{L} = 351\,\mathrm{nm}$), and the natural bandwidth of the argon-fluoride laser, another candidate broadband laser technology, is around 10 THz (Obenschain *et al.*, 2020; Dorrer *et al.*, 2020, 2021). The amount of broadening in these cases is notable. The right panels of figure 4.1 show an extreme amount of bandwidth in which virtually the full TPD hyperbolas are visible.

An increase in the electron temperature generally reduces the size of all features. At higher temperatures, the frequency $\delta\omega_\mathbf{k} = 3v_\mathrm{the}^2 k^2/(2\omega_\mathrm{pe})$ increases more sharply with k. Figure 4.1 compares the two cases relevant to (a) Omega and (b) ignition-scale NIF conditions.

In order to evaluate the peak values that the expression (4.11) attains over wave numbers, it is useful to concentrate on the middle panel of figure 4.1. We can see that the growth rate peaks at the same wave numbers as in the monochromatic case. This is due to the fact that the broadened laser spectrum peaks for the same $\mathbf{k}_0$, leading to a peak value of $\hat{I}(\delta\omega^\mathrm{em}_{Q_\mathbf{k}})$ equaling $\hat{I}(0)$. The monochromatic growth rate peaks at γ_0 (i.e. the hyperbola factor has a maximum of 1). Therefore:

$$\gamma_\mathrm{max} = \pi\gamma_0^2\,\hat{I}(0). \tag{4.12}$$

For the Lorentzian spectrum:

$$\hat{I}(\omega) = \frac{1}{\pi}\frac{\Delta\omega/2}{\omega^2 + (\Delta\omega/2)^2}, \qquad \hat{I}(0) = \frac{2}{\pi\Delta\omega}, \qquad \gamma_\mathrm{max} = \frac{2\gamma_0^2}{\Delta\omega}. \tag{4.13}$$

For a flat-top spectrum:

$$\hat{I}(\omega) = \frac{1}{\Delta\omega}\mathrm{rect}\left(\frac{\omega}{\Delta\omega}\right), \qquad \hat{I}(0) = \frac{1}{\Delta\omega}, \qquad \gamma_\mathrm{max} = \frac{\pi\gamma_0^2}{\Delta\omega}, \tag{4.14}$$

with $\mathrm{rect}(\omega) = 1$ for $|\omega| \leq 1/2$ and zero otherwise. Peak growth rates for the Lorentzian are $\simeq 60\,\%$ of those of the flat-top.

The scaling $\gamma_\mathrm{max} \propto \hat{I}(0)$ is notable in that it is different from the scalings of the TPD instability thresholds due to the density gradient inhomogeneity (c.f. the end of section 2.1). Follett *et al.* (2019) explored the dependence of those thresholds due to laser bandwidth numerically, and found that they scale to a very high degree of accuracy with a quantity, termed the coherence time, and defined as $\tau_c = \int_{-\infty}^{\infty} |g(\tau)|^2\,\mathrm{d}\tau$, where $g(\tau)$ is the Fourier transform of $\hat{I}(\omega)$ (and therefore their thresholds are proportional to $\int |\hat{I}(\omega)|^2\,\mathrm{d}\omega$). What is meant by this is that the thresholds for lasers with different spectra were identical if their coherence times as defined above were identical. This is not so for

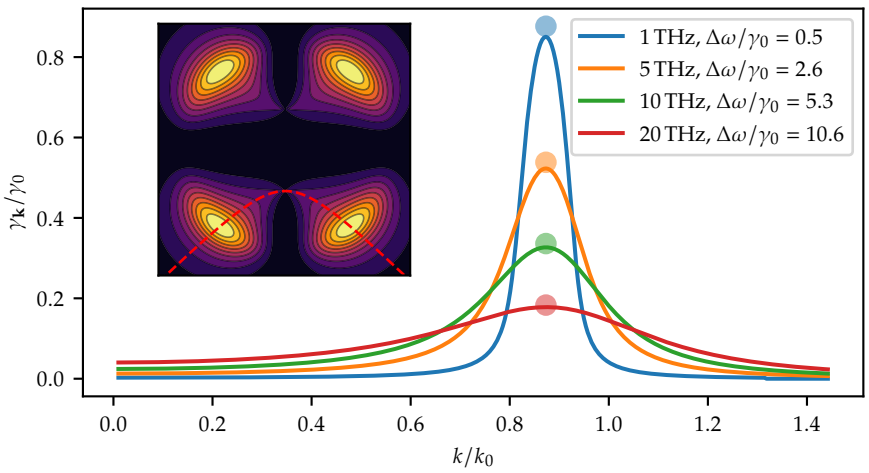


Figure 4.2: Plot of the growth rate $\gamma_{\mathbf{k}}$ obtained by the numerical evaluation of (4.6) along the lower branch of the TPD hyperbolas $k_\perp^2 = k_\parallel(k_\parallel - k_0)$. The inset shows the middle panel of figure 4.1 (a) along with the aforementioned hyperbola by the red dashed line. The laser and plasma parameters are identical to those in figure 4.1. The growth rate is normalised to the monochromatic one γ_0, and the horizontal axis is $k = \sqrt{k_\perp^2 + k_\parallel^2}$, evaluated along the hyperbola. The circles show the estimated peak growth rate from (4.18).

the peak growth rates $\gamma_{\max}$. For example $\tau_c = 2/\Delta\omega$ for the Lorentzian, and $\tau_c = 2\pi/\Delta\omega$ – a difference of a factor of π, and not $\pi/2$. One does not necessarily expect the peak growth rates in a homogeneous plasma, and the thresholds due to inhomogeneity to follow the same scaling, but the difference is worth pointing out.

Finally, let us consider the intermediate bandwidth regime in which $\Delta\omega \sim \gamma_{\mathbf{k}}$. In this case, we solve (4.6) numerically for $\gamma_{\mathbf{k}}$. The results are shown in figure 4.2. A notable feature is that the growth rate is halved for the quite modest $\Delta\omega/2\pi = 5\,\mathrm{THz}$ at an intensity of $I_L = 10^{15}\,\mathrm{W/cm^2}$. Although the exact shapes need to be calculated numerically, at least for the Lorentzian power spectrum, the peaks can be estimated well even in the intermediate bandwidth regime. Consider evaluating the integral (4.6) at the wave numbers of the monochromatic resonance (i.e. the peaks). At those points $\delta\omega_{\mathbf{k}} + \delta\omega_{\mathbf{p}} = \Omega$, and the factors from the hyperbolas evaluate to unity. Thus the integral reduces to:

$$\gamma_{\max} = \sum_{\mathbf{q}_\parallel} \frac{1}{\pi} \frac{\Delta\omega/2}{\left(\delta\omega_{\mathbf{q}}^{\mathrm{em}}\right)^2 + (\Delta\omega/2)^2} \frac{\gamma_{\max}}{\left(\delta\omega_{\mathbf{q}}^{\mathrm{em}}\right)^2 + \gamma_{\max}^2} \tag{4.15}$$

$$\simeq \gamma_0^2 \int_{-\infty}^{\infty} \mathrm{d}\omega \, \frac{1}{\pi} \frac{\Delta\omega/2}{\omega^2 + (\Delta\omega/2)^2} \frac{\gamma_{\max}}{\omega^2 + \gamma_{\max}^2} \tag{4.16}$$

$$= \frac{2\gamma_0^2}{\Delta\omega + 2\gamma_{\max}} \tag{4.17}$$

Solving for $\gamma_{\max}$:

$$\gamma_{\max} = \frac{1}{4}\left(\sqrt{16\gamma_0^2 + \Delta\omega} - \Delta\omega\right). \tag{4.18}$$

The estimate of the peak growth rate from the relation above is shown by the circles of figure 4.2.

4.2.3 Relation of the DIA to other statistical approximations

It is useful to briefly comment on how the present results relate to other studies of broad-bandwidth effects that apply statistical approximations – such as the Bourret approximation or random-phase approximation (RPA) – to the coupled-mode equations (Laval *et al.*, 1977; Pesme *et al.*, 1992; Krommes, 2002). For example, Tikhonchuk *et al.* (2026) recently compared the RPA prediction for the reduction of the growth rate $\gamma_0^2/\Delta\omega$ with a numerical solution of the coupled-mode equations, finding very good agreement. In the limit of small non-linearity, the DIA equations reduce to those of weak turbulence which are derived via an RPA ansatz. Therefore from the point of view of the statistical approximation, taking this limit is more or less equivalent to the RPA. For the present problem this occurred when the self-energy was ignored in the denominator in equation (4.4), which amounted to evaluating (4.3) with the *linear* dispersion functions $D_{\mathbf{k}}(\omega)$. Of course, the benefit of starting from the TPD equations in k-space (3.48), (3.49), the wave number dependence of the problem was explicitly retained and studied.

4.3 Parametric instabilities driven by a discrete N-line spectrum

Producing laser pulses with the broad spectra considered in the previous section is challenging. The gas excimer lasers such as the krypton fluoride or argon fluoride lasers naturally have broad bandwidth (Obenschain *et al.*, 2020), but substantial efforts are required to engineer broad spectra with more traditional drivers such as the frequency tripled Nd:Glass (Dorrer *et al.*, 2020, 2021). Therefore it is interesting to consider how a spectrum comprised of well-separated discrete spectral lines spread over some bandwidth $\Delta\omega$ such as the one shown in figure 4.3(a) might affect the instability. The argument in this section applies more generally, and is not specific to the TPD instability.

So we consider a discrete spectrum:

$$\hat{I}(\omega) = \frac{1}{N}\sum_{j=0}^{N-1} \delta\left(\omega - \frac{\Delta\omega}{2} + \frac{\Delta\omega}{N-1}j\right). \tag{4.19}$$

According to the broadband dispersion relation (4.6) each line in the spectrum will integrate to contribute a term identical to the monochromatic growth rate, resulting in a set of N rings of differing radii such as those seen in the left panels in figure 4.1. The radii of the rings are determined by the magnitude of the k which allows the Langmuir

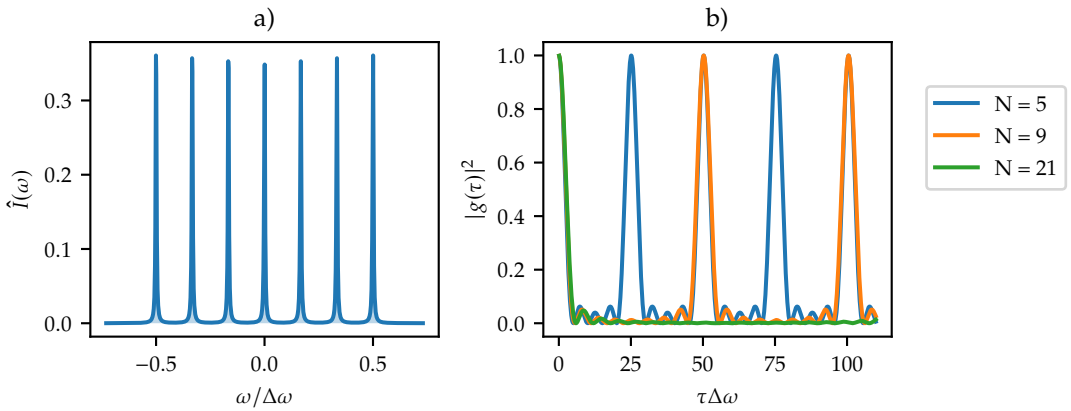


Figure 4.3: a) A power spectrum consisting of $N = 7$ discrete spectral lines spread over bandwidth $\Delta\omega$. b) The square of the correlation function $|g(\tau)|^2$ as a function of the time delay τ for a set of N discrete spectral lines spread over a bandwidth $\Delta\omega$.

modes to frequency match to each line in the spectrum. The peak growth rate in each line will be reduced according to $\Gamma_{\max} = \gamma_0/\sqrt{N}$. This is under the assumption that the lines are well separated, which means that only a single line is contained within the instability resonance $\Delta\omega/(N-1) > \gamma_0$. In this case, the reduction in the growth rate depends only on the number of lines and not on the total amount of bandwidth $\Delta\omega$. The reduction can still be significant – for example for $N = 10$ the reduction by a factor of approximately 3, is similar to 10 THz of continuous bandwidth (see figure 4.2) for $I_L = 10^{15}\,\mathrm{W/cm^2}$, and $\lambda_L = 351\,\mathrm{nm}$.

It has been argued (Bodner, 2023) that the coherence properties of the discrete spectrum cannot approximate the continuous one, since formally, if each line in the spectrum is delta-shaped, the coherence time of the signal is infinite. And so if one were following a coherence time argument for the reduction of the growth rate, or the fact that scalings of the LPI thresholds seem to depend only on τ_c and not on the shape of the spectrum (Follett *et al.*, 2019), one might be right to question the utility of the discrete spectrum, if its coherence time is indeed infinite.

This isn't necessarily the case, and it is worth exploring why. Consider the correlation function related to the spectrum (4.19):

$$g(\tau) = \int_{-\infty}^{\infty} \mathrm{d}\omega\, e^{-\mathrm{i}\omega\tau}\, \hat{I}(\omega) = \frac{1}{N} \sin\left(\frac{N\Delta\omega\tau}{2(N-1)}\right) \Big/ \sin\left(\frac{\Delta\omega\tau}{2(N-1)}\right), \tag{4.20}$$

with the coherence time again defined as:

$$\tau_c = \int_{-\infty}^{\infty} |g(\tau)|^2\, \mathrm{d}\tau. \tag{4.21}$$

The integral of $|g(\tau)|^2$ does indeed diverge for any finite N. For $N \to \infty$ it reduces to the correlation function expected from the continuous flat spectrum:

$$g(\tau) = \mathrm{sinc}\,(\Delta\omega\tau/2)\,, \tag{4.22}$$

which does have a finite coherence time. In figure 4.3(b) I show what $|g(\tau)|^2$ looks like for a varying number of discrete spectral lines N. For small τ, we see all examples following the sinc profile expected in the continuous case, but we also see "bursts" of correlation for longer τ which are like echoes of the same sinc profile. We also see that these bursts occur for longer and longer delays τ, the larger N is. It is the fact that the amplitude of these bursts is not decaying that produces the infinite coherence time. Or at least a very long coherence time if the width of each line is small but finite.

But if one imagined that the number of lines is high enough so that the bursts of correlation occurred on a time scale much longer than the scale of interest, then from the point of view of such a fast process, the discrete nature of the spectrum would not matter, and the coherence properties of the signal will be well approximated by the continuous case. More concretely, from (4.20) the first peak past the origin occurs for a delay $\tau_1 = 2(N-1)\pi/\Delta\omega$, and so if $\tau_1 \gg \gamma_0^{-1}$ (γ_0^{-1} being the time scale of the LPI), then the coherence properties of the continuous spectrum will be well approximated to the discrete one, as far as the instability is concerned. This can be cast into a condition on the number of lines:

$$N \gg \frac{1}{2\pi}\frac{\Delta\omega}{\gamma_0}. \tag{4.23}$$

For a laser intensity of $10^{15}\,\mathrm{W/cm^2}$ at a wavelength of 350 nm and bandwidth of $\Delta\omega/\omega_0 = 1\,\%$, the right-hand side is approximately equal to one, and so even a fairly low number of lines such as $N = 10$ to 15 might be enough.

This condition is also identical to the discrete lines *not* being well separated. The spectral distance between the lines is $\Delta\omega/(N-1)$. (4.23) is a statement of this distance being much smaller than the width of the resonance.

4.4 Summary

A dispersion relation for the TPD instability valid for laser fields with broadband power spectra was derived from the general formalism presented in the previous chapter. It produces the well-known monochromatic growth rate in the appropriate limit. Of primary interest was TPD driven by a single temporally incoherent laser beam. For

large laser bandwidth (in the sense of $\Delta\omega \gg \gamma_0$) an exact analytic solution for the growth rate exists, showing an increase in the range of modes excited by TPD at each density, and a decrease in peak growth rates. The practically relevant problem of using discrete laser power spectra was also examined.

But even if you do obtain a solution, you may then discover, to your delight, the existence of a whole family of enchanting though perhaps difficult problem children for whose welfare you may work, with a purpose, to the end of your days.

— Karl Popper, *Realism and the Aim of Science*

5 Concluding remarks and future work

5.1 Summary of the results

This thesis addressed two related problems: (i) investigating the potential mitigating effect of broad laser bandwidth on the two-plasmon decay instability; and (ii) investigating the influence of the strongly turbulent background in which TPD must evolve in its saturated state. Both problems were explored by applying the direct-interaction approximation to the ZakTPD system. The unifying concept of the triad interaction time – which quantified the effective time during which the three modes in the TPD resonance maintain coherence – provided a clear physical picture of the influence of the background turbulence on the instability, in conjunction with the effect of short laser coherence time. I argued that despite some known deficiencies of the DIA in *predicting* the SLT state, there are good reasons to believe that it captures the influence of the turbulence on TPD well. The main effect was understood to be one of turbulent decorrelation: the large amount of fluctuations that the free Langmuir modes must propagate through in order to resonantly interact with the laser, caused a reduction in the triad interaction time.

Balancing the total power injected by TPD with the power dissipated by the turbulence allowed for an investigation of how the fluctuation level and power absorbed from the laser scale with the laser parameters. In the regime in which the turbulent damping dominates the triad interaction time (i.e. for a monochromatic laser driver), a notable feature was the fact that the injected power is both independent of the fluctuation level and scales linearly with the laser intensity. This feature aligns with numerical work reporting a constant hot-electron fraction and constant laser anomalous absorption when TPD is driven strongly above its inhomogeneity threshold.

In the linear regime, the frequency spectrum of a single broad bandwidth laser beam was shown to "smear" the TPD growth rate in wave number space, leading to an overall reduction for the peak values, but with an associated increase for other parts of the spectrum. The coherence properties of a discrete spectrum and its effect on parametric instabilities in general were also evaluated.

5.2 Open questions and future research

Multiple avenues for future research are worth exploring. The most pressing issue is a more detailed comparison with simulation, especially regarding the scaling laws in the laser bandwidth dominated regime. The injected power is predicted to scale strongly with laser bandwidth: $(\Delta\omega)^{-5/3}$ in $D = 3$, which could be helpful in containing the deleterious effects of TPD even if it is above threshold. In the linear regime, preliminary results using the LPSE code show the expected broadening due to laser bandwidth such as the one observed in figure 4.2.

The broadband driving laser fields considered in this thesis have all involved only temporal incoherence, i.e. a broadening in wave number in the direction parallel to beam propagation. In realistic experimental geometries, using beam smoothing techniques such as random phase plates, the fields are transversely incoherent as well – there is a spread in wave number of the spectrum in the directions perpendicular to propagation. While such a spectrum is trivially incorporated in the formalism, care should be taken in applying the results. Such fields produce a speckled intensity pattern at focus, and it is well known that LPI can exhibit different behaviour based on whether there is "communication" between the speckles or not (Follett *et al.*, 2022). These issues may be related to how intermittent the fields are, and thus may question the near Gaussianity assumption of the DIA.

Questions also remain regarding the role of damping as well as the laser drive on SLT physics. Myatt *et al.* (2013) for example report that strong ion-acoustic damping may favour more efficient nucleation of the cavities and hence lead to higher fluctuation levels and more hot electron production. By studying the auto-correlation function of the Langmuir field, Vu *et al.* (2014) inferred that laser polarisation influences the caviton shape and orientation. The focus in this thesis has been on the influence of the SLT state onto TPD, but that point suggests that the reverse should also be considered.

Light emitted near odd half-integer harmonics of the driving laser ($\omega_0/2$ and $3\omega_0/2$) has been a characteristic signature of TPD (Seka *et al.*, 2009; Myatt *et al.*, 2014; Michel, 2023). Some of the properties of these features are not fully understood but the Langmuir spectrum has been determined to be very broad, consistent with SLT predictions.

Langmuir-decay-instability-produced waves have been used to explain observed features in the $3\omega_0/2$ spectrum (Russell & DuBois, 2001), as well as in ultraviolet Thomson scattering experiments (Follett, 2015; Follett *et al.*, 2015). More work is needed to establish what the expected effect of SLT on these features would be. Perhaps the most promising route to testing whether cavitation is present, is to look for the caviton continuum feature *below the local plasma frequency* (see figure 3.2), as was done for ionospheric modification experiments (DuBois *et al.*, 2001). It might be important that similar to those experiments, the measurements should be "altitude-resolved", meaning that the volume of plasma sampled by Thomson scattering is small compared to the density gradient scale length, and one is observing waves in a narrow density range. If that is not the case, both the free mode feature and the caviton continuum would be substantially blurred due to averaging over the gradient.

Finally, the triad interaction time both as a mental concept as well as a quantitative measure, appears to be extremely useful in interpreting the role of the turbulence on TPD. This should carry to the non-linear saturation of other LPI of interest such as the Raman scattering instability, and in general it would not be unreasonable to expect its utility in studying any wave-wave coupling in a turbulent medium.

Appendices

A

Relationship between real space and Fourier space response functions

The slightly unsymmetrical form for the homogeneous responses and covariances in subsection 3.3.1 stems from the fact that the response functions corresponding to an equation written in **x**-space, or to the equation written in Fourier **k**-space, fundamentally represent different things. Consider, in terms of the generalised variables, an equation of the form:

$$R_{12}^{-1}\varphi_2 = f_1, \tag{A.1}$$

which has the formal solution:

$$\varphi_1 = R_{12}f_2. \tag{A.2}$$

Here f_1 is an external source. The response function describes the evolution of a delta-shaped perturbation, which clearly means different things in different coordinate systems. To make this point clear, consider writing the above both in terms of the **x**-space response, which I will denote $G(\mathbf{x}, \mathbf{x}')$ and the Fourier space response $R_{\mathbf{k}\mathbf{k}'}$[1]:

$$\varphi(\mathbf{x}) = \int \mathrm{d}\mathbf{x}'\, G(\mathbf{x}, \mathbf{x}')f(\mathbf{x}'), \qquad \varphi_{\mathbf{k}} = \sum_{\mathbf{k}'} R_{\mathbf{k}\mathbf{k}'}f_{\mathbf{k}'}. \tag{A.3}$$

It is indeed the case that the Fourier modes corresponding to G:

$$G(\mathbf{x}, \mathbf{x}') = \sum_{\mathbf{k},\mathbf{k}'} G_{\mathbf{k}\mathbf{k}'}\, e^{\mathrm{i}\mathbf{k}\cdot\mathbf{x}}e^{\mathrm{i}\mathbf{k}'\cdot\mathbf{x}'} \tag{A.4}$$

[1]The time variables have been dropped for clarity.

will indeed obey the usual $G_{\mathbf{k}\mathbf{k}'} = G_{\mathbf{k}}\delta_{\mathbf{k}+\mathbf{k}',\mathbf{0}}$, which any function of only the difference $\mathbf{x} - \mathbf{x}'$ must obey. But consider writing:

$$\begin{aligned}\varphi(\mathbf{x}) &= \sum_{\mathbf{k}} e^{\mathrm{i}\mathbf{k}\cdot\mathbf{x}} \sum_{\mathbf{k}'} R_{\mathbf{k}\mathbf{k}'} f_{\mathbf{k}'} \\ &= \sum_{\mathbf{k}} e^{\mathrm{i}\mathbf{k}\cdot\mathbf{x}} \sum_{\mathbf{k}'} R_{\mathbf{k}\mathbf{k}'} \int \mathrm{d}\mathbf{x}' e^{-\mathrm{i}\mathbf{k}'\cdot\mathbf{x}'} f(\mathbf{x}') \\ &= \int \mathrm{d}\mathbf{x}' \underbrace{\left(\sum_{\mathbf{k},\mathbf{k}'} R_{\mathbf{k}\mathbf{k}'} e^{\mathrm{i}\mathbf{k}\cdot\mathbf{x} - \mathrm{i}\mathbf{k}'\cdot\mathbf{x}'} \right)}_{G(\mathbf{x},\mathbf{x}')} f(\mathbf{x}').\end{aligned} \tag{A.5}$$

From here immediately we see that for $G(\mathbf{x}, \mathbf{x}') = G(\mathbf{x} - \mathbf{x}')$ we need $R_{\mathbf{k}\mathbf{k}'} \propto \delta_{\mathbf{k}\mathbf{k}'}$. The relationship between the Fourier components of the $\mathbf{x}$-space response G, and the Fourier response is:

$$R_{\mathbf{k}\mathbf{k}'} = G_{\mathbf{k},-\mathbf{k}'}. \tag{A.6}$$

And thus for a homogeneous system:

$$R_{\mathbf{k}\mathbf{k}'} = R_{\mathbf{k}}\delta_{\mathbf{k}\mathbf{k}'}. \tag{A.7}$$

B

Equations for the ZakTPD system in the direct-interaction approximation

B.1 Coupling coefficients in the ZakTPD system

Having derived (3.48) and (3.50-3.52) describing the evolution of the generalised field φ_1, the application of the DIA equations (2.60-2.63) requires reading off the coupling coefficients M_{123} and the linear operators L_{12} for the system. The variables are $1 \equiv (t, \mathbf{k}, \sigma)$ with the field index σ taking the values $\sigma = \{\psi, \psi^\dagger, n, u, \xi^\mu, \xi^{\dagger\mu}\}$.

From the ψ equation (3.48), the non-linear couplings are:

$$M^{\psi n \psi}_{\mathbf{kpq}}(t, t_2, t_3) = -\frac{\mathrm{i}\omega_{\mathrm{pe}}}{2}\frac{(\mathbf{k}\cdot\mathbf{q})}{k^2}\delta_{\mathbf{k},\mathbf{p}+\mathbf{q}}\delta(t-t_2)\delta(t-t_3), \tag{B.1}$$

$$M^{\psi \psi n}_{\mathbf{kpq}}(t, t_2, t_3) = -\frac{\mathrm{i}\omega_{\mathrm{pe}}}{2}\frac{(\mathbf{k}\cdot\mathbf{p})}{k^2}\delta_{\mathbf{k},\mathbf{p}+\mathbf{q}}\delta(t-t_2)\delta(t-t_3), \tag{B.2}$$

$$M^{\psi \psi^\dagger \xi^\mu}_{\mathbf{kpq}}(t, t_2, t_3) = -\mathrm{i}\gamma_0\frac{k_\mu}{k_0}\left(\frac{k^2-p^2}{k^2}\right)e^{-\mathrm{i}\Omega t}\,\delta_{\mathbf{k},\mathbf{p}+\mathbf{q}}\delta(t-t_2)\delta(t-t_3), \tag{B.3}$$

$$M^{\psi \xi^\mu \psi^\dagger}_{\mathbf{kpq}}(t, t_2, t_3) = -\mathrm{i}\gamma_0\frac{k_\mu}{k_0}\left(\frac{k^2-q^2}{k^2}\right)e^{-\mathrm{i}\Omega t}\,\delta_{\mathbf{k},\mathbf{p}+\mathbf{q}}\delta(t-t_2)\delta(t-t_3). \tag{B.4}$$

This is the most general form of the coupling coefficients. To avoid clutter, I won't write out the delta functions for the next set of equations, as all of these will be implicitly integrated out when I give the DIA equations for the system in later sections of this appendix.

From the equation for $\psi^\dagger$ (3.50), we read off:

$$M^{\psi^\dagger n\psi^\dagger}_{\mathbf{kpq}} = \frac{\mathrm{i}\omega_{\mathrm{pe}}}{2}\frac{(\mathbf{k}\cdot\mathbf{q})}{k^2}, \tag{B.5}$$

$$M^{\psi^\dagger\psi^\dagger n}_{\mathbf{kpq}} = \frac{\mathrm{i}\omega_{\mathrm{pe}}}{2}\frac{(\mathbf{k}\cdot\mathbf{p})}{k^2}, \tag{B.6}$$

$$M^{\psi^\dagger\psi\xi^{\dagger\mu}}_{\mathbf{kpq}}(t) = -\mathrm{i}\gamma_0\frac{k_\mu}{k_0}\left(\frac{k^2-p^2}{k^2}\right)e^{\mathrm{i}\Omega t}, \tag{B.7}$$

$$M^{\psi^\dagger\xi^{\dagger\mu}\psi}_{\mathbf{kpq}}(t) = -\mathrm{i}\gamma_0\frac{k_\mu}{k_0}\left(\frac{k^2-q^2}{k^2}\right)e^{\mathrm{i}\Omega t}. \tag{B.8}$$

And from the ion equations (3.51-3.52):

$$M^{u\psi\psi^\dagger}_{\mathbf{kpq}} = M^{u\psi^\dagger\psi}_{\mathbf{kpq}} = -(\mathbf{p}\cdot\mathbf{q}). \tag{B.9}$$

Finally, the non-zero components of the linear couplings L_{12} are:

$$L^{\psi\psi}_{\mathbf{k}} = -\delta\omega_{\mathbf{k}}, \tag{B.10}$$

$$L^{\psi^\dagger\psi^\dagger}_{\mathbf{k}} = \delta\omega_{\mathbf{k}}, \tag{B.11}$$

$$L^{nu}_{\mathbf{k}} = -c_s^2k^2, \tag{B.12}$$

$$L^{un}_{\mathbf{k}} = 1. \tag{B.13}$$

B.2 From the general DIA equations to the statistically homogeneous ones

The complex conjugates entering the ZAKTPD system remove the pleasant symmetry of both the response R and the covariance C obeying the same homogeneity property, namely proportionality to $\delta_{\mathbf{kk'}}$, which we saw in sub-section (3.3.1). Furthermore the TPD terms introduce time-dependency in the couplings M. The formulas become slightly more tedious so it is useful to collect them here.

Consider the expressions for the self-energies first, and apply the homogeneity conditions $R \propto \delta_{\mathbf{kk'}}$ and $C \propto \delta_{\mathbf{k+k',0}}$:

$$\begin{aligned}
\Sigma_{11'} &= -M_{123}M_{2'3'1'}R_{22'}C_{33'} \\
\Sigma^{\sigma\sigma'}_{\mathbf{kk'}}(t;t') &= -\sum_{\substack{\mathbf{p},\mathbf{q},\mathbf{p'},\mathbf{q'}\\ \sigma_2,\sigma_2',\sigma_3,\sigma_3'}} M^{\sigma\sigma_2\sigma_3}_{\mathbf{kpq}}(t)\, M^{\sigma_2'\sigma_3'\sigma'}_{\mathbf{p'q'k'}}(t')\, R^{\sigma_2\sigma_2'}_{\mathbf{pp'}} C^{\sigma_3\sigma_3'}_{\mathbf{qq'}} \\
&= -\sum_{\substack{\mathbf{p},\mathbf{q},\mathbf{p'},\mathbf{q'}\\ \sigma_2,\sigma_2',\sigma_3,\sigma_3'}} M^{\sigma\sigma_2\sigma_3}_{\mathbf{kpq}}(t)\, M^{\sigma_2'\sigma_3'\sigma'}_{\mathbf{p'q'k'}}(t') \left(R^{\sigma_2\sigma_2'}_{\mathbf{p}}\delta_{\mathbf{pp'}}\right)\left(C^{\sigma_3\sigma_3'}_{\mathbf{q}}\delta_{\mathbf{q+q',0}}\right) \\
&= -\sum_{\substack{\mathbf{p},\mathbf{q}\\ \sigma_2,\sigma_2',\sigma_3,\sigma_3'}} M^{\sigma\sigma_2\sigma_3}_{\mathbf{kpq}}(t)\, M^{\sigma_2'\sigma_3'\sigma'}_{\mathbf{p},-\mathbf{q},\mathbf{k'}}(t')\, R^{\sigma_2\sigma_2'}_{\mathbf{p}} C^{\sigma_3\sigma_3'}_{\mathbf{q}}.
\end{aligned} \tag{B.14}$$

I've assumed that the time dependence of the couplings M is of the form which appears in the couplings of the ZAKTPD system $M(t_1,t_2,t_3) \propto \delta(t_1-t_2)\delta(t_1-t_3)$, and have performed the integrations implicitly. In a translationally invariant system, which is a necessary condition for statistical homogeneity, the couplings obey $M_{\mathbf{kpq}} \propto \delta_{\mathbf{k},\mathbf{p}+\mathbf{q}}$. Therefore:

$$\begin{aligned}\Sigma^{\sigma\sigma'}_{\mathbf{k}\mathbf{k}'}(t;t') &= -\sum_{\substack{\mathbf{p},\mathbf{q}\\ \sigma_2,\sigma_2',\sigma_3,\sigma_3'}} M^{\sigma\sigma_2\sigma_3}_{\mathbf{kpq}}(t)\, M^{\sigma_2'\sigma_3'\sigma'}_{\mathbf{p},-\mathbf{q},\mathbf{k}'}(t')\, R^{\sigma_2\sigma_2'}_{\mathbf{p}} C^{\sigma_3\sigma_3'}_{\mathbf{q}}\, \delta_{\mathbf{k},\mathbf{p}+\mathbf{q}}\, \delta_{\mathbf{p},-\mathbf{q}+\mathbf{k}'},\\ &= -\delta_{\mathbf{k}\mathbf{k}'} \sum_{\substack{\mathbf{p},\mathbf{q}\\ \sigma_2,\sigma_2',\sigma_3,\sigma_3'}} M^{\sigma\sigma_2\sigma_3}_{\mathbf{kpq}}(t)\, M^{\sigma_2'\sigma_3'\sigma'}_{\mathbf{p},-\mathbf{q},\mathbf{k}'}(t')\, R^{\sigma_2\sigma_2'}_{\mathbf{p}} C^{\sigma_3\sigma_3'}_{\mathbf{q}} \delta_{\mathbf{k},\mathbf{p}+\mathbf{q}},\end{aligned} \tag{B.15}$$

and so we see that as expected Σ obeys the same homogeneity property as R. Meaning we can write:

$$\Sigma^{\sigma\sigma'}_{\mathbf{k}}(t;t') = -\sum_{\substack{\mathbf{k}=\mathbf{p}+\mathbf{q}\\ \sigma_2,\sigma_2',\sigma_3,\sigma_3'}} M^{\sigma\sigma_2\sigma_3}_{\mathbf{kpq}}(t)\, M^{\sigma_2'\sigma_3'\sigma'}_{\mathbf{p},-\mathbf{q},\mathbf{k}}(t')\, R^{\sigma_2\sigma_2'}_{\mathbf{p}}(t;t') C^{\sigma_3\sigma_3'}_{\mathbf{q}}(t,t'). \tag{B.16}$$

An analogous calculation for F yields $F^{\sigma\sigma'}_{\mathbf{k}\mathbf{k}'}(t,t') = F^{\sigma\sigma'}_{\mathbf{k}}(t,t')\,\delta_{\mathbf{k}+\mathbf{k}',\mathbf{0}}$ with:

$$F^{\sigma\sigma'}_{\mathbf{k}}(t,t') = \frac{1}{2}\sum_{\substack{\mathbf{k}=\mathbf{p}+\mathbf{q}\\ \sigma_2,\sigma_2',\sigma_3,\sigma_3'}} M^{\sigma\sigma_2\sigma_3}_{\mathbf{kpq}}(t)\, M^{\sigma'\sigma_2'\sigma_3'}_{-\mathbf{k},-\mathbf{p},-\mathbf{q}}(t')\, C^{\sigma_2\sigma_2'}_{\mathbf{p}}(t,t')\, C^{\sigma_3\sigma_3'}_{\mathbf{q}}(t,t'). \tag{B.17}$$

(B.16) and (B.17) are the homogeneous versions of (2.62) and (2.63). For the other two equations, it is easy to check that terms such as ΣR or ΣC have the appropriate dependencies matching the homogeneity conditions in the respective equations they enter, i.e. that $\Sigma_{12}R_{21'} \propto \delta_{\mathbf{k}\mathbf{k}'}$ and $\Sigma_{12}C_{21'} \propto \delta_{\mathbf{k}+\mathbf{k}',\mathbf{0}}$. Thus:

$$\partial_t R^{\sigma\sigma'}_{\mathbf{k}}(t;t') - \sum_{\bar\sigma} L^{\sigma\bar\sigma}_{\mathbf{k}} R^{\bar\sigma\sigma'}_{\mathbf{k}}(t;t') + \sum_{\bar\sigma}\int_{t'}^{t} \mathrm{d}\bar t\; \Sigma^{\sigma\bar\sigma}_{\mathbf{k}}(t;\bar t)\, R^{\bar\sigma\sigma'}_{\mathbf{k}}(\bar t;t') = \delta_{\sigma\sigma'}\delta(t-t'), \tag{B.18}$$

$$\begin{aligned}\partial_t C^{\sigma\sigma'}_{\mathbf{k}}(t,t') - \sum_{\bar\sigma} L^{\sigma\bar\sigma}_{\mathbf{k}} C^{\bar\sigma\sigma'}_{\mathbf{k}}(t,t') + \sum_{\bar\sigma}\int_{-\infty}^{t} \mathrm{d}\bar t\; \Sigma^{\sigma\bar\sigma}_{\mathbf{k}}(t;\bar t)\, C^{\bar\sigma\sigma'}_{\mathbf{k}}(\bar t,t')&\\ = \sum_{\bar\sigma}\int_{-\infty}^{t'} \mathrm{d}\bar t\; F^{\sigma\bar\sigma}_{\mathbf{k}}(t,\bar t)\, R^{\sigma'\bar\sigma}_{\mathbf{k}}(t';\bar t).&\end{aligned} \tag{B.19}$$

This completes the derivation of the statistically homogeneous versions of the DIA equations. We have further allowed for the time dependence of the couplings M entering through the TPD non-linearity, which appears to be a fairly uncommon feature of the problem.

B.3 The ZAKTPD-DIA equations

B.3.1 Langmuir response and covariance

In this section, we combine the coupling coefficients, the homogeneous version of the DIA, and utilise the symmetry argument of sub-section 3.3.1, to compute the governing equations for the direct-interaction approximation for the ZAKTPD system. Consider first the quantities relating to the Langmuir fluctuations. Due to the symmetry argument, we assume that the only non-zero covariance is $C^{\psi\psi^\dagger}_{\mathbf{k}}$, and $C^{\psi^\dagger\psi}_{\mathbf{k}} = \left(C^{\psi\psi^\dagger}_{-\mathbf{k}}\right)^*$; similarly for the responses: $R^{\psi\psi}_{\mathbf{k}}$, together with $R^{\psi^\dagger\psi^\dagger}_{\mathbf{k}} = \left(R^{\psi\psi}_{-\mathbf{k}}\right)^*$. The equations they obey are:

$$(\partial_t + \mathrm{i}\delta\omega_{\mathbf{k}})\, R^{\psi\psi}_{\mathbf{k}}(t;t') + \int_{t'}^{t} \mathrm{d}\bar{t}\; \Sigma^{\psi\psi}_{\mathbf{k}}(t;\bar{t})\, R^{\psi\psi}_{\mathbf{k}}(\bar{t};t') = \delta(t-t')\,, \tag{B.20}$$

$$\begin{aligned}(\partial_t + \mathrm{i}\delta\omega_{\mathbf{k}})\, C^{\psi\psi^\dagger}_{\mathbf{k}}(t,t') + \int_{-\infty}^{t} \mathrm{d}\bar{t}\; \Sigma^{\psi\psi}_{\mathbf{k}}(t;\bar{t})\, C^{\psi\psi^\dagger}_{\mathbf{k}}(\bar{t},t') \\ = \int_{-\infty}^{t'} \mathrm{d}\bar{t}\; F^{\psi\psi^\dagger}_{\mathbf{k}}(t,\bar{t})\, R^{\psi^\dagger\psi^\dagger}_{\mathbf{k}}(t';\bar{t}).\end{aligned} \tag{B.21}$$

These necessitate only the computation of $\Sigma^{\psi\psi}$ – the turbulent correction to the Langmuir response – and the non-linear source $F^{\psi\psi^\dagger}$. Consider each one of these in turn.

Due to (B.16) we have:

$$\Sigma^{\psi\psi}_{\mathbf{k}}(t;t') = -\sum_{\substack{\mathbf{k}=\mathbf{p}+\mathbf{q}\\ \sigma_2,\sigma_2',\sigma_3,\sigma_3'}} M^{\psi\sigma_2\sigma_3}_{\mathbf{kpq}}(t)\, M^{\sigma_2'\sigma_3'\psi}_{\mathbf{p},-\mathbf{q},\mathbf{k}}(t')\, R^{\sigma_2\sigma_2'}_{\mathbf{p}}(t;t')\, C^{\sigma_3\sigma_3'}_{\mathbf{q}}(t,t'). \tag{B.22}$$

The non-zero coupling coefficients which match the form of the second M are $M^{\psi n\psi}$, $M^{u\psi^\dagger\psi}$, and $M^{\psi^\dagger\xi^{\dagger\mu}\psi}$. The last one introduces terms of the form:

$$\textcircled{1} = -\sum_{\substack{\mathbf{k}=\mathbf{p}+\mathbf{q}\\ \sigma_2,\sigma_3}} M^{\psi\sigma_2\sigma_3}_{\mathbf{kpq}}(t)\, M^{\psi^\dagger\xi^{\dagger\mu}\psi}_{\mathbf{p},-\mathbf{q},\mathbf{k}}(t')\, R^{\sigma_2\psi^\dagger}_{\mathbf{p}}(t;t')\, C^{\sigma_3\xi^{\dagger\mu}}_{\mathbf{q}}(t,t'). \tag{B.23}$$

Since again due to the symmetry argument we assume that the only non-zero covariance relating to the laser electric field is $C^{\xi^\mu\xi^{\dagger\nu}}$ which I shall denote as $I^{\mu\nu}_{\mathbf{q}} \doteq C^{\xi^\mu\xi^{\dagger\nu}}_{\mathbf{q}}$. Thus, the above will reduce to just:

$$\textcircled{1} = -\sum_{\mathbf{k}=\mathbf{p}+\mathbf{q}} M^{\psi\psi^\dagger\xi^\mu}_{\mathbf{kpq}}(t)\, M^{\psi^\dagger\xi^{\dagger\nu}\psi}_{\mathbf{p},-\mathbf{q},\mathbf{k}}(t')\, R^{\psi^\dagger\psi^\dagger}_{\mathbf{p}}(t;t')\, I^{\mu\nu}_{\mathbf{q}}(t,t'). \tag{B.24}$$

A summation convention over repeated indices relating to the laser field components ξ^μ will always be implied. The $M^{u\psi^\dagger\psi}$ coupling gives terms of the form:

$$\textcircled{2} = -\sum_{\substack{\mathbf{k}=\mathbf{p}+\mathbf{q}\\ \sigma_2,\sigma_3}} M^{\psi\sigma_2\sigma_3}_{\mathbf{kpq}}(t)\, M^{u\psi^\dagger\psi}_{\mathbf{p},-\mathbf{q},\mathbf{k}}(t')\, R^{\sigma_2 u}_{\mathbf{p}}(t;t')\, C^{\sigma_3\psi^\dagger}_{\mathbf{q}}(t,t'). \tag{B.25}$$

The only non-zero covariance which is allowed occurs for $\sigma_3 = \psi$, thus:

$$\textcircled{2} = -\sum_{\mathbf{k}=\mathbf{p}+\mathbf{q}} M^{\psi n\psi}_{\mathbf{kpq}}(t)\, M^{u\psi^\dagger\psi}_{\mathbf{p},-\mathbf{q},\mathbf{k}}(t')\, R^{nu}_{\mathbf{p}}(t;t')\, C^{\psi\psi^\dagger}_{\mathbf{q}}(t,t'). \tag{B.26}$$

Finally, in a completely analogous manner, $M^{\psi n\psi}$ gives:

$$\textcircled{3} = -\sum_{\mathbf{k}=\mathbf{p}+\mathbf{q}} M^{\psi\psi n}_{\mathbf{kpq}}(t)\, M^{\psi n\psi}_{\mathbf{p},-\mathbf{q},\mathbf{k}}(t')\, R^{\psi\psi}_{\mathbf{p}}(t;t')\, C^{nn}_{\mathbf{q}}(t,t'). \tag{B.27}$$

Combining all three and substituting in the relevant couplings:

$$\begin{aligned}\Sigma^{\psi\psi}_{\mathbf{k}}(t;t') = \sum_{\mathbf{k}=\mathbf{p}+\mathbf{q}} \Bigg\{ & \frac{\omega_{pe}^2}{4}\frac{(\mathbf{k}\cdot\mathbf{p})^2}{k^2p^2}\, R^{\psi\psi}_{\mathbf{p}}(t;t')\, C^{nn}_{\mathbf{q}}(t,t') \\ & + \frac{\mathrm{i}\omega_{pe}}{2}\frac{(\mathbf{k}\cdot\mathbf{q})^2}{k^2} R^{nu}_{\mathbf{p}}(t;t')\, C^{\psi\psi^\dagger}_{\mathbf{q}}(t,t') \\ & - \gamma_0^2 \frac{\left(k^2-p^2\right)^2}{k^2p^2}\frac{k_\mu k_\nu}{k_0^2} e^{-\mathrm{i}\Omega(t-t')}\, R^{\psi^\dagger\psi^\dagger}_{\mathbf{p}}(t;t')\, I^{\mu\nu}_{\mathbf{q}}(t,t') \Bigg\}.\end{aligned} \tag{B.28}$$

In the last term I have substituted $p_\nu \to k_\nu$ since $\xi^\nu_{\mathbf{q}}$ is transverse. This completes the calculation for $\Sigma^{\psi\psi}$.

Let us turn now to the non-linear source $F^{\psi\psi^\dagger}$. From (B.17):

$$F^{\psi\psi^\dagger}_{\mathbf{k}}(t,t') = \frac{1}{2}\sum_{\substack{\mathbf{k}=\mathbf{p}+\mathbf{q}\\ \sigma_2,\sigma_2',\sigma_3,\sigma_3'}} M^{\psi\sigma_2\sigma_3}_{\mathbf{kpq}}(t)\, M^{\psi^\dagger\sigma_2'\sigma_3'}_{-\mathbf{k},-\mathbf{p},-\mathbf{q}}(t')\, C^{\sigma_2\sigma_2'}_{\mathbf{p}}(t,t')\, C^{\sigma_3\sigma_3'}_{\mathbf{q}}(t,t'). \tag{B.29}$$

The couplings which result correspond to non-zero covariances are $M^{\psi n\psi}M^{\psi^\dagger n\psi^\dagger}$, $M^{\psi\psi n}M^{\psi^\dagger\psi^\dagger n}$ and $M^{\psi\psi^\dagger\xi^\mu}M^{\psi^\dagger\psi\xi^{\dagger\nu}}$, $M^{\psi\xi^\mu\psi^\dagger}M^{\psi^\dagger\xi^{\dagger\nu}\psi}$; each pair results in the same contribution after summing over wave numbers, thus:

$$\begin{aligned}F^{\psi\psi^\dagger}_{\mathbf{k}}(t,t') = \sum_{\mathbf{k}=\mathbf{p}+\mathbf{q}} \Bigg\{ & \frac{\omega_{pe}^2}{4}\frac{(\mathbf{k}\cdot\mathbf{p})^2}{k^4}\, C^{\psi\psi^\dagger}_{\mathbf{p}}(t,t')\, C^{nn}_{\mathbf{q}}(t,t') \\ & + \gamma_0^2 \frac{\left(k^2-p^2\right)^2}{k^4}\frac{k_\mu k_\nu}{k_0^2} e^{-\mathrm{i}\Omega(t-t')}\, C^{\psi^\dagger\psi}_{\mathbf{p}}(t,t')\, I^{\mu\nu}_{\mathbf{q}}(t,t') \Bigg\}.\end{aligned} \tag{B.30}$$

B.3.2 Ion response and covariance

I now turn to the equations governing the ion quantities. So far we have seen C^{nn} and R^{nu} enter the equations for the Langmuir fluctuations. Consider the latter first. It obeys:

$$\partial_t R^{nu}_{\mathbf{k}}(t;t') + c_s^2 k^2 R^{uu}_{\mathbf{k}}(t;t') = 0, \tag{B.31}$$

where I have made use of the fact that all $\Sigma^{n\sigma}$ vanish due to n coupling only linearly to u, and hence all $M^{n\sigma\sigma'} = 0$. We need R^{uu} so:

$$\partial_t R^{uu}_{\mathbf{k}}(t;t') - R^{nu}_{\mathbf{k}}(t;t') + \int_{t'}^{t} \mathrm{d}\bar{t}\; \Sigma^{un}_{\mathbf{k}}(t;\bar{t})\, R^{nu}_{\mathbf{k}}(\bar{t};t') = \delta(t-t')\,. \tag{B.32}$$

Finally:

$$\Sigma^{un}_{\mathbf{k}}(t;t') = -\sum_{\substack{\mathbf{k}=\mathbf{p}+\mathbf{q}\\ \sigma_2,\sigma_2',\sigma_3,\sigma_3'}} M^{u\sigma_2\sigma_3}_{\mathbf{kpq}}(t)\, M^{\sigma_2'\sigma_3' n}_{\mathbf{p},-\mathbf{q},\mathbf{k}}(t')\, R^{\sigma_2\sigma_2'}_{\mathbf{p}}(t;t')\, C^{\sigma_3\sigma_3'}_{\mathbf{q}}(t,t'), \tag{B.33}$$

contains two contributions: from $M^{u\psi\psi^\dagger} M^{\psi\psi n}$ and $M^{u\psi^\dagger\psi} M^{\psi^\dagger\psi n}$, resulting in:

$$\Sigma^{un}_{\mathbf{k}}(t;t') = \sum_{\mathbf{k}=\mathbf{p}+\mathbf{q}} \frac{\mathrm{i}\omega_{pe}}{2} \frac{(\mathbf{p}\cdot\mathbf{q})}{p^2} \left[R^{\psi\psi}_{\mathbf{p}}(t;t')\, C^{\psi^\dagger\psi}_{\mathbf{q}}(t,t') - R^{\psi^\dagger\psi^\dagger}_{\mathbf{p}}(t;t')\, C^{\psi\psi^\dagger}_{\mathbf{q}}(t,t') \right]. \tag{B.34}$$

For the spectra, one has:

$$\partial_t C^{nn}_{\mathbf{k}}(t,t') + c_s^2 k^2 C^{un}_{\mathbf{k}}(t,t') = 0, \tag{B.35}$$

$$\partial_t C^{un}_{\mathbf{k}}(t,t') - C^{nn}_{\mathbf{k}}(t,t') + \int_{-\infty}^{t} \mathrm{d}\bar{t}\; \Sigma^{un}_{\mathbf{k}}(t;\bar{t})\, C^{nn}_{\mathbf{k}}(\bar{t},t') = \int_{-\infty}^{t'} \mathrm{d}\bar{t}\; F^{uu}_{\mathbf{k}}(t,\bar{t})\, R^{nu}_{\mathbf{k}}(t';\bar{t}). \tag{B.36}$$

F^{un} vanishes due to $F^{un} \propto M^{n\sigma\sigma'} = 0$. F^{uu} on the other hand is:

$$F^{uu}_{\mathbf{k}}(t,t') = \sum_{\mathbf{k}=\mathbf{p}+\mathbf{q}} (\mathbf{p}\cdot\mathbf{q})^2\, C^{\psi\psi^\dagger}_{\mathbf{p}}(t,t')\, C^{\psi^\dagger\psi}_{\mathbf{q}}(t,t'). \tag{B.37}$$

The two equations for the responses can be reduced to a single second-order one:

$$\left(\partial_t^2 + c_s^2 k^2\right) \widehat{R}^{nn}_{\mathbf{k}}(t;t') + \int_{t'}^{t} \mathrm{d}\bar{t}\; \widehat{\Sigma}^{nn}_{\mathbf{k}}(t;\bar{t})\, \widehat{R}^{nn}_{\mathbf{k}}(\bar{t};t') = \delta(t-t')\,, \tag{B.38}$$

where

$$\widehat{R}^{nn}_{\mathbf{k}} = -\frac{R^{nu}_{\mathbf{k}}}{c_s^2 k^2}, \qquad \widehat{\Sigma}^{nn}_{\mathbf{k}} = -c_s^2 k^2\, \Sigma^{un}_{\mathbf{k}}. \tag{B.38a,b}$$

Similarly for the equations for the covariances:

$$\left(\partial_t^2 + c_s^2 k^2\right) C^{nn}_{\mathbf{k}}(t,t') + \int_{-\infty}^{t} \mathrm{d}\bar{t}\; \widehat{\Sigma}^{nn}_{\mathbf{k}}(t;\bar{t})\, C^{nn}_{\mathbf{k}}(\bar{t},t') = \int_{-\infty}^{t'} \mathrm{d}\bar{t}\; \widehat{F}^{nn}_{\mathbf{k}}(t,\bar{t})\, \widehat{R}^{nn}_{\mathbf{k}}(t';\bar{t}), \tag{B.39}$$

with

$$\widehat{F}^{nn}_{\mathbf{k}} = c_s^4 k^4 F^{uu}_{\mathbf{k}}. \tag{B.40}$$

Bibliography

Bates, J. W., Follett, R. K., Shaw, J. G., Obenschain, S. P., Myatt, J. F., Weaver, J. L., Wolford, M. F., Kehne, D. M., Myers, M. C. & Kessler, T. J. 2023 Suppressing parametric instabilities in direct-drive inertial-confinement-fusion plasmas using broadband laser light. *Physics of Plasmas* **30** (5), 052703.

Bingham, R., de Angelis, U. & Tsytovich, V.N. 1997 Theory of collisionless damping of cavitons and resonant particle acceleration. *Journal of plasma physics* **58** (1), 41–59.

Bingham, R., Silva, L.O., Trines, R.M.G.M., Mendonça, J.T., Shukla, P.K., Mori, W.B. & Cairns, R.A. 2005 Wave kinetic treatment of forward four-wave stimulated scattering instabilities. *Journal of plasma physics* **71** (6), 899–904.

Bodner, S.E. 2023 Comparison of an argon-fluoride gas laser with a solid-state laser for application to laser fusion energy. *Journal of Fusion Energy* **42** (2), 33.

Bowman, J.C., Krommes, J.A. & Ottaviani, M. 1993 The realizable Markovian closure. I. General theory, with application to three-wave dynamics. *Physics of Fluids B: Plasma Physics* **5** (10), 3558–3589.

Bowman, J. C. 1992 Realizable Markovian Statistical Closures: General Theory and Application to Drift-Wave Turbulence. PhD thesis, Princeton University (https://www.math.ualberta.ca/~bowman/publications/thesis.pdf).

Brandão, B., Santos, J.E., Trines, R.M.G.M., Bingham, R. & Silva, L.O. 2021 Bandwidth effects in stimulated Brillouin scattering driven by partially incoherent light. *Plasma Physics and Controlled Fusion* **63** (9), 094003.

Craxton, R. S., Anderson, K. S., Boehly, T. R., Goncharov, V. N., Harding, D. R., Knauer, J. P., McCrory, R. L., McKenty, P. W., Meyerhofer, D. D., Myatt, J. F., Schmitt, A. J., Sethian, J. D., Short, R. W., Skupsky, S., Theobald, W., Kruer, W. L., Tanaka, K., Betti, R., Collins, T. J. B., Delettrez, J. A., Hu, S. X., Marozas, J. A., Maximov, A. V., Michel, D. T., Radha, P. B., Regan, S. P., Sangster, T. C., Seka, W., Solodov, A. A., Soures, J. M., Stoeckl, C. & Zuegel, J. D. 2015 Direct-drive inertial confinement fusion: A review. *Physics of Plasmas* **22** (11), 110501.

Diamond, P.H., Itoh, S.-I. & Itoh, K. 2010 *Modern Plasma Physics. Volume 1: Physical Kinetics of Turbulent Plasmas.*. Cambridge University Press.

Dodin, I.Y. 2022 Quasilinear theory for inhomogeneous plasma. *Journal of Plasma Physics* **88** (4), 905880407.

Dorrer, C., Hill, E.M. & Zuegel, J.D. 2020 High-energy parametric amplification of spectrally incoherent broadband pulses. *Optics Express* **28** (1), 451–471.

Dorrer, C., Spilatro, M., Herman, S., Borger, T. & Hill, E.M. 2021 Broadband sum-frequency generation of spectrally incoherent pulses. *Optics Express* **29** (11), 16135–16152.

DuBois, D.F. 2000 From Kadanoff-Baym Equations to Plasma Turbulence. In *Progress In Nonequilibrium Green's Functions*, pp. 112–143. World Scientific.

DuBois, D.F., Bezzerides, B. & Rose, H.A. 1992 Collective parametric instabilities of many overlapping laser beams with finite bandwidth. *Physics of Fluids B: Plasma Physics* **4** (1), 241–251.

DuBois, D.F., Rose, H.A. & Russell, D. 1996 Saturation of radiation-induced parametric instabilities by excitation of Langmuir turbulence. *Physica Scripta* **1996** (T63), 16.

DuBois, D.F., Rose, H. A. & Russell, D. 1990 Excitation of strong Langmuir turbulence in plasmas near critical density: Application to HF heating of the ionosphere. *Journal of Geophysical Research: Space Physics* **95** (A12), 21221–21272.

DuBois, D.F., Russell, D. A. & Rose, H. A. 1995*a* Saturation spectra of the two-plasmon decay instability. *Physical Review Letters* **74** (20), 3983.

DuBois, D. F. & Espedal, M. 1978 Direct interaction approximation and plasma turbulence theory. *Plasma Physics* **20** (12), 1209.

DuBois, D. F. & Rose, H. A. 1981 Statistical theories of Langmuir turbulence. i. Direct-interaction-approximation responses. *Phys. Rev. A* **24**, 1476–1504.

DuBois, D. F., Russell, D. & Rose, H. A. 1995*b* Reduced description of strong Langmuir turbulence from kinetic theory. *Physics of Plasmas* **2** (1), 76–96.

DuBois, D. F., Russell, D. A., Cheung, P. Y. & Sulzer, M. P. 2001 High-power high-frequency-induced langmuir turbulence in the smooth ionosphere at arecibo. i. theoretical predictions for altitude-resolved plasma line radar spectra. *Physics of Plasmas* **8** (3), 791–801.

Follett, Russell 2015 The multiple-beam two-plasmon-decay instability. PhD thesis, Laboratory For Laser Energetics, University of Rochester.

Follett, R.K., Shaw, J.G., Myatt, J.F., Wen, H., Froula, D.H. & Palastro, J.P. 2021 Thresholds of absolute two-plasmon-decay and stimulated raman scattering instabilities driven by multiple broadband lasers. *Physics of Plasmas* **28** (3), 032103.

Follett, R.K., Wen, H., Froula, D.H., Turnbull, D. & Palastro, J.P. 2022 Independent-hot-spot approach to multibeam laser-plasma instabilities. *Physical Review E* **105** (6), L063201.

Follett, R. K., Edgell, D. H., Henchen, R. J., Hu, S. X., Katz, J., Michel, D. T., Myatt, J. F., Shaw, J. & Froula, D. H. 2015 Direct observation of the two-plasmon-decay common plasma wave using ultraviolet thomson scattering. *Phys. Rev. E* **91**, 031104(R).

Follett, R. K., Myatt, J. F., Shaw, J. G., Michel, D. T., Solodov, A. A., Edgell, D. H., Yaakobi, B. & Froula, D. H. 2017 Simulations and measurements of hot-electron generation driven by the multibeam two-plasmon-decay instability. *Physics of Plasmas* **24** (10), 102134.

Follett, R. K., Shaw, J. G., Myatt, J. F., Dorrer, C., Froula, D. H. & Palastro, J. P. 2019 Thresholds of absolute instabilities driven by a broadband laser. *Physics of Plasmas* **26** (6), 062111.

Frisch, U. 1995 *Turbulence: The Legacy of A. N. Kolmogorov*. Cambridge University Press.

Froula, D. H., Dorrer, C., Colaïtis, A., Edgell, D. H., Follett, R. K., Hill, E. M., Igumenshchev, I. V., Milder, A. L., Palastro, J. P., Shah, R. C., Solodov, A. A., Turnbull, D., Goncharov, V. N., Regan, S. P., Sorce, C., Zuegel, J. & Deeney, C. 2025 A future of inertial confinement fusion without laser-plasma instabilities. *Physics of Plasmas* **32** (5), 052713.

Goodman, J.W. 2015 *Statistical optics*. John Wiley & Sons.

Grams, J. 2021 Ripple: An Investigation of the World's Most Advanced High-Yield Thermonuclear Weapon Design. *Journal of Cold War Studies* **23** (2), 133–161.

Hurricane, O. A., Patel, P. K., Betti, R., Froula, D. H., Regan, S. P., Slutz, S. A., Gomez, M. R. & Sweeney, M. A. 2023 Physics principles of inertial confinement fusion and u.s. program overview. *Rev. Mod. Phys.* **95**, 025005.

Kadomtsev, B. B. 1965 *Plasma turbulence*. Academic Press, New York.

Kline, J. L., Montgomery, D. S., Yin, L., DuBois, D. F., Albright, B. J., Bezzerides, B., Cobble, J. A., Dodd, E. S., DuBois, D. F., Fernández, J. C., Johnson, R. P., Kindel, J. M., Rose, H. A., Vu, H. X. & Daughton, W. 2006 Different $k\lambda_D$ regimes for nonlinear effects on Langmuir waves. *Physics of Plasmas* **13** (5), 055906.

Kolmogorov, A. N. 1941 Local structure of turbulence in incompressible viscous fluid at very large Reynolds numbers. *Dokl. Acad. Nauk SSSR* **30** (299).

Kraichnan, R. H. 1959 The structure of isotropic turbulence at very high Reynolds numbers. *Journal of Fluid Mechanics* **5** (4), 497–543.

Krommes, J. A. 1984 Statistical descriptions and plasma physics. In *Handbook of Plasma Physics, Vol. 2* (ed. A. A. Galeev & R. N. Sudan), pp. 184–268. North-Holland Publishing Company.

Krommes, J. A. 2002 Fundamental statistical descriptions of plasma turbulence in magnetic fields. *Physics Reports* **360** (1-4), 1–352.

Krommes, J. A. 2015 A tutorial introduction to the statistical theory of turbulent plasmas, a half-century after Kadomtsev's Plasma Turbulence and the resonance-broadening theory of Dupree and Weinstock. *Journal of Plasma Physics* **81** (6), 205810601.

Krommes, J. A. & Kim, C.-B. 2000 Interactions of disparate scales in drift-wave turbulence. *Phys. Rev. E* **62**, 8508–8539.

Laval, G., Pellat, R. & Pesme, D. 1976 Absolute parametric excitation by an imperfect pump or by turbulence in an inhomogeneous plasma. *Physical Review Letters* **36** (4), 192.

Laval, G., Pellat, R., Pesme, D., Ramani, A., Rosenbluth, Marshall N. & Williams, E. A. 1977 Parametric instabilities in the presence of space-time random fluctuations. *The Physics of Fluids* **20** (12), 2049–2057.

Martin, P. C., Siggia, E. D. & Rose, H. A. 1973 Statistical dynamics of classical systems. *Phys. Rev. A* **8**, 423–437.

Michel, P. 2023 *Introduction to Laser-Plasma Interactions*, 1st edn. Springer Cham.

Myatt, J.F., Zhang, J., Short, R.W., Maximov, A.V., Seka, W., Froula, D.H., Edgell, D.H., Michel, D.T., Igumenshchev, I.V., Hinkel, D.E., Michel, P. & Moody, J.D. 2014 Multiple-beam laser–plasma interactions in inertial confinement fusion. *Physics of Plasmas* **21** (5), 055501.

Myatt, J. F., Vu, H. X., DuBois, D. F., Russell, D. A., Zhang, J., Short, R. W. & Maximov, A. V. 2013 Mitigation of two-plasmon decay in direct-drive inertial confinement fusion through the manipulation of ion-acoustic and Langmuir wave damping. *Physics of Plasmas* **20** (5), 052705.

Nicholson, D.R. 1983 *Introduction to Plasma Theory*. Wiley New York.

Nuckolls, J. 2007 Contributions to the Genesis and Progress of ICF. In *Inertial Confinement Nuclear Fusion: A historical Approch by its Pioneers* (ed. G. Velarde & N. Santamaria). Foxwell & Davies Ltd (UK).

Obenschain, S.P., Schmitt, A.J., Bates, J.W., Wolford, M.F., Myers, M.C., McGeoch, M.W., Karasik, M. & Weaver, J.L. 2020 Direct drive with the argon fluoride laser as a path to high fusion gain with sub-megajoule laser energy. *Philosophical Transactions of the Royal Society A* **378** (2184), 20200031.

Pesme, D., Berger, R.L., Williams, E.A., Bourdier, A. & Bortuzzo-Lesne, A. 1992 A statistical description of parametric instabilities with an incoherent pump; effet de l'incohérence spatiale induite sur les instabilités paramétriques. *Tech. Rep.* CEA-N-2692. Commissariat à l'énergie atomique et aux énergies alternatives, arXiv: 0710.2195.

Robinson, P. A. 1997 Nonlinear wave collapse and strong turbulence. *Reviews of modern physics* **69** (2), 507.

Robinson, P. A. & Newman, D. L. 1990 Two-component model of strong Langmuir turbulence: Scalings, spectra, and statistics of Langmuir waves. *Physics of Fluids B: Plasma Physics* **2** (12), 2999–3016.

Rosen, M.D. 2024 The long road to ignition: An eyewitness account. *Physics of Plasmas* **31** (9), 090501.

Rosenberg, M. J., Solodov, A. A., Myatt, J. F., Seka, W., Michel, P., Hohenberger, M., Short, R. W., Epstein, R., Regan, S. P., Campbell, E. M., Chapman, T., Goyon, C., Ralph, J. E., Barrios, M. A., Moody, J. D. & Bates, J. W. 2018 Origins and scaling of hot-electron preheat in ignition-scale direct-drive inertial confinement fusion experiments. *Phys. Rev. Lett.* **120**, 055001.

Rovere, E., Colaïtis, A., Follett, R. K. & Casner, A. 2023 Hot electron scaling for two-plasmon decay in icf plasmas. *Physics of Plasmas* **30** (4), 042104.

Ruskov, R.T., Bingham, R., Silva, L.O., Harper, M., Aboushelbaya, R., Myatt, J.F. & Norreys, P.A. 2024 Statistical theory of the broadband two-plasmon decay instability. *Journal of Plasma Physics* **90** (6), 905900621, arXiv: 2404.17384.

Russell, D., DuBois, D.F. & Rose, H.A. 1986 Collapsing-caviton turbulence in one dimension. *Phys. Rev. Lett.* **56**, 838–841.

Russell, D. A. & DuBois, D. F. 2001 $\frac{3}{2}\omega_0$ Radiation from the Laser-Driven Two-Plasmon Decay Instability in an Inhomogeneous Plasma. *Phys. Rev. Lett.* **86**, 428–431.

Sagdeev, R.Z., Solov'ev, G.I., Shapiro, V.D., Shevchenko, V.I. & Yusupov, I.U. 1982 Plasma turbulence and dissipation of a strong electromagnetic wave in the vicinity of the $n_c/4$ resonance. *Sov. Phys. JETP* **55** (1).

Sagdeev, R. Z. & Galeev, A. A. 1969 *Nonlinear Plasma Theory*. W.A. Benjamin, Inc.

Santos, J.P. & Silva, L.O. 2005 Wigner-Moyal description of free variable mass Klein-Gordon fields. *Journal of mathematical physics* **46** (10), 102901.

Santos, J.E., Silva, L.O. & Bingham, R. 2007 White-light parametric instabilities in plasmas. *Physical review letters* **98** (23), 235001.

Schekochihin, A. A. 2026 Lectures on Kinetic Theory and Magnetohydrodynamics of Plasmas. *Lecture Notes for the Oxford MMathPhys programme* (URL: http://www-thphys.physics.ox.ac.uk/people/AlexanderSchekochihin/KT/2015/KTLectureNotes.pdf).

Schmitt, A.J. & Obenschain, S.P. 2023*a* The importance of laser wavelength for driving inertial confinement fusion targets. I. Basic physics. *Physics of Plasmas* **30** (1), 012701.

Schmitt, A.J. & Obenschain, S.P. 2023*b* The importance of laser wavelength for driving inertial confinement fusion targets. II. Target design. *Physics of Plasmas* **30** (1), 012702.

Seka, W., Edgell, D. H., Myatt, J. F., Maximov, A. V., Short, R. W., Goncharov, V. N. & Baldis, H. A. 2009 Two-plasmon-decay instability in direct-drive inertial confinement fusion experiments. *Physics of Plasmas* **16** (5), 052701.

Silin, V. P. & Tikhonchuk, V. T. 1986 Parametric plasma turbulence. *Physics Reports* **135** (1), 1–46.

Silva, L.O. & Bingham, R. 2013 *Laser-Plasma Interactions and Applications*, chap. Theory of Underdense Laser-Plasma Interactions with Photon Kinetic Theory, pp. 3–18. Springer.

Simon, A., Short, R.W., Williams, E.A. & Dewandre, T. 1983 On the inhomogeneous two-plasmon instability. *The Physics of fluids* **26** (10), 3107–3118.

Thomson, J.J. 1975 Finite-bandwidth effects on the parametric instability in an inhomogeneous plasma. *Nuclear Fusion* **15** (2), 237.

Thomson, J. J. & Karush, Jack I. 1974 Effects of finite-bandwidth driver on the parametric instability. *The Physics of Fluids* **17** (8), 1608–1613.

Tikhonchuk, V., Blackman, D., Loiseau, P. & Ruyer, C. 2026 Effect of spectral bandwidth on the stimulated scattering of laser beams in plasma. *Physics of Plasmas* **33** (1), 012107.

Tikhonchuk, V. T. 2019 Physics of laser plasma interaction and particle transport in the context of inertial confinement fusion. *Nuclear Fusion* **59** (3), 032001.

Tracy, E.R., Brizard, A.J., Richardson, A.S. & Kaufman, A.N. 2014 *Ray tracing and beyond: phase space methods in plasma wave theory*. Cambridge University Press.

Trines, R.M.G.M., Bingham, R., Silva, L.O., Mendonça, J.T., Shukla, P.K., Murphy, C.D., Dunlop, M.W., Davies, J.A., Bamford, R., Vaivads, A. & Norreys, P.A. 2009 Applications of the wave kinetic approach: From laser wakefields to drift wave turbulence. *Physics of Plasmas* **16** (5), 055904.

Tsytovich, V. 1970 *Nonlinear Effects in Plasma*. Plenum Press, New York.

Vu, H.X., DuBois, D.F., Myatt, J.F. & Russell, D.A. 2012*a* Hot-electron production and suprathermal heat flux scaling with laser intensity from the two-plasmon–decay instability. *Physics of Plasmas* **19** (10), 102703.

Vu, H.X., DuBois, D.F., Russell, D.A. & Myatt, J.F. 2010 The reduced-description particle-in-cell model for the two plasmon decay instability. *Physics of Plasmas* **17** (7), 072701.

Vu, H.X., DuBois, D.F., Russell, D.A. & Myatt, J.F. 2012*b* Hot-electron generation by "cavitating" Langmuir turbulence in the nonlinear stage of the two-plasmon–decay instability. *Physics of Plasmas* **19** (10), 102708.

Vu, H. X., DuBois, D. F., Russell, D. A., Myatt, J. F. & Zhang, J. 2014 Nonlinear development of the two-plasmon decay instability in three dimensions. *Physics of Plasmas* **21** (4), 042705.

Yan, R., Maximov, A.V. & Ren, C. 2010 The linear regime of the two-plasmon decay instability in inhomogeneous plasmas. *Physics of Plasmas* **17** (5), 052701.

Zakharov, V. E. 1972 Collapse of Langmuir waves. *Sov. Phys. JETP* **35** (5), 908–914.

Zaslavskii, G. M. & Sagdeev, R. Z. 1967 Limits of statistical description of a nonlinear wave field. *Soviet physics JETP* **25** (718-724).